Square and Slant Fatigue Crack Growth in Al 2024

Cover: Two constant ΔK tests for ΔK=20 MPa$\sqrt{m}$ and R=0.1
frequency=20 Hz (above)
frequency=0.2 Hz (below)

Rechte en Schuine Vermoeiingscheurgroei in Al 2024

proefschrift

ter verkrijging van de graad van doctor
aan de Technische Universiteit van Delft
op gezag van de Rector Magnificus, prof. ir. K. F. Wakker
in het openbaar te verdedigen ten overstaan van een commissie
aangewezen door het College van Dekanen
op dinsdag 21 november 1995 te 16.00 uur

door

Jan ZUIDEMA

metaalkundig ingenieur
geboren te Veenendaal.

Dit proefschrift is goedgekeurd door de promotoren
prof. dr. ir. J. Schijve en
prof. dr. ir. A. Bakker.

Samenstelling promotiecommissie:
Rector Magnificus, voorzitter
Prof. dr. ir. J. Schijve, promotor, Lucht&Ruimtevaart, T.U. Delft.
Prof. dr. ir. A. Bakker, promotor, Materiaalkunde, T.U. Delft.
Prof. ir. L. Katgerman, Materiaalkunde, T.U. Delft.
Prof. Dr. G. den Ouden, Materiaalkunde, T.U. Delft.
Prof. ir. L.B. Vogelesang, Lucht&Ruimtevaart, T.U. Delft.
Dr. ir. M. Janssen, Materiaalkunde, T.U. Delft.

Published and distributed by:

Delft University Press
Stevinweg 1
2628 CN Delft
The Netherlands
Telephone +31 15 2783254
Fax +31 15 2781661

CIP-DATA KONINKLIJKE BIBLIOTHEEK, DEN HAAG

Zuidema, Jan

Square and Slant Fatigue Crack Growth in Al 2024/ Jan Zuidema. -Delft:
Delft University Press. -III.
Thesis Delft University of Technology. -With ref. -With summary in Dutch.
ISBN 90-407-1191-7
NUGI 841
Keywords: shear lips/crack closure/fatigue crack growth.

Printed in The Netherlands

Acknowledgments

The research described in this dissertation was carried out at the Laboratory of Materials Science of the Faculty of Chemical Engineering and Materials of the Delft University of Technology. The favorable research conditions in this laboratory are gratefully acknowledged.
When I started to work in the field of Fracture Mechanics and Fatigue Bert Ewalds suggested me to do also research on shear lips, a topic he was highly interested on. So I did.

I wish to express my appreciation to my colleagues in the "vakgroep Toepassing van Materialen in Constructies" for their cooperation, support, loyalty and belief in a successful end to this thesis.

Special appreciation is expressed to the former students (afstudeerders) Huib Blaauw, Eric de Jong, Marco Kanaar , Jos Krabbe, Mark Mannesse, Peter Mense and Fred Veer who all had a contribution or participated in this research project.

Special appreciation is also expressed to Michael Janssen for many discussions about fatigue crack growth, to Anton Wachters for reading the concept manuscript and to Theo van Soest who always solved all technical problems.

I thank my promotor, Jaap Schijve, for tirelessly reading and rereading my concept thesis.

Finally, I thank my wife Rita and my sons Jan and Joost for their patience and unfailing support and belief in a successful end.

Rechte en Schuine Vermoeiingscheurgroei in Al 2024

Samenvatting:

Alhoewel schuine vermoeiingsscheurgroei, door middel van zgn. shear lips, veelvuldig is waargenomen, werd de oorzaak en de betekenis ervan voor de scheurgroeisnelheid tot op heden niet onderkend.
Het onderhavige promotieonderzoek werd primair uitgevoerd om deze dip in onze kennis van de vermoeiingscheurgroei op te vullen. Als onderzoeks materiaal werd de aluminium legering 2024 T351 gekozen. Enerzijds omdat dit materiaal zeer duidelijke shear lips vertoont, en anderzijds omdat het een belangrijk technisch materiaal betreft. Het wordt zeer veel gebruikt in vliegtechnische toepassingen vanwege zijn lichte gewicht en gunstige vermoeiingseigenschappen.
Voor het verkrijgen van kwantitatieve informatie over de effecten van shear lips op de vermoeiingsscheurgroeisnelheid (da/dN) bleek de constante ΔK proef onontbeerlijk. In een constante ΔK test groeit de shear lip naar een evenwichtstoestand die bij deze ΔK hoort. Tegelijkertijd daalt de da/dN ook naar een evenwichtswaarde. De vermoeiingsscheurgroeisnelheid kan maximaal met een factor 3 dalen, wanneer een rechte vermoeiingsscheur wordt vergeleken met een schuine scheur. Er wordt een model gepresenteerd dat naast scheurdrijvende kracht (ΔK) ook rekening houdt met scheurweerstand en scheursluiting. Vreemd is de rol die de frequentie van de vermoeiingsbelasting speelt. Bij 10 Hz, in lucht, is er een aanzienlijk verschil in scheurgroeisnelheid tussen rechte en schuine vermoeiingsscheuren bij dezelfde belasting. Indien we de frequentie verlagen wordt dit verschil minder. Bij 1 Hz en lager is er geen verschil in da/dN meer merkbaar.
De schuine scheur blijkt ook een aanzienlijke invloed te hebben op de kritische K waarde, die gevonden wordt in een K_{Ic} test. Aangezien meestal shear lips voorafgaan aan het uiteindelijk bezwijken heeft dit belangrijke consequenties voor de veiligheid en levensduur van een constructie.
Van praktisch belang is verder dat het onderzoek aangeeft dat in scheurgroeivoorspellings modellen rekening moet worden gehouden met de breukmode (recht of schuin). Verder is informatie over shear lips van belang voor de fractografie. Het geeft aanvullende informatie over de redenen cq oorzaken van falen van op vermoeiing belaste constructies.

Contents:

Nomenclature

a	= half crack length in a center cracked tension specimen (mm).
a_0	= half initial crack length.
a_c	= half critical crack length.
c	= Paris coefficient or a constant.
c_1 ,c_2 ,c_3	= constants.
da/dN	= the crack length increase per cycle (μm/cycle).
$(da/dN)_{10}$	= da/dN at 10 mm after the start of the constant ΔK test.
$(da/dN)_{eq}$	= da/dN in the (stable) equilibrium situation.
$(da/dN)_{tensile}$	= da/dN in the (often unstable) tensile mode.
Δa	= a crack length interval.
ΔK	= K_{max} - K_{min}
ΔK_{eff}	= effective ΔK = K_{max} - K_{cl}
ΔN	= the number of delay cycles.
ΔS	= S_{max} -S_{min}
f	= frequency of the fatigue cycles (Hz).
K	= stress intensity factor (in MPa$\sqrt{m}$).
K_c	= the critical stress intensity factor.
K_{cl}	= the value of K where the crack is just closed.
$K_{eq,m}$	= the mean equivalent stress intensity.
$K_{I,m}$	= the mean mode I stress intensity.
K_{Ic}	= the valid critical plane strain stress intensity factor.
K_{max}	= maximum value of K during a cycle.
K_{min}	= minimum value of K during a cycle.
K_{op}	= the value of K where the crack is just fully open.
ℓ	= transverse crack length (mm).
m	= Paris exponent.
n	= reduction number.
N	= the number of cycles.
OL	= overload.
P	= load (in kN)
P_{max}	= maximum value of the load during a cycle.
P_{min}	= minimum value of the load during a cycle.
R	= load ratio = P_{min}/P_{max} = K_{min}/K_{max}
S	= value of the stress during a cycle (MPa)
S_{max}	= maximum value of the stress during a cycle.
S_{min}	= minimum value of the stress during a cycle.

t	= specimen thickness (mm).
t_s	= shear lip width (mm).
$t_{s,eq}$	= equilibrium shear lip width.
t_t	= width of tensile part of the crack surface.
U	= $\Delta K_{eff}/\Delta K$.
UL	= underload.
w	= specimen width.

About the Author

The author is employed by the Technical University of Delft as assistant professor since 1971. After a graduate study in metallurgy, on the diffraction contrast of antiphase boundaries in Cu_3Au in the transmission electron microscope, he teached and did research in fast deformation loading, plasticity and texture of metals. Since 1982 he teaches and does research in the field of fracture mechanics and fatigue (crack growth) of several materials.

1. Introduction

1.1. Introduction

The growth of fatigue cracks in plate and sheet material occurs in various structures. The fatigue load can have the character of constant-amplitude loading, sinusoidal in many cases, which is the more simple type of a fatigue load. However, in many practical situations the load history in service has a variable amplitude character. It is a well recognized technical problem how to predict the growth of fatigue cracks under constant amplitude and variable amplitude loading.

The possibilities for predictions of fatigue crack growth have been considerably improved by the introduction of the stress intensity factor K. Especially for constant amplitude loading, the literature seems to suggest that such predictions are possible for design problems, provided that the K factor can be calculated. In addition, the relation between the crack growth rate (da/dN) and the cyclic variation of the stress intensity factor (ΔK) must be available for the material under consideration. For variable amplitude loading the situation is more complex, but also for that problem the stress intensity factor is generally considered to be an essential tool for the analysis of the problem.

As a consequence of the above problem setting, the application of fracture mechanics to fatigue crack growth prediction has seen an extensive evolution. Our ability to calculate stress intensity factors for various geometries has been developed considerably, notable by various calculation techniques now possible on modern computers. The basic fatigue crack growth resistance in the format of da/dN - ΔK relations has been determined experimentally for many materials. If such a relation is not available, experimental techniques are well known and documented in standards. The remarkable "paradox" of the development is that many analysts have paid little attention to the fatigue crack growth phenomenon as it occurs in plate and sheet materials. In fracture mechanics it is simply assumed that cracks are perfectly flat and growing in the so-called mode I, i.e. in a plane perpendicular to the direction of the main principal stress (i.e. perpendicular to the loading direction if the fatigue load is cyclic tension). Unfortunately, this is not always true. A slowly growing fatigue crack in a plate is largely growing in the "tensile mode", but at both surfaces of the material

"shear lips" are frequently observed, see figure 1.1. It is obvious that such shear lips imply that the crack front is no longer a straight line. It is also not a curved line in a plane perpendicular to the loading direction. In the latter case, it still would be a mode I crack. Shear lips imply that the fatigue crack growth occurs in a mixed mode (I+III).

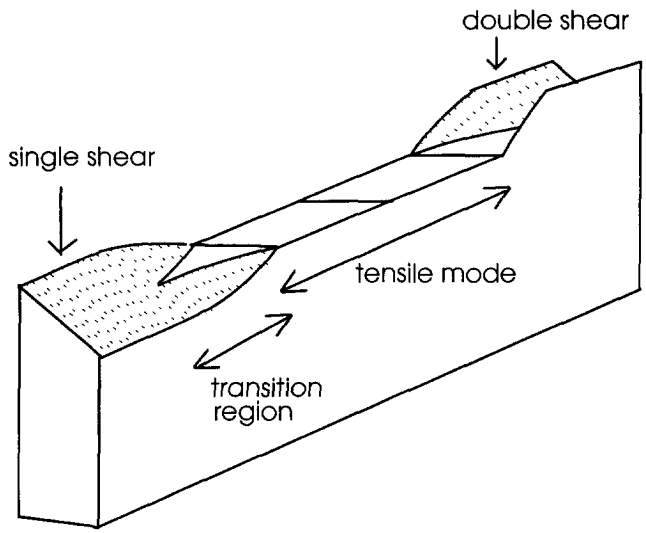

Figure 1.1. Schematic drawing of the development of shear lips in a constant amplitude test on a center cracked plate.

The shear lips have received some attention in the literature. Frequently it is associated with a plane stress situation at the surface, whereas in the center of a plate the predominant state of stress will be plane strain. Actually, until now it is not well understood why shear lips occur or why in other cases they do not. Moreover, shear lips need some crack growth to develop to a larger size. As will be shown in the present study, the shear lip width is not a single function of the cyclic stress intensity. It also depends on how fast a crack is growing. For that reason many tests in the present investigation have been done under a constant ΔK cyclic load in order to let the crack grow until a stable shear lip width is obtained. Besides that shear lips do also depend on the environment and/or the frequency. The frequency effect is also investigated.
The shear lips also have consequences for crack growth under variable-amplitude loading, another problem covered in the present study.

1.2. Scope of this thesis

The essential phenomenon studied in this work is the development of shear lips and the consequence of shear lips for crack growth predictions.
The contents of the thesis are as follows:

In chapter 2 basic aspects of fatigue crack growth are introduced. Shear lip development and slant crack growth are defined. Attention is paid to the concept of crack closure and of crack growth resistance.

Chapter 3 gives a discussion of some general measurement methods used. Where needed, more specific measurement techniques are discussed in the appropriate chapters.

Chapter 4. In this chapter a large amount of experimental observations on shear lip development is presented. A number of measurement techniques are used in measuring the shear lip width. Two thicknesses of Al 2024 T351 plate (unclad) are chosen to account for possible thickness effects. Most of the tests are performed at constant ΔK and R as this is the only possible manner to find the steady state behaviour of shear lips.
Attention is also paid to the shear lip behaviour under constant amplitude loading and to the effect of shear lips on da/dN.
An important variable in the shear lip development is the frequency. The majority of the tests have been done at 10 Hz. A number of tests have been performed at other frequencies.
At the end of this chapter some attention is paid to results of static tensile tests. Some differences between these fracture surfaces and fatigue fracture surfaces will be discussed.

Chapter 5 presents a model for predicting slant fatigue crack growth rate, when the rate in the tensile mode is known. Based on the model the da/dN versus a for constant amplitude tests at different R ratio's, thicknesses and frequencies can also be predicted. An explanation for the observed temporary decrease of da/dN in some constant amplitude tests is given.

Chapter 6. Tests with large numbers of underloads are performed. Larger numbers of underloads, large enough to give rise to shear lips, give rise to retardation effects comparable with the effects of overloads.

Chapter 7. A pulsed direct current potential drop method is applied to measure the crack closure level in fatigue crack growth tests on Al 2024 at different R values. In principle the measurement method allows finding the R level above which no closure occurs ($\Delta K_{eff} = \Delta K$). The resulting closure equations are compared with well-known closure relations for Al 2024 from the literature.

Chapter 8. The thesis is completed with a general evaluation of the significance of shear lips and a number of conclusions.

2. Growth of Fatigue Cracks

2.1. Introduction to Metal Fatigue

About a hundred years ago discussions were taking place on the fracture of wrought-iron railway axles. It was generally accepted that the failures were a consequence of the cyclic nature of the loading. There was also agreement about the crystalline appearance of the fracture faces. The problem was defined as metal fatigue, a fracture phenomenon caused by repeated loading. It is the most common cause of failures in service [1].

Although around 1920 it was known that fatigue failure is a progressive and localized process, involving both initiation of a crack and its progressive growth, there was no general acceptance of the fact that fatigue consists of crack initiation and growth. This led to considerable confusion about the nature of fatigue. For a long time fatigue was considered as a gradual deterioration of a material subjected to repeated loads.

Since the mid-1950s there has been considerable interest in the growth of fatigue cracks, an interest stimulated by the realization that fatigue crack growth can comprise a significant part of the fatigue lifetime of a cyclically loaded structure. The treatment of this subject has been advanced by developments in the field of fracture mechanics, the introduction of servohydraulic test systems, and the availability of transmission and scanning electron microscopes for fractographic examination.

In the 1950s metallurgists were actively developing fractography. In the case of fracture surfaces created by a fatigue crack, line markings termed striations were seen on the fracture surface in an electron microscope. The striations indicated the position of the crack tip in successive load cycles. The striation spacing could be shown to be equal to the local increment of growth in one stress cycle. On a macroscopic scale other line markings, termed beach markings, were found, indicating changes of the cyclic load. Further work elucidated the mechanisms of striation formation and fatigue crack growth. Plastic deformation at the crack tip

changes the geometry of the tip during each load cycle. The nature of the fatigue crack growth mechanism means that theories cannot be based simply on the accumulation of 'damage' in the material. The growth mechanism of alternately blunting and resharpening of the crack tip explains why cracks can grow under cyclic loads too low to cause failure under a single load application. Although striations are not always observed, it is generally accepted that cracks grow by the same basic mechanism except that growth is not necessarily continuous along the whole crack front.
A rigorous definition of metal fatigue is difficult. In reference [2] it is defined as:" Failure of a metal under a repeated or otherwise varying load which never reaches a level sufficient to cause failure in a single application."
Perhaps the most significant advance in metal fatigue during the past decade is the general realization that most structures contain crack-like defects which are either introduced during manufacturing (especially in case of welding), or form early in service. Thus virtually the whole life of the structure is occupied by fatigue crack growth from flaws. An understanding of fatigue crack growth is therefore essential for the understanding and prediction of fatigue behavior of many structures.

Ever since the optical microscope was used for fatigue studies, it became clear that the fatigue process had to be associated with cyclic microplasticity. A much better picture was obtained after the electron microscope became available, although macroscopic observations are still important. Some relevant observations are:

- If a finite fatigue life applies, microcracks are initiated early in the fatigue life.
- In several materials (sub)microscopic crack extension occurs in every load cycle. If the crack extension in a load cycle is large enough, it can leave a ridge of microscopic plastic deformation on the fracture surface (a striation). The striation spacing indicates the local crack growth rate (μm/cycle).
- Usually, fatigue cracks do not produce visible macro-plastic deformation.
- The fatigue crack shows a tendency to grow perpendicular to the main principal stress, in general perpendicular to a tensile load direction. A noteworthy exception occurs in thin sheet material, discussed later.

The fatigue process is usually divided into three stages: crack initiation, crack propagation to a critical size and unstable fast fracture. If cycling occurs at a low stress amplitude with an expected fatigue life of 10^6 cycles or greater, the major

part of the life is consumed by crack initiation and early stages of crack propagation. At higher stress amplitudes, when the expected fatigue life is from 10^3 to 10^5 cycles or less, the major part of the life is spent in crack propagation. Thus the fatigue life is usually divided to cover two main phases:

1. Crack initiation period.
2. Crack growth period.

For engineering purposes, predictions for the two periods should be made separately. The definition of the end of the second period appears to be simple. It is the occurrence of the quasi-static failure of the remaining uncracked cross section in the last cycle of the life. However, the transition from the first to the second period is more problematic. The crack initiation period is supposed to include microcrack growth until some macrocrack is present. This transition of a microcrack to a macrocrack does not easily lead to a quantitative definition. Three suggestions were made by Schijve [3].

(i) The transition is characterized by the fact that a macrocrack is a visible crack, whereas a microcrack is still invisible.

(ii) A second approach is based on the fact that microcrack growth still depends on the material surface conditions, whereas a macrocrack depends on the crack growth resistance of the material as a bulk property.

(iii) The last suggestion starts from the idea that the stress intensity factor is not yet meaningful for a microcrack, whereas ΔK can be used for macrocracks. None of these definitions leads to a straightforward quantitative definition of the beginning of the crack growth period. It should be pointed out here, that in the present investigation visible cracks are considered, where application of fracture mechanics is justified. Moreover, through cracks are studied only. For sheet materials through cracks are important, especially in thin skin structures, such as used in aircraft.

If a crack is growing perpendicularly to a cyclic tensile load, the crack is opened perpendicular to the plane of the crack, i.e. perpendicular to the fatigue fracture surface. This is called mode I crack opening.

According to the theory of fracture mechanics, crack surface displacements are possible in three different ways, as shown in figure 2.1. Viewed macroscopically, cracks in isotropic materials under essentially elastic conditions tend to grow in Mode I under both static and fatigue loading, irrespective of their initial orientation [2]. This can at best be regarded as a useful generalization based on observation, and it is not a general rule. The mode I crack growth is sometimes used, assuming elastic behavior, as a test of isotropy; or, assuming isotropy, as a

test of essentially elastic behavior [4]. An equivalent consideration is the criterion of local symmetry.

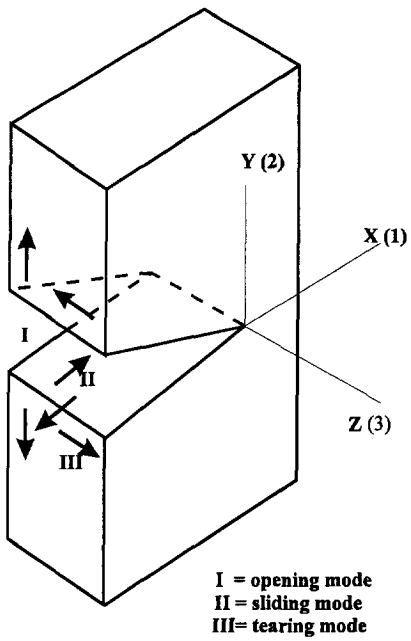

Figure 2.1. Three modes of crack loading.

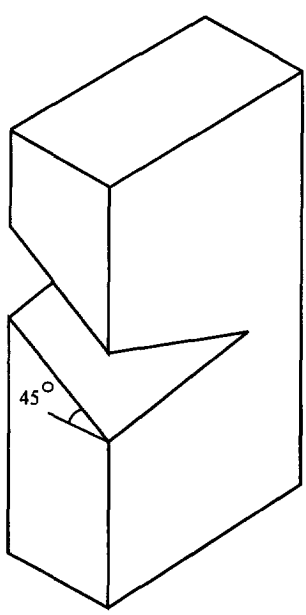

Figure 2.2. Slant crack growth.

This criterion implies that it is self-evident that a crack tends to grow such that the crack tip stress field becomes symmetrical [5]. The main exceptions to mode I growth are when a crack follows a plane of "material weakness", or when a crack grows on planes at 45 ° through the thickness. The latter slant crack growth usually occurs in thin sheets and is sometimes called shear mode crack growth, because the growth is on the planes of maximum shear stress in an uncracked plate (figure 2.2). Crack propagation then occurs in a combination of mode I and mode III. Slant crack growth is addressed in section 2.5 of this chapter.

2.2. Crack Growth Rate and the Paris Relation

As was already stated, the application of fracture mechanics principles to fatigue permits separate consideration of a crack initiation stage, and crack propagation and final failure stages. In many engineering applications, crack-like defects exist when the component is put into service, eliminating the initiation part of the fatigue life. Crack propagation behavior then becomes the most important damage regime in developing fatigue life predictions. Normally, in a fatigue (crack growth) test the crack length (a) and the associated number of cycles (N) are recorded. The crack growth rate is defined as the crack increment per cycle da/dN.

A typical fatigue crack propagation curve is shown in figure 2.3.

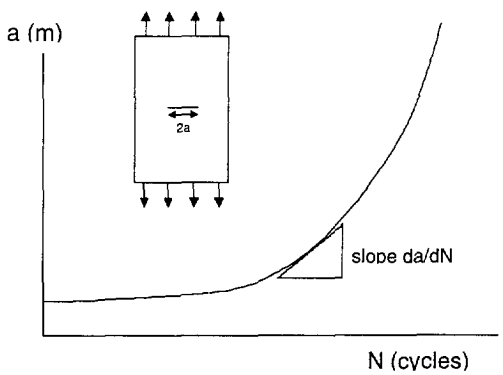

Figure 2.3. Typical fatigue test result.

Figure 2.3 shows a crack growth curve as it can be obtained for a center cracked tension specimen under a cyclic load with a constant S_{max} and S_{min} (also called a constant ΔS test, $\Delta S = S_{max} - S_{min}$ or a constant amplitude test). The slope of the curve gives the crack growth rate da/dN. The cyclic stress implies a cyclic stress intensity factor K for the crack tips with $\Delta K = K_{max} - K_{min}$.

It was found that da/dN could be correlated by the stress intensity factor K as defined in fracture mechanics. That means that different geometries show about the same da/dN when the same ΔK is applied. In other words, the same ΔK-cycle will always produce the same crack growth rate da/dN (= f(ΔK)).

Paris [6] found a linear relation between da/dN and ΔK on a log-log scale for intermediate crack growth rates, which implies:

$$da/dN = c\,\Delta K^m \qquad 2.1$$

The equation is frequently referred to as the Paris relation or Paris law. The Paris law is a simplification, because other influences are not explicitly considered. These influences were thought to be secondary to the ΔK effect and as a consequence they were neglected. The stress ratio effect (effect of R, $R = S_{min} / S_{max}$) was supposed to be also a secondary effect, but later experiments have shown that the R-effect is significant for many materials.
For low and high crack growth rates deviations from the power law occur. There are two vertical asymptotes in a da/dN-ΔK diagram. The lower one, $\Delta K = \Delta K_{th}$, indicates that a minimum ΔK is required for fatigue crack growth. The upper one is a consequence of static failure if K_{max} is large enough to cause immediate failure ($K_{max} = K_{critical}$ = "fracture toughness"). In the middle regime of figure 2.4 the Paris relation represents the crack growth behavior rather well. Fortunately, this regime is relatively large for many technical materials, which implies that the power law can be used in algorithms for crack growth predictions.

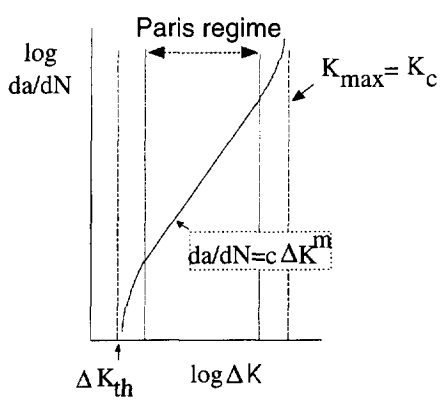

Figure 2.4. Fatigue crack growth rate as a function of ΔK.

2.3. Crack Driving Force and Similitude

As mentioned in the previous section, the crack growth rate da/dN can be correlated by ΔK. ΔK can be considered as the crack driving force. This driving force has to overcome the resistance of the material against cracking. If a crack grows, it is as a consequence of a variation in K.
The correlation of ΔK and da/dN was a very important discovery. It means that for every structure the crack growth rate can be predicted if the K factor for this structure is known and if a da/dN - ΔK relation can be found for the material. If it is not available, it can be obtained by measurements on a standard specimen with a known K versus crack length relation.

The application of $da/dN = f(\Delta K)$ is known as the similitude approach, with ΔK as a similitude parameter. The approach is defined as [7]: "similar conditions applied to the same system will have similar consequences".
More specifically, "a similar K-cycle applied to a crack in a standard specimen and to a crack in a structure of the same material, will induce the same crack length increment in both cases".
This rule seems logical and physically sound enough, but careful examination is needed to assure that similar conditions do indeed apply. In the case of fatigue crack growth it is often found that besides ΔK the crack growth rate also depends on the frequency, the loading cycle shape, the temperature, the mean stress , the fracture mode and in general the load history during crack growth. If these conditions are not satisfied, the similitude can be adopted only if these variables do not affect the crack extension mechanism. The same system obviously includes a similar fatigue crack geometry in the same material with the same material structure and heat treatment. Moreover, it also includes the same material thickness in view of having the same state of stress. *One important aspect of our problem, which is the subject of this thesis, is easily recognized. A crack with shear lips or a fully slant crack does not have the same crack tip geometry as a flat pure mode I crack.*

2.4. Fatigue Crack Closure

One of the problems encountered with the similitude approach is the dependence of da/dN on the stress ratio (see section 2.2).
For many materials (but not for all) different crack growth rates are obtained at the same ΔK for different values of the stress ratio R ($R = S_{min} / S_{max} = K_{min} / K_{max}$). A solution for this problem was found by Elber [8]. He discovered that

fatigue cracks are closed for a significant portion of a tensile load cycle, owing to residual plastic deformation left in the wake of a growing crack. He introduced an effective ΔK, which is the K variation during which the crack is fully open. By using a relation, experimentally found, between ΔK_{eff} and the stress ratio R, he was able to fit da/dN - ΔK curves at various R values into a narrow scatterband. The similitude concept could be restored by using da/dN and ΔK_{eff} instead of da/dN and ΔK.
The closure phenomenon is considered to be involved in several other fatigue crack growth phenomena, such as the R ratio effect on fatigue crack thresholds; differences in crack growth rates in vacuum, air, humid gas, hydrogen and corrosive environments; effects of microstructure that contribute to crack path tortuosity; retardation due to overloads; effects of underloads and acceleration of short cracks.
Since Elber's discovery, hundreds of papers have been written on this subject. Closure has made the application of the similitude approach more difficult. A prediction of da/dN in a cracked structure not only demands that the K applied to the structure is known, but also the previous history of K as a function of the crack length should be known. The amount of crack closure depends on the K history of the previous load cycles. Although models have been developed to predict the variation of crack closure for an arbitrary K history, the problems involved are difficult, and several assumptions are necessary.

For loading situations with a slowly changing K (low dK/da), the situation is less difficult, since standard relations as presented by Elber [8] or Schijve [9] can be adopted to calculate ΔK_{eff} (see chapter 4, equations 4.6 and 4.10 respectively).

However there are still conflicting ideas about the existence of plasticity induced closure in a plane strain situation [10,11,12]. The cause probably is that accurate measurement of crack closure is very difficult and that the result strongly depends on the techniques used [13,10]. Usually less crack closure is measured in a thicker material (more plane strain) than in a thin sheet.
Elber performed his closure measurements in a loading situation where shear lips are normally present. He performed direct measurements of the value of K-opening or K-closure (K_{op} and K_{cl}). He showed that the empirical relation, between ΔK_{eff} and R was able to shift all da/dN - ΔK curves, at different R values, into one scatterband. For ΔK_{eff} he used K_{max} -K_{cl} or $\Delta K_{eff} = U(R)\ \Delta K$, with $U(R) = 0.5 + 0.4\ R$.

It is generally believed that a plane stress situation is a necessary condition for the development of shear lips. Thus if there are shear lips the stress situation is by definition plane stress. If there are no shear lips we do not know the stress situation. Thus the existence of shear lips is an indication for a plane stress situation and Elber's crack closure formula is strictly only valid for a plane stress situation with shear lips. The results of Elber are certainly not a proof for the existence of crack closure under plane strain conditions.

Schijve [9] found his ΔK_{eff} relation by correlating da/dN values , obtained in tests with different R - values, with different quadratic (in R) formulas for ΔK_{eff} until one scatterband was reached. He performed no direct closure measurements. However, Schijve used test results with and without shear lips for the correlation. It is reasonable to assume that plane strain implies a situation without shear lips, but a situation without shear lips is *not* necessarily a plane strain situation (although it will often be the case). However let us assume for the moment (for simplicity) that a plane strain situation is a situation without shear lips and that the reverse is also true; this means: a situation without shear lips is plane strain. Thus (flat) tensile mode and plane strain are equivalent concepts. Then the results found by Schijve can be a proof for the correctness of the closure relation and for the existence of closure also in plane strain.
The existence of closure under plane strain conditions may then be clear from the following reasoning. Suppose that the tensile mode situation (thus without shear lips) does not lead to crack closure. All curves for different R values will then show an excellent correlation with ΔK in the tensile mode area, because there is no R effect, and thus not with ΔK_{eff} , when for ΔK_{eff} the standard relation of Schijve is used.
Suppose also that the shear lips have an enhancing effect on crack closure and that Schijve's relation correlates da/dN values in this area with ΔK_{eff} . The overall result will be a da/dN - ΔK_{eff} figure with a lot of divergence in the lower, tensile mode regime and a high correlation in the higher, shear mode regime. This was not found by Schijve, which leads to the conclusion that also in the lower da/dN range crack closure is present. However, the present author found some divergence in the tensile mode regime and convergence for the shear mode regime. This is shown in figures 2.5 and 2.6 for 8 constant amplitude tests at 10 Hz with R ratios ranging from 0.1 to 0.7. In this R-range the crack closure relations of Elber and Schijve show about the same result.
A new crack closure model was developed by the author [14]. The crack closure stress was calculated for each crack length for the eight tests shown in figures 2.5

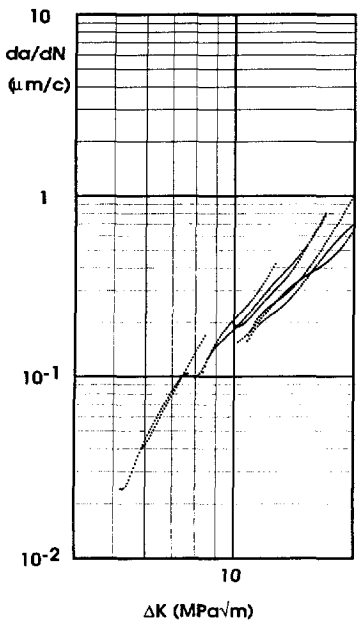

Figure 2.5. da/dN versus ΔK as measured.

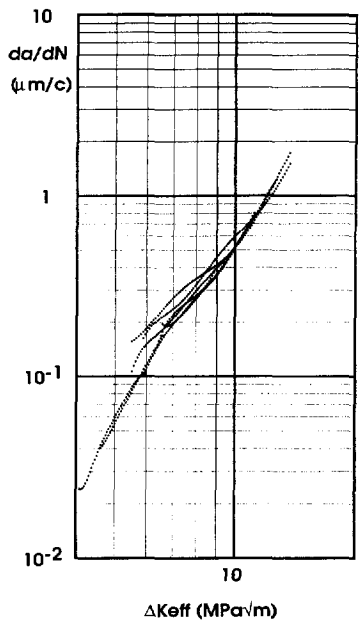

Figure 2.6. da/dN versus ΔKeff using the crack closure relation of Elber.

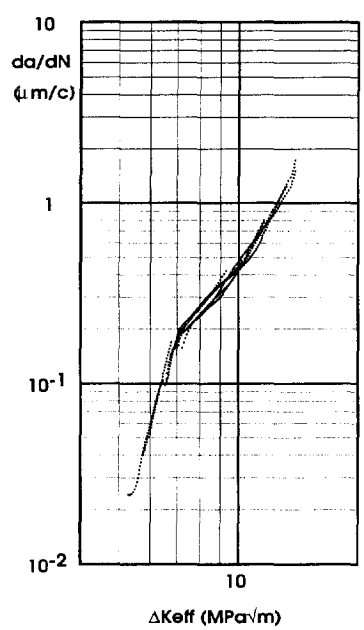

Figure 2.7. da/dN versus ΔKeff using a crack closure calculation model

and 2.6. Then the da/dN results, experimentally found, were plotted against the ΔK_{eff} calculated from the closure stresses. The results are shown in figure 2.7. The results in the figures 2.5, 2.6 and 2.7 show that the closure behaviour is (somewhat) different in the plane strain and plane stress areas.
Although Elber found his empirical relation between ΔK_{eff} and the nominal ΔK for crack growth occurring in the shear mode , his crack closure formula is able to reasonable correlate da/dN - ΔK data for different R values in the tensile mode area. Schijve [3] proved that when there is a satisfactory correlation between da/dN and ΔK_{eff} (= U(R) ΔK, with U(R)= a +bR + cR^2), exactly the same correlation will be found for: $\Delta K_{eff}{}^{*}$=q U(R) ΔK = U(R)* ΔK. This result implies that the ratios of the coefficients of the U(R) and U(R)* are the same, i.e. a/b/c= qa/qb/qc.

Thus if a good correlation is found for crack growth in the tensile mode as well as in the shear mode, the conclusion is *not* that crack closure is the same in the tensile mode and the shear mode parts. When the same correlation is found for tensile and shear mode parts, the ratio's of the coefficients of the quadratic crack closure function will be the same in both areas, but it is very likely that the total amount of closure in both area's will be different. This means that the absolute values of the coefficients are different. (more about this topic in chapter 4, section 4.2.5.).

A weakness of the approaches used by Elber and Schijve is the assumption that crack closure is responsible for all load ratio effects, and that the crack closure ratio U = ΔK_{eff} / ΔK is a function of R alone.
Moreover, Schijve's (and also Elber's) formula can also correlate da/dN in other environments and at other frequencies [15].
It is assumed that there is no dependence of K_{cl} of the environment, when tests on Al - 2024 in vacuum, air and artificial seewater are compared [16,17].

The good correlation in other environments means also that the ratios of the coefficients of the closure function U are environmentally independent. The fact that K_{cl} was found to be independent of the environment is a strange result, because it contradicts the findings that the shear lip width depends on the environment, see next section, where greater shear lip width (or slant growth) is associated with more closure [18,19,20,21], and thus a higher K_{cl} . An explanation of this inconsistency will be given in chapter 7.
The conclusion is that closure relations like that of Elber and Schijve can

correlate da/dN - ΔK results from constant amplitude tests at different R ratios. The correlation is valid both in the plane strain area and in the plane stress area, and also in different environments and at different frequencies.

The above considerations are related to plasticity induced crack closure as found in many metals and metal alloys. The conclusion is not necessarily true for other (non-metals) materials. Exceptions are found for completely elastic, non ductile, ceramic materials and for very ductile polymers.
The work of Suresh [22] in ceramics has shown that closure-like behavior can occur without the effects of wake plasticity, which is assumed to be responsible for crack closure in ductile materials. Another non-closure mechanism will be responsible in this case.
A reversed R effect , meaning that a higher R leads to a lower da/dN, has been found in some polymers. A clear effect of the stress ratio R on the fatigue crack growth rate was measured, while the crack was macroscopically open during the whole test [23].
In the literature other mechanisms leading to crack closure with $\Delta K_{eff} < \Delta K$ have also been reported, such as surface roughness induced crack closure, fiber bridging, oxide induced crack closure, etc. The material used in the present investigation is a reasonably ductile Al-alloy (2024-T351). For this material plasticity induced crack closure under plane stress conditions cannot be ignored. Very recently, in reference [13] a mathematical analysis using dislocation theories has been performed to show that plasticity induced crack closure does not exist, except if shear lips are present.
However, the mathematical analysis only applies to constant amplitude tests or tests with a low dK/da. The existence and role of closure after overloads cannot be denied. So the possible absence of closure in plane strain and in plane stress without shear lips will not have a dramatic influence on crack growth predictions based on closure.
When variable amplitude test results are compared with results from constant amplitude tests caution is needed, because the fracture mode is often not the same. The similitude concept can now break down.

2.5. Slant Crack Growth and Shear Lips

introduction:
In thin sheets a transition from mode I crack growth to slant crack growth is often observed. It is an exception to the generalization that crack growth tends to take place in mode I. The major features of the transition are shown in figure 2.8.

After the transition crack growth occurs in a mixture of modes I and III, but in calculations it is usual to treat it as if it still happens in mode I. The transition to slant crack growth originates in the development of shear lips which increase in width until they reach a material dependent maximum size [24]. In sufficiently thin specimens the shear lips meet at midthickness, which completes the transition to full slant crack growth.

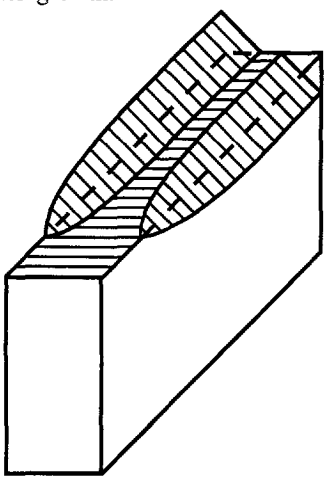

Figure 2.8. Development of (single) shear lips.

In (static) fracture testing the transition from the tensile mode to the shear mode is reasonably predictable, as it is related to the relative dimensions of the monotonic crack tip plastic zone and the plate thickness [25]. Under cyclic loading the process appears to be more complicated [26]. The transition usually starts when a critical value of da/dN or ΔK_{eff} for a given material and thickness is exceeded [27,28,29,30,31]. Investigations on Al 2024 T3 and Al 7075 T6 have shown that the change in fracture mode starts at a critical rate of growth of the order of 0.01 μm/cycle. The completion of the transition occurs at higher values (about 1 μm/cycle) [32,33,34], depending on the material thickness [30,35]. The transition can be reversed by reducing the cyclic load level [36].
At this moment the only generalizations that can be made with reasonable confidence are that the attainment of a critical value of ΔK_{eff} (or da/dN) is a necessary condition for the appearance of shear lips, and a state of plane stress (at the maximum load in the fatigue cycle) is a necessary condition for completion of the transition, but neither condition is by itself sufficient [37].
The mechanisms responsible for the transition to slant growth in thin sheets are not clear, although the actual crack growth mechanisms (by striations) are the same as in mode I fatigue crack growth [37,38,39].

An argument against the association of shear lips with a plane stress situation is the observation that higher R values promote tensile mode crack growth [40]. In chapter 4, section 4.5, of this work it will be shown that the start of shear lips is not dependent on K_{max} , whereas normally the plane stress situation is assumed to depend on K_{max} .
Shear lips often show up on fracture surfaces of thin sheets and are sometimes thought to result from general out-of-plane sliding which allows an antiplane strain (K_{III}) mode of fracture to operate. This seems to occur easily in thin sheet (tensile) specimens, because of elastic crack edge buckling (out-of-plane displacements), which develop into concentrated shear on 45 ° planes [38]. However, the fact that shear lips are also present in thick specimens rules out buckling as a major cause. In reference [37] it is stated that a possible explanation of the transition is that the development of shear lips is an instability effect.

effect of shear lips on da/dN:
Forman et al.[27] observed an effect of the fracture mode on da/dN. They suggested that two independent equations of the same basic form (power law) were needed to describe the da/dN - ΔK behavior, one covering flat fracture, and a second one for shear mode cracking.
The present author and his co-workers [41] introduced the constant ΔK test to study shear lip behavior and crack growth rate during growth of shear lips. This type of test is the only test to get reliable quantitative information on both shear lip width and associated da/dN behavior (see chapters 4 and 5). A decrease of about a factor 3 in da/dN was found for crack growth in Al 2024 going from a tensile situation to a situation of complete shear. This was later confirmed by Ling and Schijve [42], who found a decrease with a factor 3 to 4. They also performed constant ΔK tests. In their investigation the da/dN decrease was found from fractographic measurements of striation width.

thickness dependence:
The transition can lead to a thickness dependence in fatigue crack growth behavior [43]. Indications were obtained that the effect of sheet thickness on da/dN mainly occurs in the transitional area [44,45]. No thickness effect on da/dN is found for cracks in the tensile mode [46], see chapter 5 for more on this topic.

effects of frequency and environment:

Shear lips are often associated with plane stress conditions which exist at free surfaces even of thick specimens. This cannot be the only explanation because environmental effects are also reported. The transition from a tensile mode to a shear mode fracture in Al 2024 and Al 7075 depends on the environment. A more aggressive environment shifts the transition to higher values of ΔK [47,48]. Similar indications are reported for steels in air and seawater. In seawater no transition was observed for the ΔK range which produced fracture mode transition in air [49].
At least part of the environmental or frequency influence on da/dN in Al alloys can be associated with the presence of shear lips. Before the transition is completed, different values of the crack growth rate in dry and wet air are found, while above this point there is no effect left [50]. The same effect has been found for crack growth in Titanium in air and salt water [51].

practical relevance:
The width of shear lips and their growth would only be of scientific interest if there were no effects on the crack growth rate. Some authors found higher crack growth rates due to shear lips [19,37,52,53], while others found just the reverse with a decrease in da/dN by a factor of 2 to 3 [30,39,54,55,56].
In most tests constant amplitude loading was used. For this type of test it is difficult to estimate the effect of shear lips on da/dN. The authors who found higher growth rates, did so on the basis of different slopes of the log(da/dN)-log(ΔK) lines below and above the (end) transition point. After the transition had ended the slope was found to be higher than before.
The same result was found by the present author. In chapter 5 it will be shown that the slope in the transitional area is lower than beyond the transition point. However, this fact does not mean that shear lips have an accelerating effect on da/dN, but rather that they have a retarding effect on da/dN in the transitional area.
The significance of the transition from an engineering point of view is twofold [57]. First, as was already mentioned, it may cause a change of the slope in the log (da/dN) - log (ΔK) relationship [27,43,54,56]. Secondly, if shear lips are present, the R ratio sensitivity under constant amplitude conditions increases. Under variable amplitude loading the effect of the load sequence will be much more important when shear lips are present, because the effect of crack closure is much larger when shear mode growth occurs [18,58,59].
Although shear mode crack growth is observed in laboratory specimens, this behavior is rarely observed in cracks in general engineering structures. An

exception is found for aerospace structures, although also here the shear lip width development is much more limited. This means that the load sequence under random loading is less important than might be supposed from the results of laboratory tests involving isolated overloads. Historically the majority of crack growth rate data have been generated under constant amplitude conditions. Because of the simplicity of the tests it is expected that this will not change in the future. Therefore the need remains for a method capable of predicting crack growth in different geometries using data generated in a constant amplitude test.

2.6. Crack Growth Resistance

The crack growth resistance is defined as the resistance of the material to the growth of cracks. In the case of fatigue the da/dN - ΔK curve can be considered as a measure of crack growth resistance. The material response to the crack driving force ΔK is da/dN.

An equivalent definition can be found in reference [2]. Here the crack growth resistance is defined as $(da/dN)^{-1}$, that is the number of cycles dN needed to get a crack extension da. A low value of $(da/dN)^{-1}$, represents a low resistance, a high value a high resistance.

In this work the resistance is defined in a more physical way.

Following Griffith and Irwin [60] the crack growth resistance is supposed to be mainly the energy that is needed for the introduction of new crack surfaces (surface energy term) and for plastic deformation accompanying the crack growth. For ductile materials the surface energy can often be neglected in comparison to the energy involved in the plastic deformation accompanying fatigue crack growth.

For an accurate description of the effect of shear lips on da/dN behavior, the effects of shear lips on both the crack driving force and on the crack growth resistance have to be considered. It is very difficult to separate these effects, because normally only the sum of both effects (for example the resulting da/dN) is measured. However, the crack driving force can be calculated.

Recently three dimensional finite element calculations [61,62] were performed on the stress intensity distribution in center cracked plates. A decrease of about 40% in K_I was found when a complete single shear situation is compared with a tensile situation. Even so, a translation of this result to fatigue crack growth is difficult, because we not only have to consider crack growth resistance, but often also crack closure as an extra complicating factor.

The conclusion is that the crack growth resistance cannot be calculated or measured independently. There is always a need for a driving force to get a

resistance, thus the measured effects result from both.

2.7. References

1. A.S. Tetelman and A.J. McEvily, Fracture of Structural Materials, p. 347, John Wiley & Sons, New York, 1967.
2. L.P. Pook, The Role of Crack Growth in Metal Fatigue, The Metals Society, London, 1983.
3. J. Schijve, Engng Fracture Mech., Vol.11, 1979, pp. 167-221.
4. B. Cotterell, Int J. Fract. Mech, 1965, 1, pp. 96-103.
5. R.V. Goldstein and R.L. Salganik, Int. J. Fract., 1974, 10, pp. 507-523.
6. P.C. Paris and F. Erdogan, Trans. ASME, J. Bas. Eng., 1963, 85, (4), pp. 528-553.
7. J. Schijve, Four Lectures on Fatigue Crack Growth, Delft University of Technology, Department of Aerospace Engineering, Report LR-254, October 1977.
8. W. Elber, Fatigue crack closure under cyclic tension, ASTM STP 486, pp.230-242 (1971).
9. J. Schijve, Engng Fracture Mech. 14, pp. 467-475 (1981).
10. T.C. Lindley and C.E. Richards, Materials Science and Engineering, 14, 1974, pp. 281-293.
11. H.R. Shercliff and N.A. Fleck, Fatigue Fract. Engng Mater. Struct., Vol. 13, No 3, pp. 287-296, 1990.
12. J. Weertman, Phys. Stat. Sol. (b) 172, 1992, pp. 27-40.
13. N. Louat, K. Sadananda, M. Duesbury and A. K. Vasudevan Metallurgical Transactions A, Vol. 24A, October 1993, pp. 2225-2232.
14. J. Zuidema, A calculation of the effective ΔK under various fatigue loading conditions, in Proceedings of ECF 9. Conference pp 391-396 ,Varna, Bulgaria, 1992.
15. J. Zuidema, P.J.M. Mense and R.A.H. Edwards. Engng Fracture Mech. 26, 1987, pp. 349-356.
16. H.L. Ewalds, Engng Fract. Mech., Vol 13, 1980, pp. 1001-1007.
17. J. Schijve and W.J. Arkema, Crack Closure and the Environmental Effect on Fatigue Crack Growth, report VTH - 217, Department of Aerospace Engineering, Delft University of Technology, 1976.
18. H.L. Ewalds and R.T. Furnee, Crack Closure along the Fatigue Crack Front of Center Cracked Specimens, Second European Colloquium on Fracture (ECF 2), Darmstadt, October 9 - 11, 1978, pp. 349-360.
19. G. Marci and P.F. Packman, Int. J. Fract, Vol. 16, No2, 1980, pp. 133-

153.

20.J. Schijve, Fatigue Crack Closure: Observations and Technical Significance, Mechanics of Fatigue Crack Closure, ASTM STP 982, American Society for Testing and Materials, Philadelphia, 1988, pp. 5-34.

21.W.J.D. Shaw and I. Le May, Crack Closure During Fatigue Crack Propagation, Fracture Mechanics, ASTM STP 677, American Society for Testing and Materials, 1979, pp. 233-246.

22.S. Suresh, Micromechanisms of Variable Amplitude Load Effects during Fatigue Crack Growth in Metals and Ceramics, in Fatigue Crack Growth under Variable Amplitude Loading, Elsevier Applied Science, London and New York, 1988, pp. 146-162.

23.A. Riemslag, personal communication.

24.M.O. Lai and W.G. Ferguson, Mater. Science & Eng. 45, pp. 183-188 (1980).

25.G.R. Irwin, Plastic Zone near a Crack and Fracture Toughness, Proc. 7th Sagamore Ordnance Materials Research Conf., Session IV, p. 63, 1960.

26.J.F. Knott, Fundamentals of Fracture Mechanics, Butterworths, London, 1973.

27.R.G. Forman, V.E. Kearney and R.H. Engle, Numerical Analysis of Crack Propagation in Cyclic Loaded Structures, Trans. ASME (Ser. D) 69,1967, pp. 459-463.

28.R.W. Hertzberg and E.F.J. von Euw, Int. Journ. of Fracture Mech., 7 (1971), pp. 349-353.

29.C.M. Hudson and J.T. Scardina, Engng Fract. Mech., Vol. 1, 1969, pp. 429-446.

30.S. R. Swanson, F. Cicci and W. Hoppe, Crack Propagation in Clad 7079-T6 Aluminum Alloy Sheet Under Constant and Random Amplitude Fatigue Loading, ASTM STP 415, American Society for Testing and Materials, 1967, pp. 312-362.

31.D.P. Wilhem Investigation of Cyclic Crack Growth Transitional Behavior, ASTM STP 415, American Society for Testing and Materials, 1967, pp. 363-383.

32.J. Schijve, Eng.Fract Mech, 1981, 14, (4), pp. 789-800

33.D. Rhodes, L.E. Culver and J.C. Radon, The influence of Fracture Mode Transition on the Compliance of Thin Section Fracture Specimens, Proc. 3rd Coll. on Fract., London, 1980 , pp. 287-296.

34.D. Broek and J. Schijve, The Influence of the Mean Stress on the Propagation of Fatigue Crack in Aluminium Alloy Sheet, report NLR-

TR M.2111, Nationaal Lucht- en Ruimtevaart Laboratorium, October 1965, Amsterdam.

35.D. Broek, P. de Rijk and P.J. Sevenhuijsen, The Transition of Fatigue Cracks in Alclad Sheet, Report NLR-TR M.2100, Nationaal Lucht- en Ruimtevaart Laboratorium, 1962, Amsterdam.

36.J. Schijve, Eng.Fract. Mech., 1974,6,(2),pp. 245-252.

37.L.P. Pook Met. Sci., 1976,10,(9), pp. 334-335.

38.R.O. Ritchie, R.F. Smith and J.F. Knott, Met. Sci., 1975, 9,(11), pp. 485-492.

39.G.G. Garrett, Metallurgical Transactions A, Vol. 10A, may 1979, pp. 648-651.

40.A. Storey, Int. J. Fatigue, october 1979, pp. 195-204.

41.R.A.H. Edwards, E.M. de Jong and J. Zuidema . The Fracture Mode Transition and its Effect on Crack Growth Retardation. Proc. Fatigue 84. University of Birmingham, UK, 1984, pp. 463-478.

42.M.R. Ling and J. Schijve, Fatigue Fract. Engng Mater. Struct., Vol 13, No 5, 1990, pp. 443-456.

43.J.J. McGowan and H.W. Liu, Journal of Engng Mater. And Techn. Vol. 102, 1980, pp. 341-346.

44.D. Broek and J. Schijve, The Effect of Sheet Thickness on the Fatigue Crack Propagation in 2024-T3 Alclad Sheet Material, report NLR-TR M.2129, Nationaal Lucht- en Ruimtevaart Laboratorium, April 1963, Amsterdam.

45.D. Broek and J. Schijve, The Influence of Sheet Thickness on Crack Propagation, Aircraft Engineering 1966, pp. 31-33.

46.A.J. McEvily, ASTM STP 811, 1983, pp. 283-312.

47.L.B. Vogelesang and J. Schijve, Fatigue Engng Mater. Struct., Vol. 3, pp. 85-98, 1980.

48.J.H. Wilson, T.S. Sudarshan and H.H. Mabie, Journal of Materials Science Letters 3 (1984), pp. 773-775.

49.S. Horibe, M. Nakamura and M. Sumita, Int. J. Fatigue, 7, No 4, 1985, pp 224-227.

50.K. Walker, The Effect of Stress Ratio During Crack Propagation and Fatigue for 2024-T3 and 7075-T6 Aluminum, ASTM STP 462, American Society for Testing and Materials, 1970, pp. 1-14.

51.K. Walker, S. Pendleberry and R. McElwee, Tensile and Shear Mode Cracking of Titanium Sheet in Air and Salt Water, ASTM STP 462, American Society for Testing and Materials, 1970, pp. 234-240.

52.R.O. Ritchie, R.F. Smith and J.F. Knott, Metal Science, Vol. 9, 1975, pp.

485-492.

53.L.P. Pook and N.E. Frost, Int. J. Fract, 9, (1), 1973, pp. 53-61.

54.W.D. Dover and N.F. Boutle, Journal of Strain Analysis, Vol. 13, No 3, 1978, pp. 129-139.

55.S.M. El-Soudani and R.M. Pelloux, Metallurgical Transactions, Vol. 4, febr. 1973, pp. 519-531.

56.D.G. Rickerby and P. Fenici, Engng Fract. Mech., Vol. 19, No 4, 1984, pp. 585-599.

57.R.J. Allen, G.S. Booth and T. Jutla, Fatigue Fract. Engng Mater. Struct., Vol. 11, No. 1, pp. 45-69, 1988.

58.T.C. Lindley and C.E. Richards, The influence of Crack Closure and Plastic Zone Geometry on Fatigue Crack Propagation, Paper 11, Conference on Mechanics and Mechanisms of Crack Growth, Churchill College, Cambridge, British Steel Corp., 1973.

59.W. Elber, Engng Fract. Mech. 2, pp. 37-45, 1970.

60.H.L. Ewalds and R.J.H. Wanhill, Fracture Mechanics, Delftse Uitgevers Maatschappij and Edward Arnold, ISBN 90 6562 024 9, London 1984.

61.A. Bakker, Fatigue Fract. Engng Mater. Struct., Vol 15, No 11, pp 1051-1069, 1992.

62.Yoshoika, in Stress Intensity Factors Handbook by Y. Murakami, Vol. 2, Pergamon Press, pp. 833-836, 1987.

3. Experimental Procedures

3.1. Introduction

In this chapter some general remarks about the experimental procedures will be made. More specific information can be found in the appropriate chapters. Unless specified otherwise, all fatigue crack growth experiments were performed on center cracked tension specimens 100 mm wide and 300 mm long with thicknesses of 2, 5, 6 and 10.3 mm (see table 3.1). The crack growth direction was always perpendicular to the rolling direction. The formula which is used for K is:

$$K = \frac{P}{wt}\sqrt{\pi a}\sqrt{\sec\frac{\pi a}{w}} \qquad 3.1$$

P is the (sinusoidal in this work) load, w is the width and t the thickness of the plate. The accuracy of this equation is: 0.3% for $2a/w \leq 0.7$ and 1% for $2a/w = 0.8$. The fatigue tests were conducted in lab air (or vacuum) of about 20° Celsius on computer controlled closed-loop servo-hydraulic fatigue machines made by MTS and Schenck. All test conditions matched the experimental standards set in [1]. Most of the tests were performed under load control. Unless specified otherwise, mainly two types of tests were performed, constant load amplitude tests and constant stress intensity amplitude tests, with constant ΔS and constant ΔK respectively. The latter type of test is performed by measuring the crack length and adjusting the load if necessary to keep ΔK constant. Cracks were started from an initial sawcut or a spark eroded machined notch (with a length of 3 mm on both sides in most of the tests). First a prefatigue loading was applied to get a fatigue crack growth increment of several mm. The prefatigue loading was such that no shear lips were present at the start of the tests. A schematic figure of the specimen is shown in chapter 2, in figure 2.3.

3.2. Crack Length Measurements and da/dN Calculation

The crack length was measured using a direct current potential drop method or a pulsed direct current potential drop method. Crack growth increases the electrical resistance, thus the potential drop over the crack is a measure for the crack length. Several fatigue tests were performed to calibrate the crack length

measured with the potential drop against the crack length measured with a travelling microscope directly at the specimen surfaces. A third order polynomial was fitted through the measurement points and fed into the controlling computer of the fatigue machine. More details about the potential drop techniques can be found in reference [2]. With the pulsed direct current potential drop method measurements were done in current-on and current-off situations to compensate for thermoelectric effects. The crack length measurements were very often checked by eye and corrected if necessary. The absolute accuracy for the Al 2024 specimens is claimed to be better than 0.4 mm [2]. In a normal fatigue crack growth test the crack length a and the number of cycles N are recorded, see figure 3.1 as an example. In this figure the results are shown of a constant amplitude test with S_{max} = 120 MPa, R= 0.1 and a frequency of 0.1 Hz. The specimen had a length of 300 mm, was 160 mm wide and had a thickness of 2 mm. The data were recorded at intervals of Δn = 2 cycles. In the case of potential drop measurements it is possible to get a large number of a(N) results. The slope da/dN is the crack growth rate (in mm per cycle).

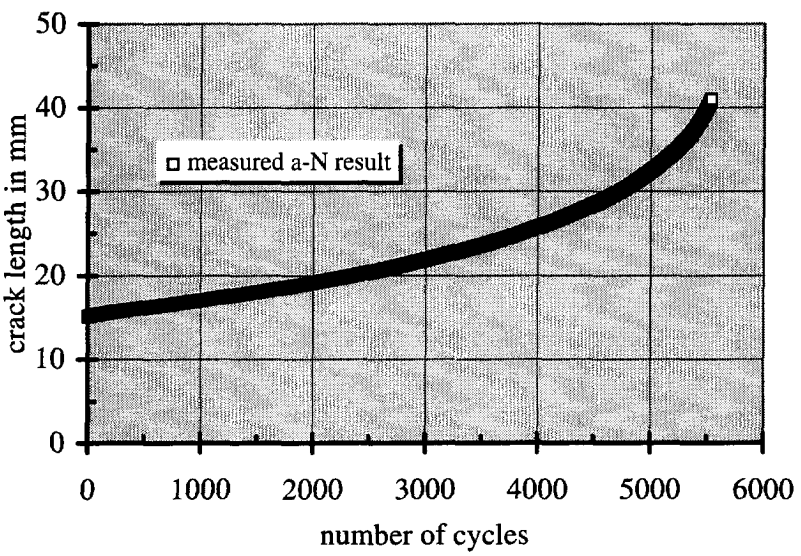

Figure 3.1. Crack length versus number of cycles.

The secant method for obtaining da/dN, as described in reference [1], can give much scatter if there are many measurement points with the same measured crack length, owing to the discrete measurement levels of the potential drop apparatus. Due to scatter in the potential drop measurements it is even possible to obtain negative crack growth rate values. In figure 3.2 the crack growth rates da/dN found using the data presented in figure 3.1 are plotted as a function of the

crack length. Due to the large spread a data reduction is needed. A computer program (in Basic) was written to perform this task. Two data reduction and smoothing methods were developed.

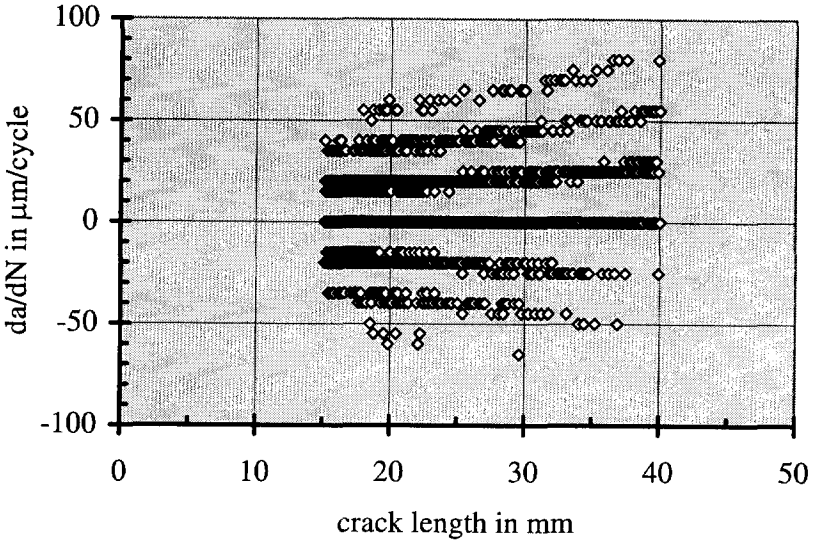

Figure 3.2. da/dN versus crack length using the ASTM secant method.

In the first one a constant reduction number n is defined to find a da/dN value defined over 2n+1 measurement points (i.e. a(N) results):

$$da/dN(i)=(a_{i+n}-a_{i-n})/(N_{i+n}-N_{i-n}) \qquad 3.2$$

The corresponding crack length value $a(i) = (a_{i+n}+a_{i-n})/2$.
The advantage of this simple method is that n can be chosen significantly high to obtain a meaningful crack increment. da/dN then has a realistic value without much scatter. A drawback of this method is related to the choice of the reduction number n. In the beginning of crack growth a large number of measurement points are recorded at about the same crack length. A high reduction number n would be needed for smoothing the da/dN. However, in the area of higher da/dN the same reduction number covers a far greater crack length increment than in the beginning of crack growth. A lower reduction number would then be sufficient for a smooth result. In figure 3.3 the reduction number n = 3 is apparently too low at the beginning of crack growth. At the end a better smoothing is reached. The choice of the reduction number is quite arbitrary. The best n is that number that gives insignificant scatter without destroying characteristic crack growth properties.

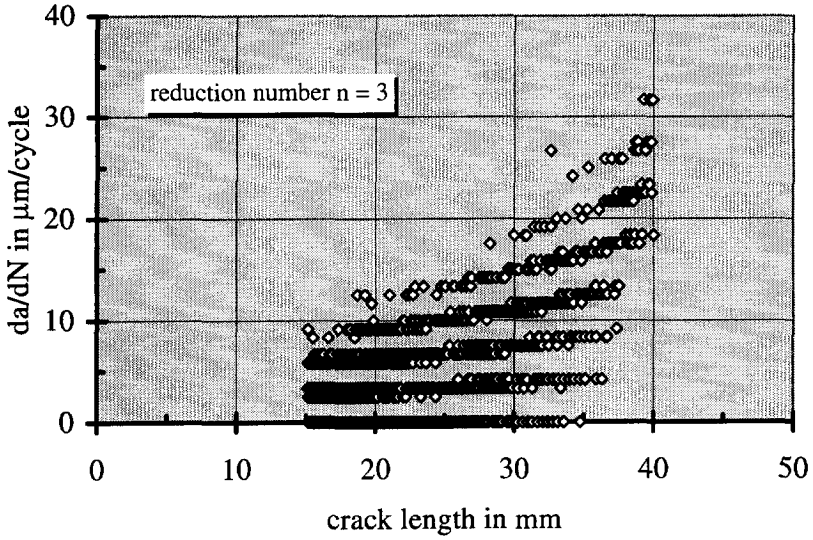

Figure 3.3. Crack growth rate versus crack length.

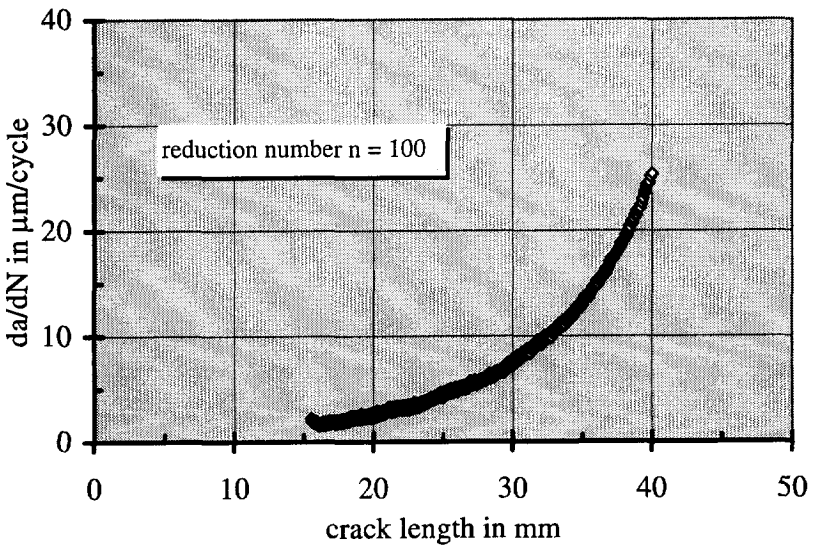

Figure 3.4. Crack growth rate versus crack length.

Thus the choice of the value of n is based on a compromise between the beginning and the end of the a(N) curve. In the beginning a large n is needed to avoid much scatter; at the end a large n is to be avoided. Figures 3.3 and 3.4 show da/dN - a curves for n = 3 and n = 100 respectively, using the data of figure 3.1. Although the reduction number is high in figure 3.4, a decrease in da/dN just

after the start of the constant amplitude test can be observed. Owing to much scatter this effect cannot be observed in figure 3.3. Note that a high reduction number clips a part of the da/dN figure at the highest and lowest crack lengths.

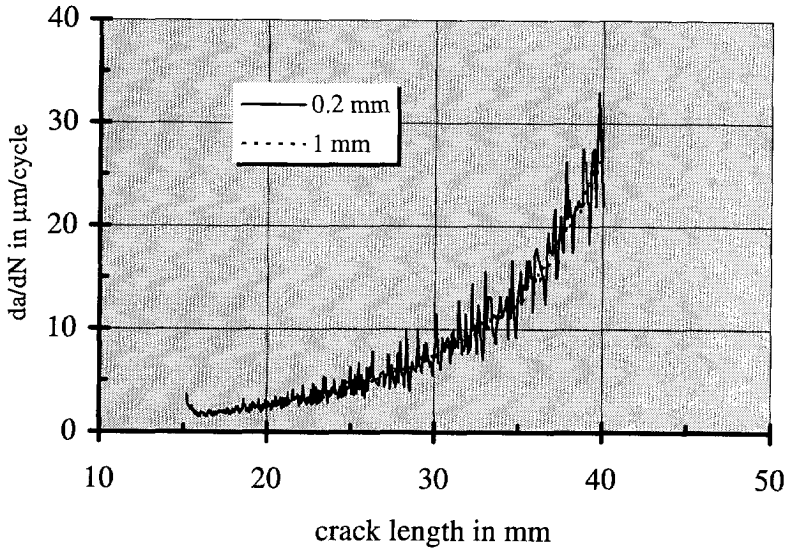

Figure 3.5. Crack growth rate versus crack length.

In the second method we define a significant crack growth increment. Significant means that we have the possibility to define an arbitrary crack length increment for obtaining a smooth result, or an increment with a physical meaning with respect to the material structure. For example in a material with very coarse (second phase) particles it is possible to choose the increment larger than these particles. The da/dN is taken over this crack growth increment. da/dN is defined analogously to equation 3.2:

$$da/dN(i) = (a_{i+k}-a_{i-k})/(N_{i+k}-N_{i-k}) \qquad 3.3$$

with the restriction that k is chosen such that $a_{i+k} - a_{i-k}$ has the smallest value just greater or equal to the crack growth increment chosen. The corresponding crack length value $a(i) = (a_{i+k}-a_{i-k})/2$. The datafile number i varies from i = k+1 to the last number minus k.

The advantage of this method is that a crack growth increment with a more or less physical significance with respect to the material structure, or with respect to the accuracy or smoothness demanded, can be taken . The beginning and end of the da/dN(a) results are handled with the same accuracy. In figure 3.5 the da/dN results for crack growth increments of 0.2 and 1 mm are shown. The results are

almost the same, as they should be. These results are also based on the data shown in figure 3.1.

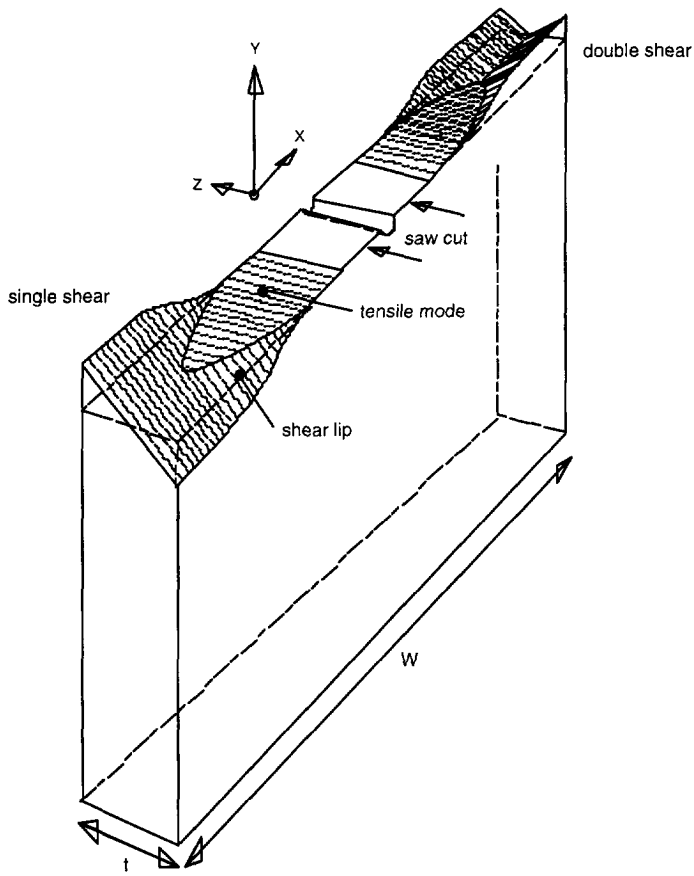

Figure 3.6. Single and double shear lips.

In this work the simpler first method is used because both methods give about the same result for the large number of measurement points made by the potential drop apparatus. Both methods can be applied equally well to results from constant amplitude and constant ΔK tests. However, in the case of crack growth under spectrum loading care should be taken to avoid annihilation of local da/dN variations associated with the load history of the spectrum loading.

3.3. Shear Lip Width Measurements

The shear lip width of broken specimens was measured as a function of crack length. Specimens were sacrificed by grinding successive cross sections perpendicular to the crack growth direction, after Δa steps of 0.5 to 2 mm. A

transparent sketch was made or a photograph (negative) was taken of the cross sections under a microscope. The crack length of each section was determined by measuring the length of the remaining part of the specimen by a micrometer. The transverse length of the tensile part t_t (see figure 3.7) of the fracture surface was measured. The shear lip width t_s is defined as:

$$t_s = (t - t_t) / 2 \qquad 3.4$$

t is the plate thickness. In figure 3.6 shear lip development in a constant load amplitude test is schematically shown. The start of the test was in the tensile mode.

In figure 3.7 an example is given of the shear lip width development for increasing crack length. The data shown in this figure are from a test with a constant $\Delta K = 28$ MPa$\sqrt{m}$ and $R = 0.067$. So with constant ΔK the shear lips increase with increasing crack length.

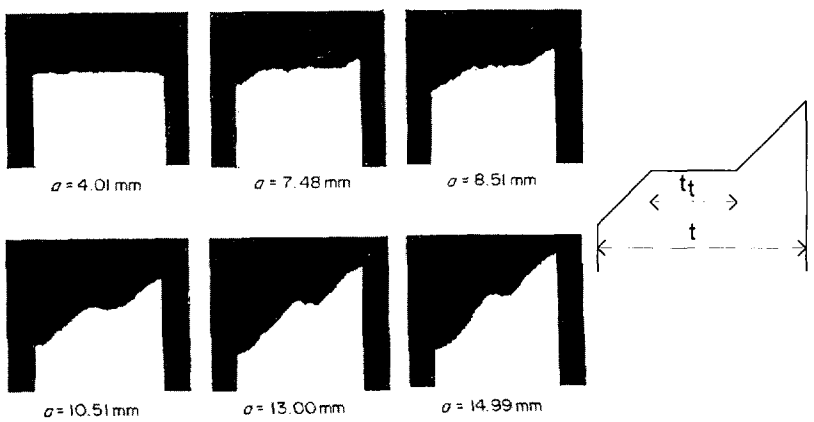

Figure 3.7. Transverse sections at increasing crack lengths.

Measured contours of another crack surface are shown in figure 3.8. The results apply to a two step test with a constant $K_{max} = 20.6$ Mpa$\sqrt{m}$ during the whole test and where $R = K_{min} / K_{max}$ has a constant value of 0.05 up to a crack length of about a = 30 mm. Above this crack length R is increased to a constant value of 0.52. The shear lips obtained in the first part of the test became significantly smaller in the second part for a lower ΔK.

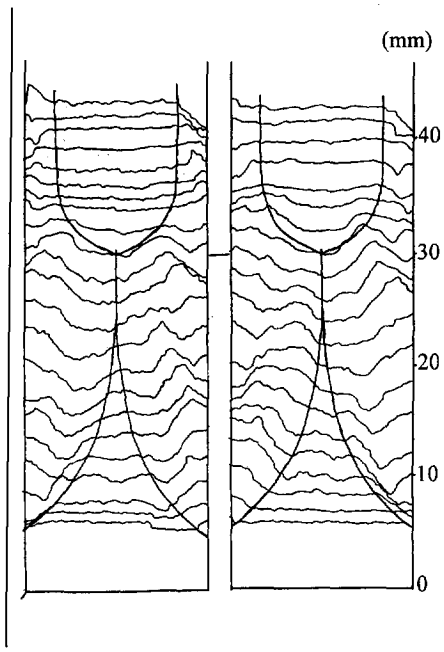

Figure 3.8. Shear lip development in a two step constant ΔK test. ΔK changes at about a = 30 mm.

The equilibrium width of the shear lips of some specimens was measured directly on the fracture surface (see chapter 4, section 4.2.3).

3.4. References

1. Standard Test Method for Measurement of Fatigue Crack Growth Rates, E 647-93, Annual book of ASTM Standards, Volume 03.01, 1993.
2. F.A. Veer, Doctor Thesis T.U. Delft, October 1993.

Table 3.1. Chemical composition and mechanical properties of the 2024 AL materials used.

Composition :

Elements	6 mm plate	10.3 mm	2 mm	5 mm
Cu	4.43 %	4.34 %	4.74 %	4.70 %
Mg	1.40	1.36	1.58	1.62
Mn	0.70	0.63	0.63	0.64
Zn	0.06	0.07	0.07	0.05
Ni	0.03	0.03		
Cr	0.01	0.01	< 0.01	< 0.01
Ti	0.02	0.02		
Fe	0.20	0.25	0.17	0.19
Si	0.06	0.08	0.04	0.06

Mechanical Properties:

	6 mm plate	10.3 mm plate
$\sigma_{0.2}$	395 MPa	366 MPa
σ_{max}	500 MPa	457 MPa
ε_{max}	17 %	19 %
E	71900 MPa	70800 MPa

4. Shear Lips on (Fatigue) Fracture Surfaces

4.1. Introduction

Shear lips obtained under constant ΔS loading were shown in figure 3.6. One crack front has transformed to single shear, and the other one to double shear. The shear lip width is defined as:

$$t_s = \frac{(t - t_t)}{2} \qquad 4.1$$

where t is the plate thickness and t_t is the width of the tensile part of the surface (see figure 3.7). Schijve [1] made shear lip width measurements on 2024-T3 specimens (t = 4.16 mm) tested in air at different R values. He proposed the following relation:

$$\frac{t_s}{t} = 0.00285\ \Delta K_{eff}^2 \qquad 4.2$$

with ΔK_{eff} in MPa$\sqrt{m}$. However, we know that because the tests were carried out under constant amplitude loading, stable shear lip width values were not obtained. Equation 4.2 thus cannot have a general validity. Based on the results of Schijve the author and his co-workers introduced the constant ΔK test for shear lip width measurements [2]. In the present investigation more constant ΔK tests were carried out on bare 2024-T351 plate material in order to arrive at the steady state behaviour of shear lips. It requires some crack growth before this steady state is reached. Both the steady state and the non-steady state are described in this chapter. The results obtained in the constant ΔK tests can be used to explain the behaviour under constant amplitude loading.
Two thicknesses were used, t = 6.0 mm and t = 10.3 mm, to explore a possible thickness effect.

It is also found that the crack growth rate da/dN decreases with increasing shear lip width. A preliminary explanation of this phenomenon will be given in this chapter. A more rigorous explanation follows in chapter 5.
Another important variable in the shear lip development is the frequency. The majority of the tests are executed at 10 Hz. Using a number of tests performed at other frequencies, it will be shown that a reasonable mathematical description of the equilibrium shear lip width as a function of frequency and of the (effective) ΔK is possible.
At the end of this chapter some attention is paid to results of static tensile tests. Some differences between these fracture surfaces and fatigue fracture surfaces will be discussed.

4.2. Shear Lip Width Development under Constant ΔK Loading

4.2.1. Shear Lip Width Results

In figure 4.1 photographs of fatigue fracture surfaces with a typical shear lip width development are shown.
Details of the photographs will not yet be explained here, but it will be clear from figure 4.1 that at 10 Hz the fracture surface is rougher than at 0.1 Hz. At 10 Hz the shear lips reinitiate several times which implies that a new shear lip with the opposite angle of about 45° with the plate surface is growing in the existing one. The new shear lip replaces the old one when the crack grows.

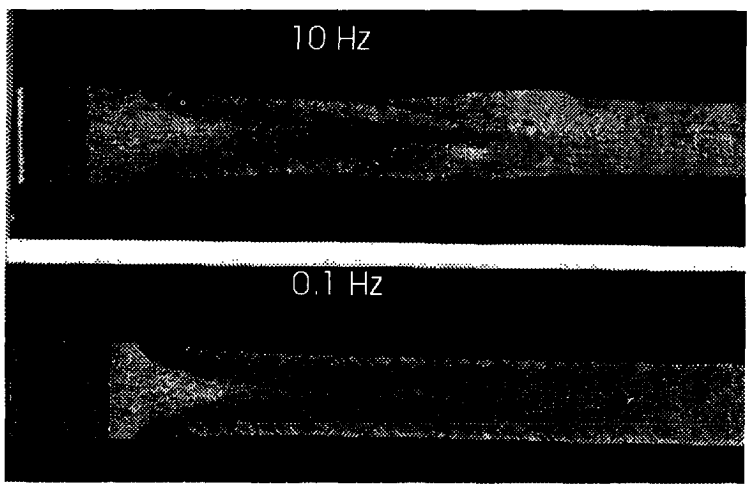

Figure 4.1. Shear Lip width at test frequencies of 10 Hz and 0.1 Hz.

This process is repeated several times. The reinitiation effect is not found at 0.1 Hz. Here an existing shear lip will keep the same angle of about 45° with the plate surface. The result is a more smooth, regular shear lip. The frequency effects will be discussed in section 4.5. The effects of smooth and rough shear lips are addressed in chapter 7.
The shear lip width t_s as a function of the crack length a was measured in 33 tests performed at constant ΔK and R and a frequency of 10 Hz. The tests and the results are summarized in table 4.1. A graphical representation of the test conditions at 10 Hz is shown in figure 4.2. Results of some tests are shown in figures 4.3 through 4.9. The fracture mechanics parameters that were applied in these tests can be found in the figure captions and in table 4.1. The solid line through the data points is discussed in section 4.3.3.

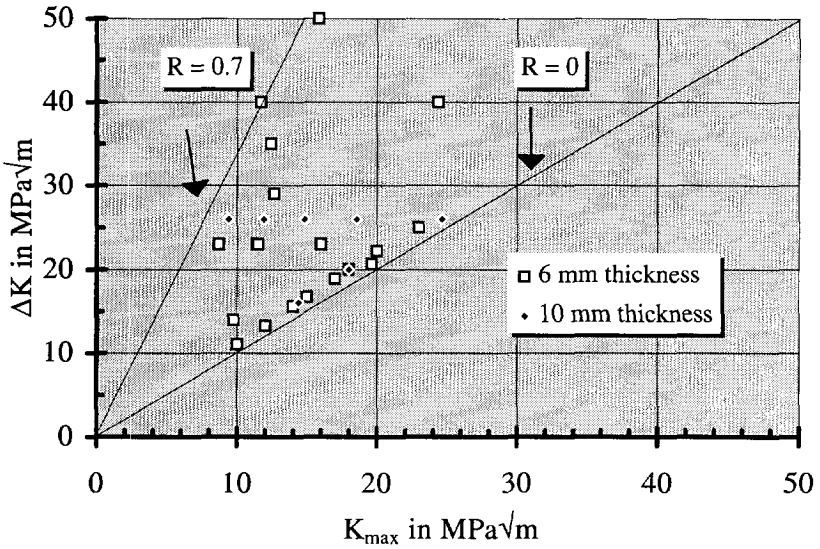

Figure 4.2. Summary of tests performed at 10 Hz.

4.2.2. A Mathematical Description

From the results in figures 4.3 to 4.9 two empirical trends are observed.

1. There is a clear trend for the shear lip width to grow asymptotically to an equilibrium value.
2. The rate of increase of the shear lip width becomes smaller during this growth process.

In order to arrive at a mathematical description of the shear lip width development, a physical assumption valid for all shear lips is adopted. This assumption consists of two parts based on the empirical trends.

First it is assumed that for a constant ΔK and R test the shear lip width t_s will tend to reach an equilibrium value denoted as $t_{s,eq}$. It can take a considerable amount of crack growth before this equilibrium situation is reached. Further the material must be thick enough to physically reach $t_{s,eq}$. However it will be shown that $t_{s,eq}$ can also be found when the material is not thick enough.

Secondly it is assumed that the rate of widening of the shear lips is governed by the difference of $t_{s,eq}$ and t_s. The widening rate decreases when the shear lip width t_s grows. Therefore the widening rate is assumed to be proportional to the difference $t_{s,eq} - t_s$. The widening rate thus has a maximum at the start of the shear lip formation, when t_s is zero, and it becomes nearly zero when t_s approaches $t_{s,eq}$.

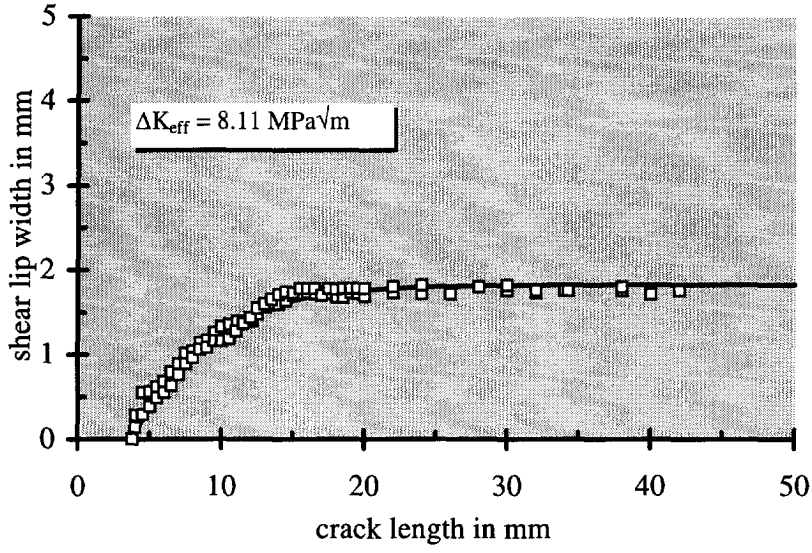

Figure 4.3. Shear Lip results; 6.0 mm plate thickness; c=0.200 mm^{-1}; $t_{s,eq}$=1.83 mm; K_{max} =16.7 MPa√m and R=0.10.

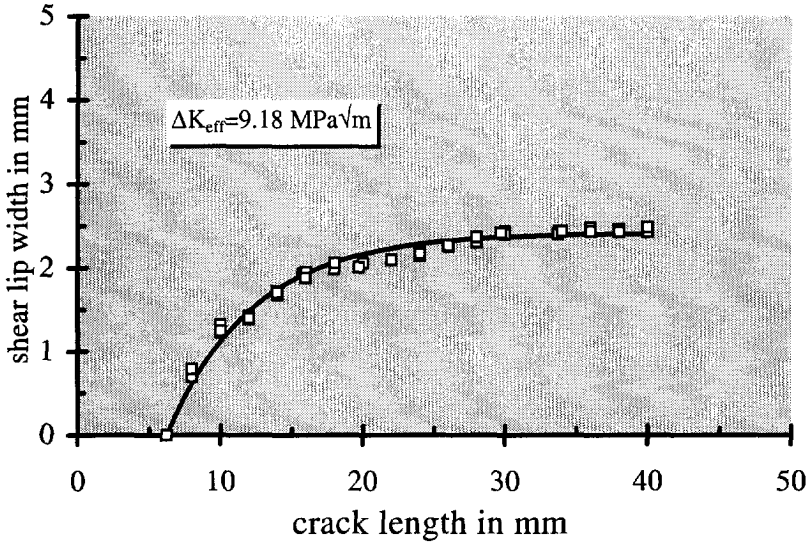

Figure 4.4. Shear Lip results; 6.0 mm plate thickness; c=0.164 mm^{-1}; $t_{s,eq}$=2.42 mm; K_{max} =18.9 MPa√m and R=0.10.

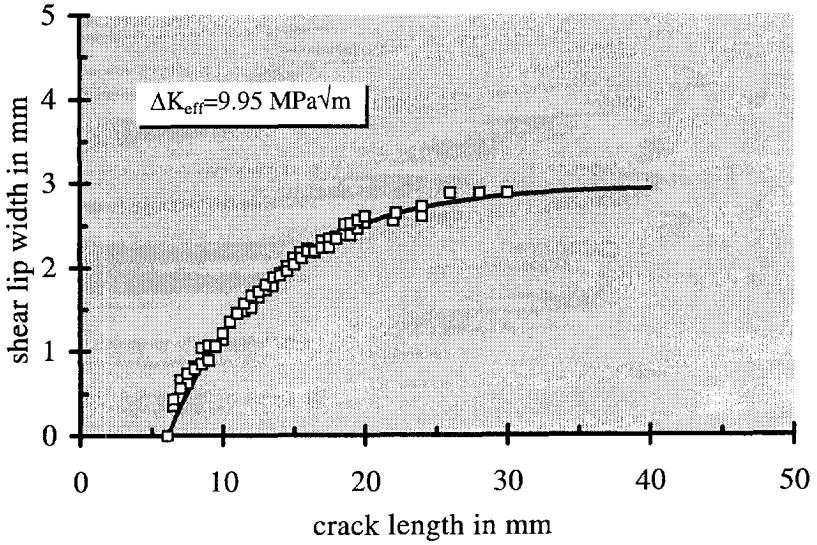

Figure 4.5. Shear Lip results; 6.0 mm plate thickness; c=0.137 mm^{-1}; $t_{s,eq}$=2.96 mm; K_{max} =23 MPa√m and R=0.30

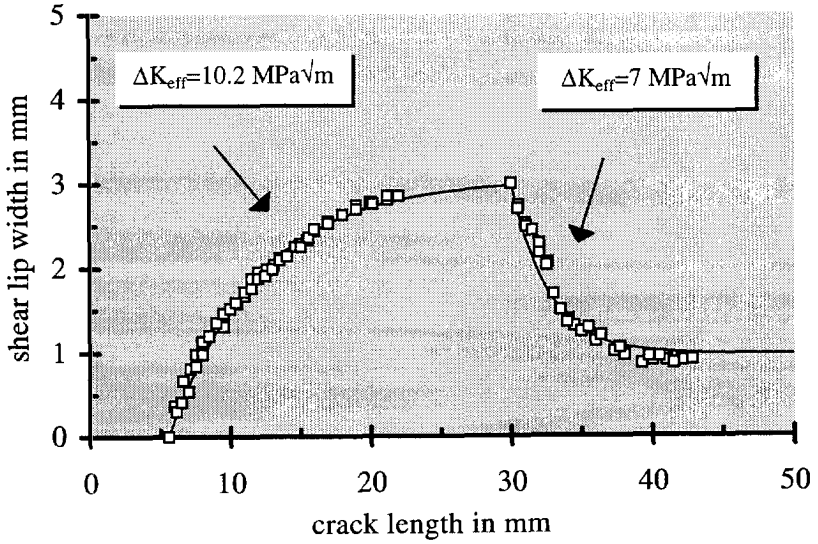

Figure 4.6. Shear Lip growth and shear lip shrinkage; 6.0 mm plate thickness; K_{max} =20.6 MPa√m ; R=0.05 until 30 mm, then 0.52 .

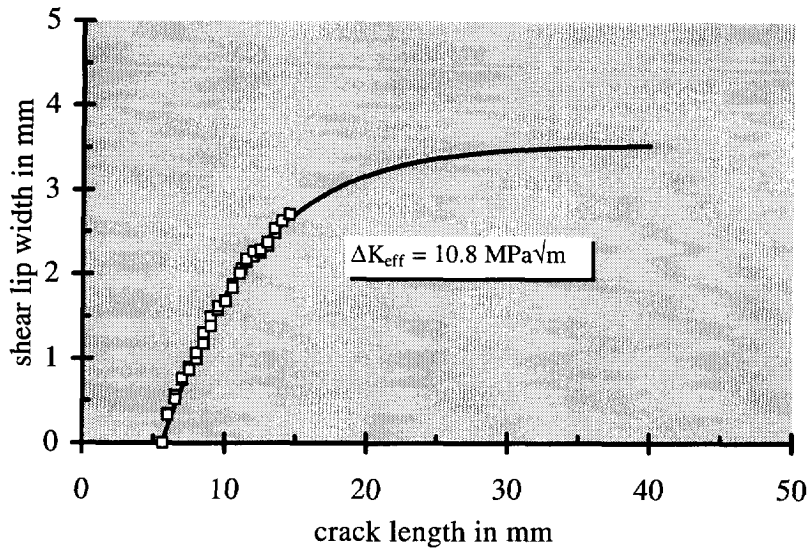

Figure 4.7. Shear Lip results; 6.0 mm plate thickness; c=0.156 mm^{-1}; $t_{s,eq}$=3.55 mm; $t_{s,eq}$> t/2; K_{max} =22.2 MPa√m and R=0.10.

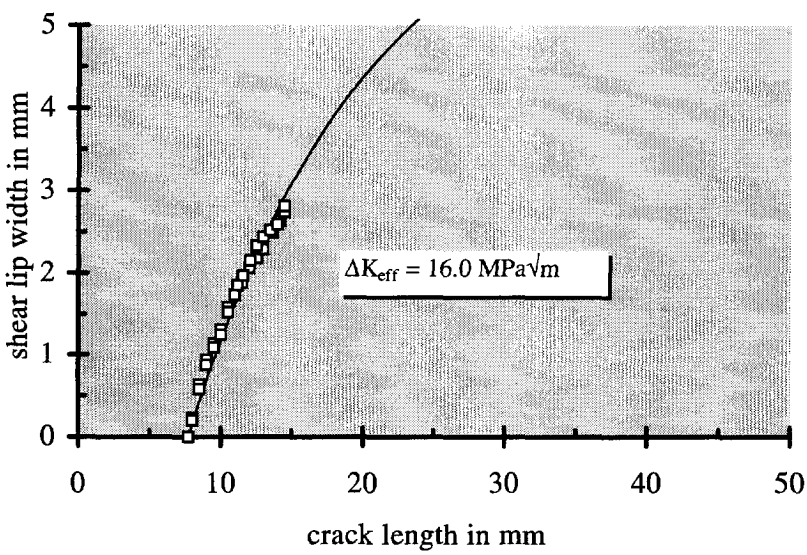

Figure 4.8. Shear Lip results; 6.0 mm plate thickness; ΔK_{eff}=16.0 MPa√m; c=0.080 mm^{-1}; $t_{s,eq}$=7.00 mm; K_{max} =40.0 MPa√m and R=0.39.

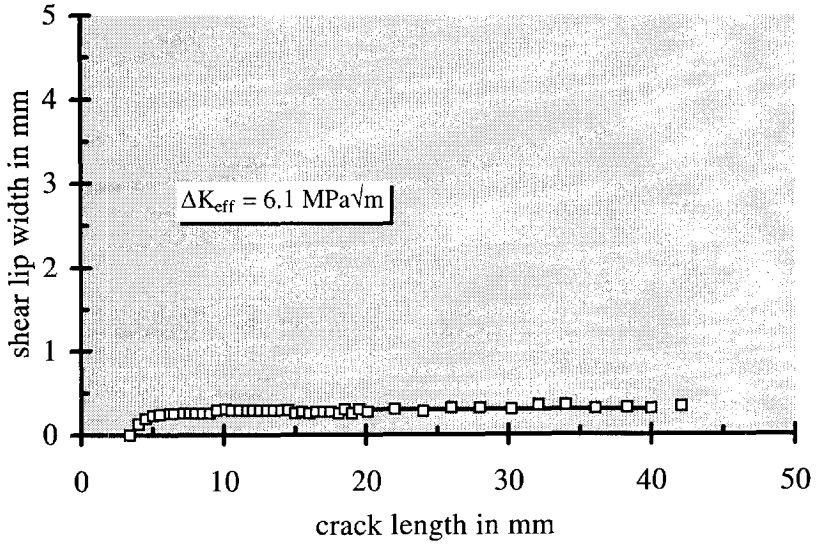

Figure 4.9. Shear Lip results; 6.0 mm plate thickness; c=0.813 mm^{-1}; $t_{s,eq}$=0.30 mm; K_{max} =14.0 MPa√m and R=0.30.

In mathematical format the assumption implies:

$$\frac{dt_s}{da} = c\,(t_{s,eq} - t_s) \qquad 4.3$$

The constant c has to be found, just like $t_{s,eq}$, for each test. It is a measure of how fast the equilibrium position $t_{s,eq}$ is reached. Integration of equation 4.3 leads to:

$$t_s = t_{s,eq}\,(1-e^{-c(a-a_o)}) \qquad 4.4$$

a_o is the crack length where the shear lip starts growing.
Equation 4.4 is valid for an initial width of $t_{s,o}$=0. Before this there is a shear lip free flat fracture surface which is called a tensile mode fracture surface. If a shear lip width $t_{s,o}$ is already present at the start of the crack growth period to be considered, the integration of equation 4.3 yields:

$$t_s - t_{s,o} = (t_{s,eq} - t_{s,o})(1-e^{-c(a-a_o)}) \qquad 4.5$$

Normally $t_{s,o}$ is smaller than $t_{s,eq}$. However, it will be shown that a test where $t_{s,o} > t_{s,eq}$ can also be described by equation 4.5.

Most of the tests started at $t_{s,o} = 0$. Values of $t_{s,eq}$ and c in equation 4.4 were determined by a least square method. This was done by varying $t_{s,eq}$ and c independently until the least squares sum $\Sigma (t_{s,cal} - t_{s,meas})^2$ has a minimum. $t_{s,cal}$ and $t_{s,meas}$ denote calculated and measured t_s values respectively. Results of the fitting procedure are shown as the solid lines through the data points in the figures 4.3 - 4.9. The regression analysis can lead to problems if the shear lips grow to a width of t/2 (full slant mode). A larger shear lip width is physically impossible. In such cases t_s - a data, where $t_s \approx t/2$, were omitted, because otherwise a good fit was not obtained. It had to be assumed that $t_{s,eq}$ could theoretically be higher than half the plate thickness t/2.
An example of such a case is given in figure 4.7 for a plate thickness of 6 mm. For crack length values $a \geq 18$ mm, it was found that $t_s = 3$ mm, which is half the plate thickness. The whole crack surface then is in the shear mode. The regression analysis leads in the case of figure 4.7 to $t_{s,eq} = 3.55$ mm, which is more than half the plate thickness.
It thus seems that at high ΔK_{eff} (10.8 MPa$\sqrt{m}$ in figure 4.7) there is a tendency for shear lips to grow wider than half the plate thickness. The larger shear lip width can actually be obtained only in a thicker specimen.

For a reliable fit it is necessary to have sufficient measurement points. This limits the magnitude of ΔK_{eff} with respect to the plate thickness. Too high a ΔK_{eff} means that not enough measurement points are available before t_s reaches half the plate thickness. The fitting procedure now gives an unreliable result because the extrapolation to find $t_{s,eq}$ is too large (see figure 4.8). These cases have been marked with a (*) in table 4.1. The value of $t_{s,eq}$ in these cases was estimated with equation 4.7 (presented in the next section) and the curve was fitted through the measurement points with c as the only parameter.
The best fit combinations of $t_{s,eq}$ and c are presented in table 4.1. The ΔK_{eff} used is the ΔK value corrected for crack closure using Elber's [3] crack closure formula:

$$\Delta K_{eff} = U \Delta K \text{ with } U = (0.5 + 0.4R) \qquad 4.6$$

Equation 4.6 is valid for - $0.1 \leq R \leq 0.7$. Until now all constant ΔK_{eff} tests discussed were performed in a situation of growing shear lips with $t_{s,o} = 0$. In principle equation 4.5 should also be able to predict shear lip shrinkage, starting from a higher shear lip width level $t_{s,o}$ and shrinking to a lower level $t_{s,eq}$ belonging to a second ΔK_{eff} applied. To test this conjecture a two step constant ΔK_{eff} test was performed. The same K_{max} was used in both steps to avoid

overload effects. For the first step ΔK_{eff} = 10.2 MPa$\sqrt{m}$ was used, leading to a situation of complete shear at 30 mm. At this crack length the test was continued with the same K_{max} (= 20.64 MPa$\sqrt{m}$), but a lower ΔK_{eff} = 7.0 MPa$\sqrt{m}$. The results of this test are shown in figure 4.6, while the fracture surface was already presented in figure 3.8.

4.2.3. Dependence of c and $t_{s,eq}$ on Some Fracture Mechanics Parameters

In order to explore whether the values of c and $t_{s,eq}$ as shown in table 4.1, might be related to fracture mechanics parameters, these values were plotted against K_{max}, ΔK and ΔK_{eff}. The graphs for $t_{s,eq}$ against K_{max}, ΔK and ΔK_{eff} are presented in figures 4.10 to 4.12 respectively. For the last 10 tests in table 4.1 a c value is not given. The $t_{s,eq}$ values of these tests were not found by the regression procedure. They have been estimated directly from the fracture surface.

Sometimes very narrow shear lips are present on specimens that are largely in the tensile mode. It was decided to neglect shear lip width smaller then about 0.1 mm and to consider it to be zero.

Obviously there is a poor correlation with K_{max} and ΔK, whereas the correlation with ΔK_{eff} is surprisingly good. Linear regression leads to equation 4.7:

$$t_{s,eq} = 0.67\ \Delta K_{eff} - 3.72 \qquad 4.7$$

where $t_{s,eq}$ is given in mm and ΔK_{eff} in MPa$\sqrt{m}$. Equation 4.7 is based only on the results from Table 4.1 that are found by the fitting procedure. However all results of the table are shown in the figures.

The regression line is shown in figure 4.12. In this figure a thickness effect is not observed. The results suggest a unique relation between shear lip width and crack growth rate. The shear lip starts at about 5.6 MPa$\sqrt{m}$, which corresponds to a crack growth rate da/dN of about 0.16 µm/cycle, using a da/dN - ΔK_{eff} relation for this material given as equation 5.5 in chapter 5. About the same result was reported in reference [18] where 0.14 µm/cycle was found for da/dN at the start of shear lips. In this reference a da/dN value of 0.5 µm/cycle was found for completion of the transition in a plate with 3 mm thickness. It should be recognized that it is often difficult to accurately indicate the completion of the transition. However, if this result is compared with the result predicted here for $t_{s,eq}$ = 1.5 mm, a value of ΔK_{eff} = 7.79 MPa$\sqrt{m}$ is found with relation 4.7. Using again equation 5.5 results in da/dN = 0.51 µm/cycle, which is the same result as

obtained in reference [18].

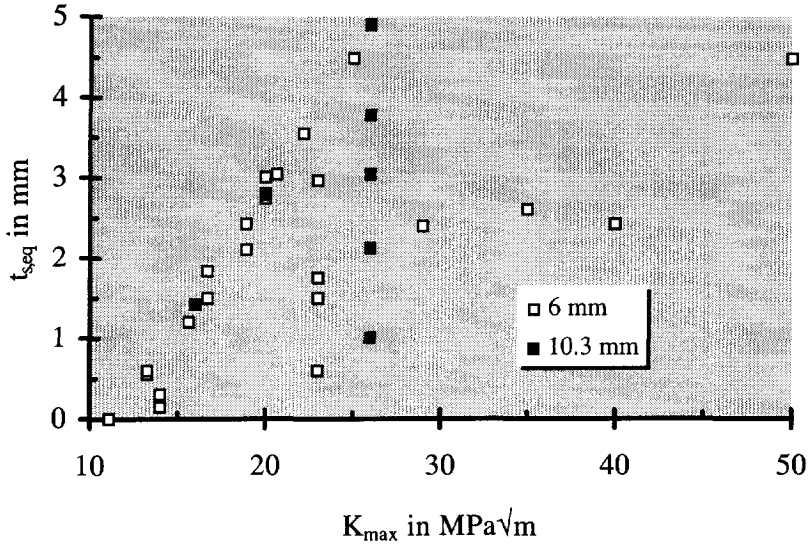

Figure 4.10. $t_{s,eq}$ versus K_{max}.

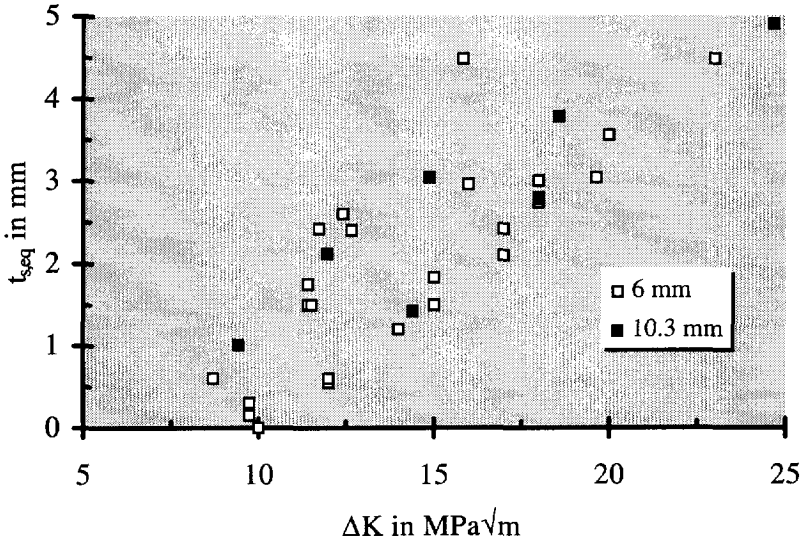

Figure 4.11. $t_{s,eq}$ versus ΔK.

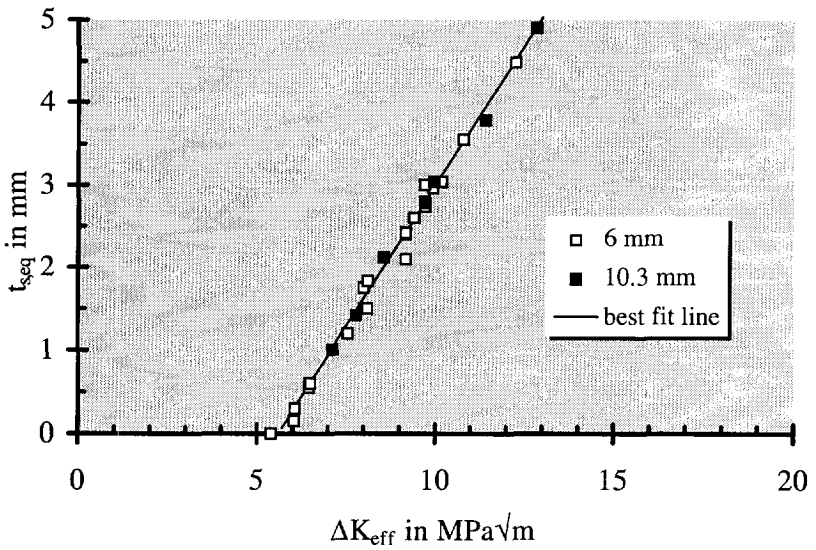

Figure 4.12. $t_{s,eq}$ versus ΔK_{eff}.

The excellent agreement could still be questionable, because equation 5.5 is found for the tensile mode situation. In chapter 5 a correction on ΔK_{eff} due to shear lips is discussed. The ΔK_{eff} correction for shear lips, with equations 5.8 , 5.9 and 5.10, should be used instead.

Here it is concluded that the same da/dN (in a stationary situation) will always be accompanied by the same $t_{s,eq}$ and vice versa. However, note that for other materials the shear lips must be measured again, even for the same alloy of another manufacturer. An example of this is a difference in shear lip width between Al 2024 T351 from Alcoa (thickness 6.35 mm, σ_{ys} = 324 Mpa) and Pechiney (our 2024 T351 alloy of 6 mm thickness and σ_{ys} = 395 MPa) . The Pechiney material showed the wider shear lips.

The values of c have also been plotted against ΔK_{eff} in figure 4.13. Here the results are less good.

Several mathematical functions were tried to get a good fit for the c - ΔK_{eff} results. A reasonable fit of the average trend can be represented by:

$$c = 0.0167e^{\frac{22.1}{\Delta K_{eff}}} \qquad 4.8$$

with c in mm^{-1} and ΔK_{eff} in MPa$\sqrt{m}$.

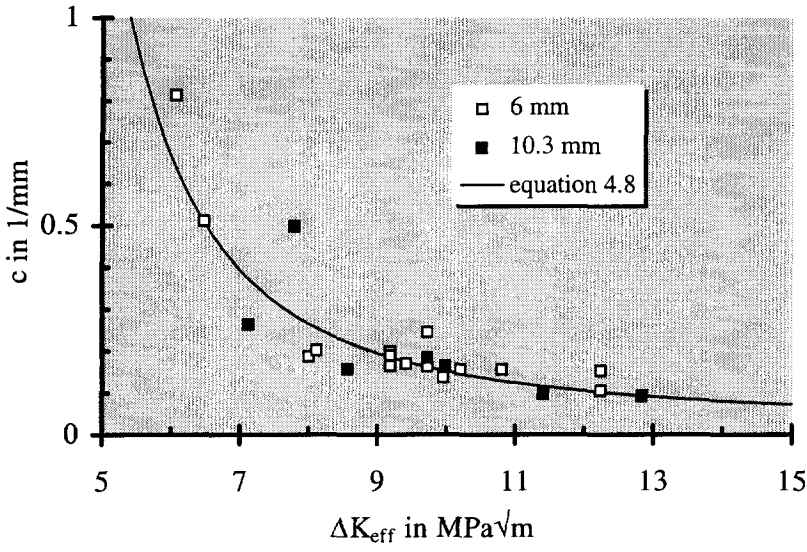

Figure 4.13. c versus ΔK_{eff}.

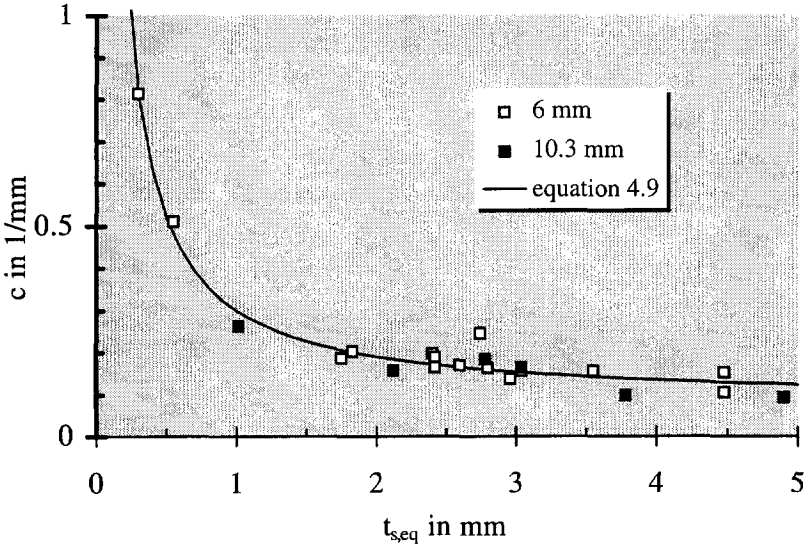

Figure 4.14. c versus $t_{s,eq}$

Figure 4.13 shows a considerable amount of scatter when equation 4.8 is drawn through the data points.

As both c and $t_{s,eq}$ can be expressed as functions of ΔK_{eff}, it seems reasonable to

assume that the parameter c depends on the equilibrium shear lip width $t_{s,eq}$. By plotting c directly against $t_{s,eq}$ a new fit was found. In figure 4.14 this fit is shown for all available c values (one extreme point was omitted). The formula based on the result given in figure 4.14 will be used in the present analysis:

$$c = \frac{0.22}{t_{s,eq}} + 0.08 \qquad 4.9$$

with $t_{s,eq}$ in mm, and c in mm^{-1}.

4.2.4. Thickness Dependence

As discussed before, $t_{s,eq}$ can be larger than half the plate thickness t. This surprising result means that $t_{s,eq}$ in such cases cannot be measured directly on the fracture surface when 100% shear is present. In these cases only the extrapolation procedure by fitting t_s-a results can be used to find $t_{s,eq}$, or a thicker specimen should be used. The results presented in figure 4.12 suggest that $t_{s,eq}$ is not dependent on the specimen thickness, but only on ΔK_{eff}. It will be assumed that the thickness independence has a general validity. The consequence is illustrated by figure 4.15. The same $t_{s,eq}$ value is used for three plate thicknesses. Only in thicker plates can $t_{s,eq}$ be measured directly on the fracture surface.

The fact that $t_{s,eq}$ is only dependent on ΔK_{eff} and not on the plate thickness is important for the transition length, that is the crack length at which a shear lip has grown to a complete slant mode. It will be clear from figure 4.15 that the transition length is larger for a thicker sheet. For $t_{s,eq} < t/2$ there is no transition length. The independence of $t_{s,eq}$ on the plate thickness, which leads to a longer transition length in thicker plates, is also experimentally confirmed by references [4] and [5] .

4.2.5. Shear Lip Behaviour and Crack Closure

The best linear and quadratic closure relations

It is well-known that for the 2024 T3 Al alloy a higher R value leads to a higher da/dN value at the same ΔK. In this section it will be shown that the shear lip width shows an analogous R effect as da/dN, i.e. a higher R shifts the shear lip width to a higher value at the same ΔK. Further the best linear and quadratic crack closure functions will be calculated using a linear $t_{s,eq}$ dependence of ΔK_{eff} . In figure 4.12 the relation between $t_{s,eq}$ and ΔK_{eff} ,using Elber's linear crack closure function (equation 4.6), was shown.

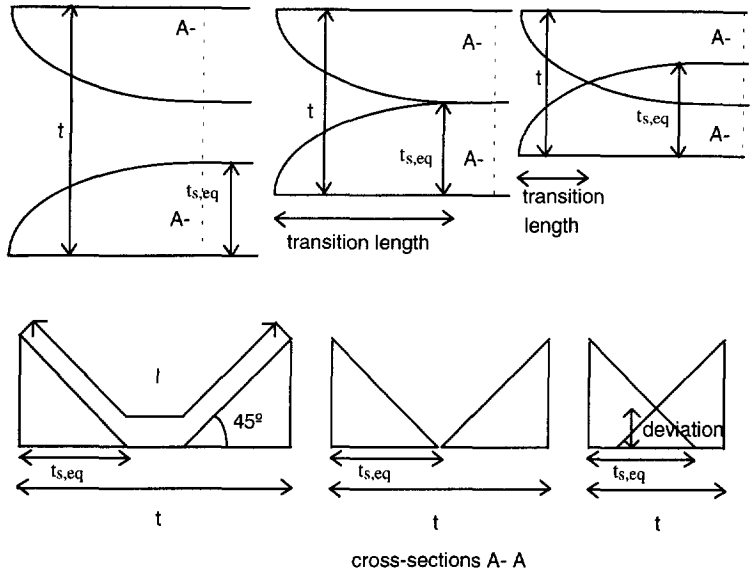

a) $2t_{s,eq} < t$ b) $2t_{s,eq} = t$ c) $2t_{s,eq} > t$

Figure 4.15. Double shear lip width development in a constant ΔK_{eff} test.

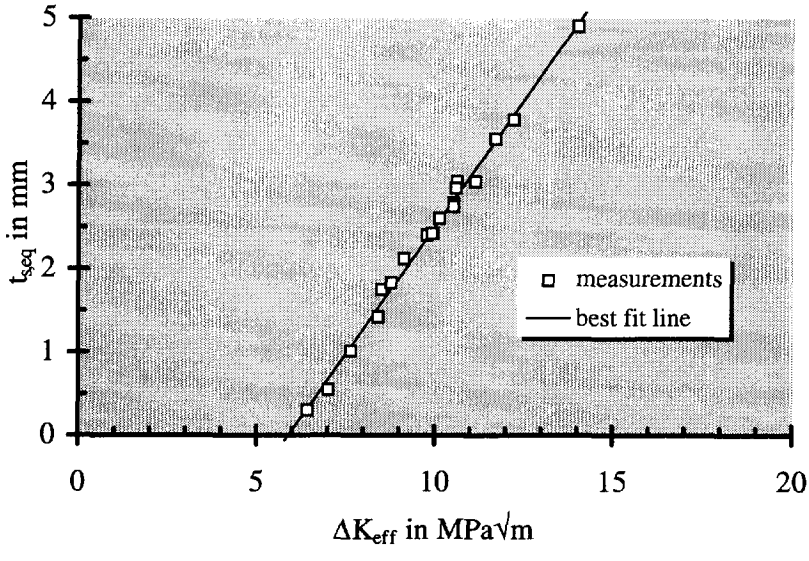

Figure 4.16. $t_{s,eq}$ versus ΔK_{eff} using the crack closure relation of Schijve.

Another well-known quadratic crack closure function for Al-2024 is that of Schijve [6]:

$$\Delta K_{eff} = U\,\Delta K \quad \text{with } U = 0.55 + 0.33\,R + 0.12\,R^2 \text{ and } -1 \le R \le 1 \qquad 4.10$$

A graph of $t_{s,eq}$ versus this ΔK_{eff} is shown in figure 4.16. There is little difference between results found with both closure functions.

As discussed by Schijve [22], if there is a satisfactory correlation between ΔK_{eff} (= U(R)ΔK) and da/dN obtained at different R values, exactly the same correlation will be found for $\Delta K_{eff}^{*} = q\,\Delta K_{eff}$, where q is a constant. The relation simply implies that the ΔK_{eff} scale is multiplied by a constant factor q, which does not affect the quality of the correlation. On a logarithmic scale it involves a horizontal shift with log(q).

The same argument applies to the correlation between $t_{s,eq}$ and ΔK_{eff}. This is illustrated by figure 4.17, which shows the same correlation for different q values. If the ΔK_{eff} values are multiplied with the same constant, it simply means a linear scaling of the horizontal axis. The correlation is not affected, but the slope of the best fit line changes. The normal Elber result is given by q=1. A consequence of the above reasoning is that a good correlation with some ΔK_{eff} does not prove that a satisfactory U(R) relation correctly indicates the crack opening stress level. A physically valid U(R) function can only be obtained by crack closure measurements.

The ΔK_{eff} equation can also be written as :
$\Delta K_{eff}^{*} = q\,U(R)\Delta K = U^{*}(R)\Delta K_{eff}$ with $U^{*}(R)=qU(R)$.
In terms of the polynomial U(R) equations of Elber and Schijve it leads to:
$U^{*}(R) = qa + qb\,R + qc\,R^2 = a^{*} + b^{*}\,R + c^{*}\,R^2$
(c = 0 for the Elber equation). In other words, the ratio of the constants (a^{*} /b^{*} /c^{*}) does not change. An improved correlation would require that a, b and c are multiplied with different factors. A computer program was written to arrive at an improved correlation. It recognizes that crack closure should decrease for higher R values, and disappear at R = 1, i.e. $\Delta K_{eff} \leq \Delta K$ for all R. This restricts the sum of a, b and c to:

$$a+b+c \leq 1 \qquad 4.16$$

In the computer program the constants were varied in small steps. For each combination of a and b, or a, b and c, a linear $t_{s,eq}$ versus ΔK_{eff} (= UΔK) fit was assumed with:

$$U = a + bR \text{ or } U = a + bR + cR^2 \qquad 4.17$$

The combinations were chosen such that $0 \leq U \leq 1$ for all $-1 \leq R \leq 1$.

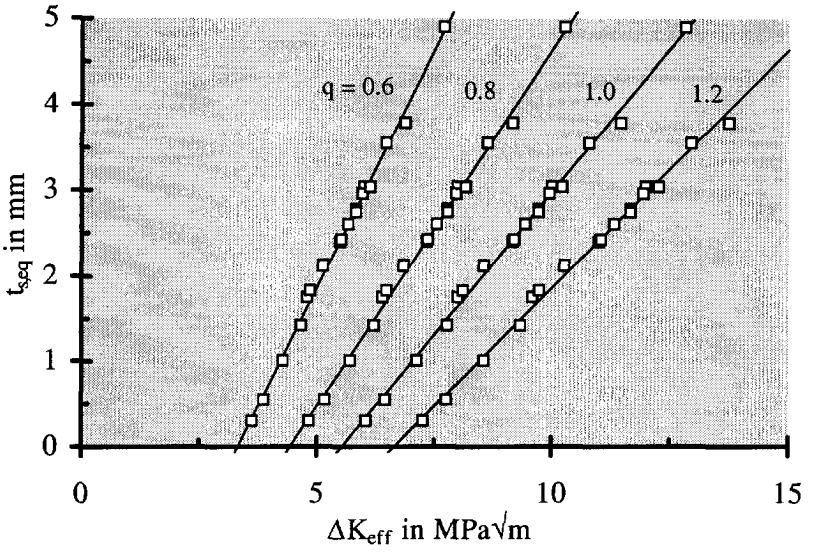

Figure 4.17. Lines with the same correlation for b/a = 0.8 (Elber).

The linear U formula showed maximum correlation for a/b = 1.22. The quadratic U formula had maximum correlation for a/b/c = 4.83/3.33/1.
The best correlations for the linear and the quadratic equation were obtained for:

$$U = 0.55 + 0.45\,R$$
$$U = 0.53 + 0.36\,R + 0.11\,R^2 \qquad 4.18$$

The ratios hardly deviate from the original ratios of Elber and Schijve, which are a/b = 1.25 and a/b/c = 4.58/2.75/1 respectively. This is not surprising, because the correlation in figures 4.12 and 4.16 is already very good.
In this chapter Elber's U formula will be used, unless specified otherwise, since it is the simplest formula leading to a good result within the R boundaries given.

The crack closure relation of Newman
Newman [7-9] has proposed crack closure equations which include a constraint factor α. The constraint factor should account for differences between plane strain and plane stress conditions. The formulae were checked with results of constant amplitude tests on center cracked tension specimens of 2219 T851 Al alloy sheet. We will apply his formulae on our Al 2024. If the crack opening stress level is denoted as S_o an effective R is introduced by:

$$R_{eff} = S_o/S_{max} \qquad 4.19$$

The material is assumed to yield in tension when the stress is $\alpha\sigma_o$, and to yield in compression for $-\sigma_o$. The flow stress σ_o is assumed to be the average of the uniaxial yield stress and the ultimate tensile strength of the material. It has been taken here as 447.5 MPa for the Al 2024 used (see chapter 3). Plane stress or plane strain conditions are simulated in the model with $\alpha = 1$ or 3 respectively. This gives an opportunity to find the difference in shear lip behaviour in both stress situations.
Newman adopted the following equations:

$$R_{eff} = A_0 + A_1 R + A_2 R^2 + A_3 R^3 \text{ for } R \geq 0$$
$$R_{eff} = A_0 + A_1 R \text{ for } -1 \leq R < 0 \qquad 4.20$$

The coefficients, found by regression analysis, are:

$$\begin{aligned} A_0 &= (0.825 - 0.34\,\alpha + 0.05\,\alpha^2)[\cos(\pi S_{max} / 2\sigma_0)]^{\frac{1}{\alpha}} \\ A_1 &= (0.415 - 0.071\,\alpha) S_{max} / \sigma_0 \\ A_2 &= 1 - A_0 - A_1 - A_3 \\ A_3 &= 2A_0 + A_1 - 1 \end{aligned} \qquad 4.21$$

The equations will be applied here on $t_{s,eq}$ results as found in constant ΔK tests, instead of in constant amplitude tests. In all constant ΔK and R tests the shear lip width had reached its equilibrium value $t_{s,eq}$ at 35 mm crack length. As S_{max} is needed in Newman's equations it was decided to calculate S_{max} at 35 mm crack length with:

$$S_{max} = \frac{K_{max}}{\sqrt{\pi a \sec(\frac{\pi a}{w})}} \qquad 4.22$$

Using this S_{max} , values of ΔK_{eff} are calculated for all tests:

$$\Delta K_{eff} = U_N \Delta K \quad \text{with } U_N = \frac{1 - R_{eff}}{1 - R} \qquad 4.23$$

and $t_{s,eq}$ is plotted as a function of these ΔK_{eff} values in figure 4.18. According to equations 4.21 the value of ΔK_{eff} is influenced by the constraint parameter α. The results have been plotted in figure 4.18 for plane stress with $\alpha = 1$ and for plane strain with $\alpha = 3$.

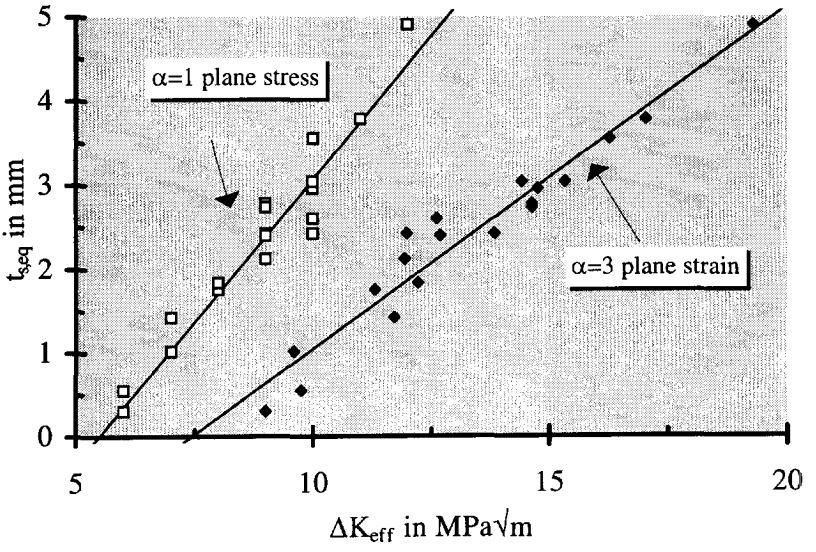

Figure 4.18. $t_{s,eq}$ versus ΔK_{eff} using the crack closure model of Newman for plane stress and plane strain.

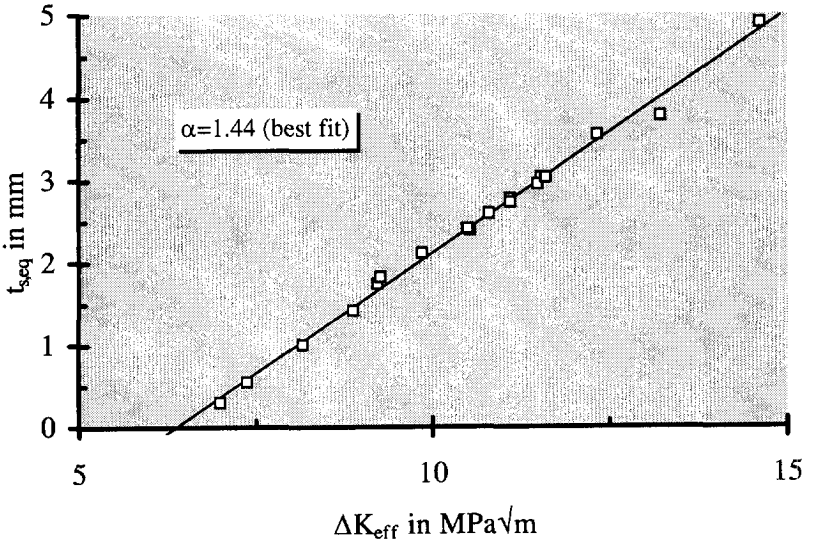

Figure 4.19. $t_{s,eq}$ versus ΔK_{eff} using the crack closure model of Newman.

Neither of both α values leads to a high correlation coefficient. The best result is found for $\alpha = 1.44$ as shown in figure 4.19. Newman used $\alpha = 1.8$ for correlating

da/dN versus ΔK_{eff} at different R ratios. In figure 4.20 it is shown that this α value correlates $t_{s,eq}$ versus ΔK_{eff} data less well than $\alpha = 1.44$.

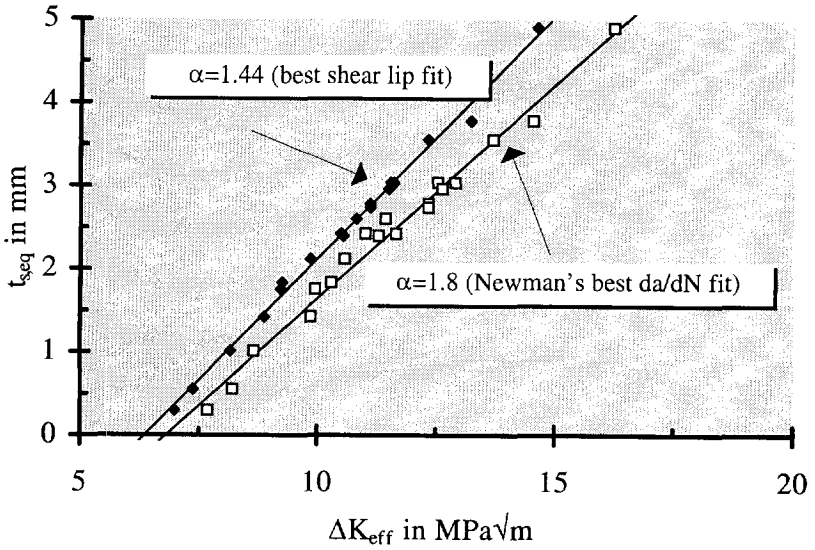

Figure 4.20. $t_{s,eq}$ versus ΔK_{eff} using the crack closure model of Newman.

Apart from the fact that two different Al alloys are compared, this result can be qualitatively explained if one thinks that the da/dN correlation was performed by Newman with results of constant amplitude tests.
It is unlikely that the equilibrium value of the shear lip width, $t_{s,eq}$, was reached in these tests, where $\Delta K_{(eff)}$ was continually increasing. The shear lip width then lags behind the current ΔK_{eff} development.
As a consequence the fracture mode in a constant amplitude test is thus more in the tensile mode than it will be for a constant ΔK test. The $t_{s,eq}$ data have been obtained with the latter type of tests. If it is assumed that shear lips often occur in a plane stress situation, and that the tensile mode is favoured by plane strain, it will be obvious that α for the best $t_{s,eq}$ - ΔK_{eff} fit is lower (more plane stress) than α for the best da/dN - ΔK_{eff} fit.

4.3. Prediction of Shear Lip Width at Constant ΔS and R Loading

For crack growth under constant ΔK and R loading it was found that the shear lip width development could be described by equation 4.5. When a constant stress amplitude (constant ΔS) is applied, at constant R, the ΔK_{eff} will increase

continuously during the crack growth. The "constants" $t_{s,eq}$ and c in equation 4.3 will change too because they are functions of ΔK_{eff}. Now equation 4.5 cannot be used to predict the width of shear lips as a function of the growing crack length (a). Thus t_s lags behind the equilibrium value $t_{s,eq}$.
A numerical incremental method is used to predict the width of shear lips in this case. It is based on the formula:

$$t_s(a + \Delta a) = t_s(a) + \frac{dt_s}{da}\Delta a \qquad 4.25$$

For every small increment Δa the values of ΔK_{eff}, $t_{s,eq}$, c and $\frac{dt_s}{da}$ are calculated with equations 4.6, 4.7, 4.9 and 4.3 respectively, and substituted in equation 4.25 to find the new t_s. It implies that for each small interval of crack growth (Δa) the prediction is made in the same way as for a constant ΔK test.
The predictions are verified with the results of five constant amplitude tests (see the following table).
The tests were carried out on 6 mm thick specimens. In figure 4.21 the result is shown for a test with a constant S_{max} = 120 MPa and R = 0.1. The test was started in the tensile mode at a = 10 mm reached by a careful prefatigue period with $\Delta K_{eff} \leq 5$ MPa$\sqrt{m}$. In figure 4.22 the result is shown for similar conditions, except R = 0.4. The prediction is quite good for both tests.

Test	initial condition	S_{max}	R	figure
1	10 mm prefatigue	120 MPa	0.1	4.21
2	10 mm prefatigue	120 MPa	0.4	4.22
3	2.5 mm saw cut	120 MPa	0.1	4.23
4	2.5 mm sawcut	120 MPa	0.4	4.24
5	10 mm saw cut	120 MPa	0.1	no figure

The prediction is not satisfactory in the two following cases, shown in figures 4.23 and 4.24. Here the same tests (S_{max} = 120 MPa, R = 0.1 or R = 0.4) were performed, starting from a sawcut of about a = 2.5 mm notch length. It was not possible to predict the shear lip behaviour from the sawcut beginning. When the prediction was made starting at about 10 mm crack length for R = 0.1 and 14 mm for R = 0.4 the results fitted the prediction reasonably well. The start-value of t_s is non-zero now.

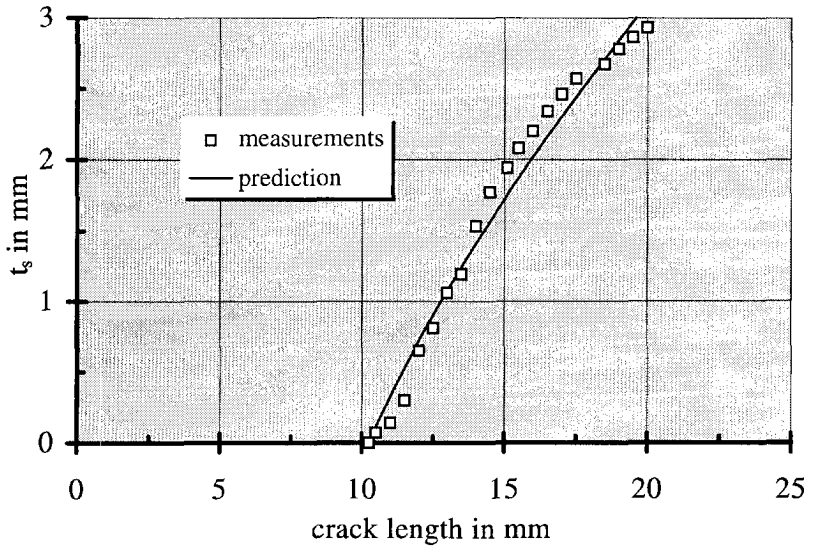

Figure 4.21. Constant amplitude test, S_{max}=120 MPa , R = 0.10.

A sawcut has two effects. First the K-factor might be lower due to the blunt notch. Secondly, there are no mode I residual stresses on the crack flanks of the sawcut. Thus at the start of fatigue crack growth there is no closure effect and ΔK_{eff} is about equal to ΔK, i.e. larger than for a fatigue crack. Unfortunately da/dN values were not available for these tests in order to check this conjecture. The second effect is probably more important than the first one, as shear lips are detected immediately after crack growth started from the sawcut (see figures 4.23 and 4.24).

The two series of data points in figure 4.23 are due to scatter between the left and right cracks in the same specimen. The (small) shear lip starts at a = 2.35 mm in figure 4.23. The value of ΔK_{eff} using equation 4.6 is now 4.1 MPa$\sqrt{m}$. This value is too small for shear lips, because equation 4.7 predicts ΔK_{eff} = 5.5 MPa$\sqrt{m}$ for the beginning of shear lips. The first sawcut effect mentioned before would make the value of 4.1 MPa$\sqrt{m}$ even lower, so this effect cannot explain the presence of shear lips.

The second effect implies that $\Delta K_{eff} \approx \Delta K$ at the start. For a = 2.35 mm a value of ΔK = 6.2 MPa$\sqrt{m}$ is obtained. This effect thus can explain the immediate presence of the shear lips, because ΔK_{eff} is high enough for creating visible shear lips.

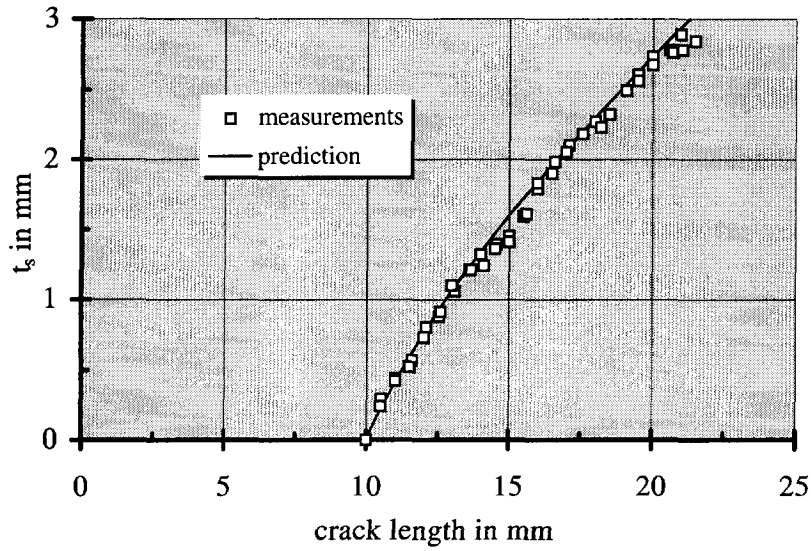

Figure 4.22. Constant amplitude test, S_{max}=120 MPa , R = 0.40.

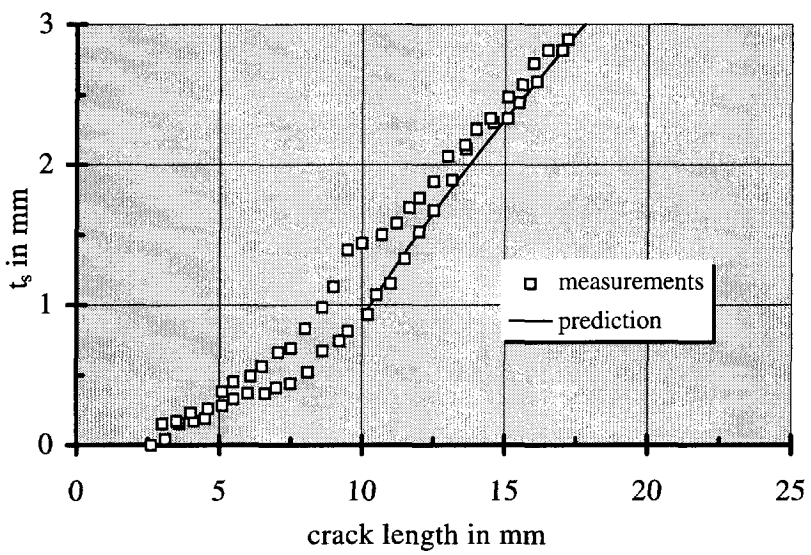

Figure 4.23. Constant amplitude test, S_{max}=120 MPa , R = 0.10, start at sawcut at 2.5 mm.

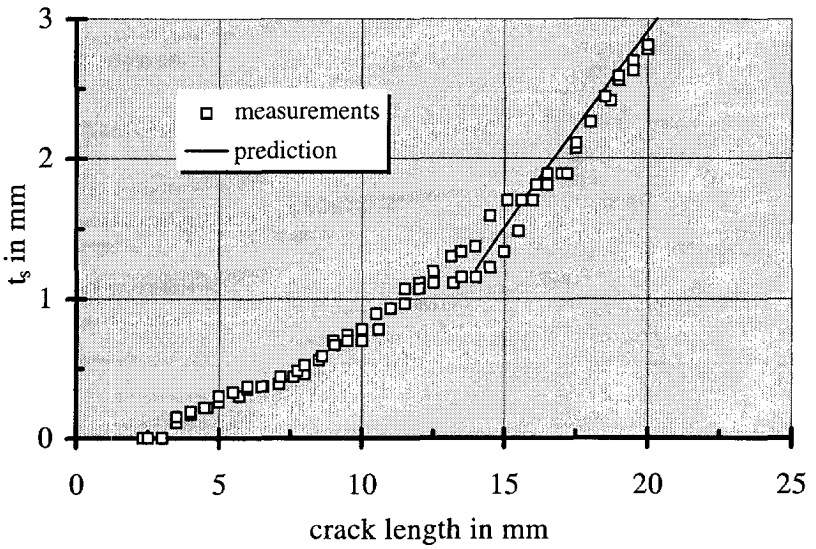

Figure 4.24. Constant amplitude test, S_{max}=120 MPa , R = 0.40, start at sawcut at 2.5 mm.

An extra complication for an accurate prediction of t_s lies in the use of equation 4.9. The inaccuracy in c becomes higher for lower values of ΔK_{eff} (or $t_{s,eq}$). This may be clear from the following. The consequence of a low $t_{s,eq}$ is a fast rising t_s (a) curve, see for example figure 4.9. The fit from which c is evaluated is now based on only a few data points before $t_{s,eq}$ is reached. The parameter c is found from the fast rising part of the t_s (a) curve.

Thus at a low ΔK_{eff} ($t_{s,eq}$) the c evaluation is based on only a few measurement points leading to a larger inaccuracy than at higher ΔK_{eff}. $t_{s,eq}$ can be found accurate for these cases, but there is a range of c values with about the same correlation.

For very high ΔK_{eff} this effect is reversed, now c can be found more accurately and $t_{s,eq}$ less accurately than at lower ΔK_{eff}.
The tests shown in figures 4.21 and 4.22 have been started at 10 mm crack length. The ΔK_{eff} values at the start of the constant amplitude crack growth are now 10.6 MPa$\sqrt{m}$ and 8.6 MPa$\sqrt{m}$ respectively. Parameter c can be found accurate for these ΔK_{eff} values. Besides that, the c has a value now that alters only slightly when ΔK_{eff} changes. In this region a ΔK_{eff} that is twice as high

only shows a little reduction of c (see figure 4.13).
In view of the foregoing it is not surprising that a fifth test, performed at S_{max} = 120 MPa and R = 0.1 and with a beginning of constant amplitude crack growth from a sawcut of 10 mm length, predicted the results quite well, comparable to figure 4.21. The results of both tests were qualitatively compared by viewing both fracture surfaces with the naked eye. No further measuring of t_s (a) for the last test was performed.

4.4 Non-Equilibrium Crack Growth Rate at Increasing Shear Lip Width

The equilibrium behaviour is covered by chapter 5, but in this section the non-equilibrium da/dN behaviour during shear lip growth in a constant ΔK test is studied. Some examples are shown in figures 4.25 and 4.26. During the shear lip development at constant ΔK_{eff} a decrease in the crack growth rate was observed. After a large initial decrease periodic variations in crack growth rate were observed, although a constant ΔK_{eff} was applied. Also changes in the crack growth direction were observed. The minima in the crack growth rate appeared to coincide with the sudden changes in direction of crack growth (although it is difficult to be sure using the potential drop method for crack length measurement, because the up-and-down cycles in the crack growth rate were rarely exactly in phase on both sides of the specimen).
In order to describe the da/dN decrease, a proportionality between the change of the crack growth rate and the change of the shear lip width is assumed:

$$d\left(\frac{da}{dN}\right) = k\, dt_s \qquad 4.26$$

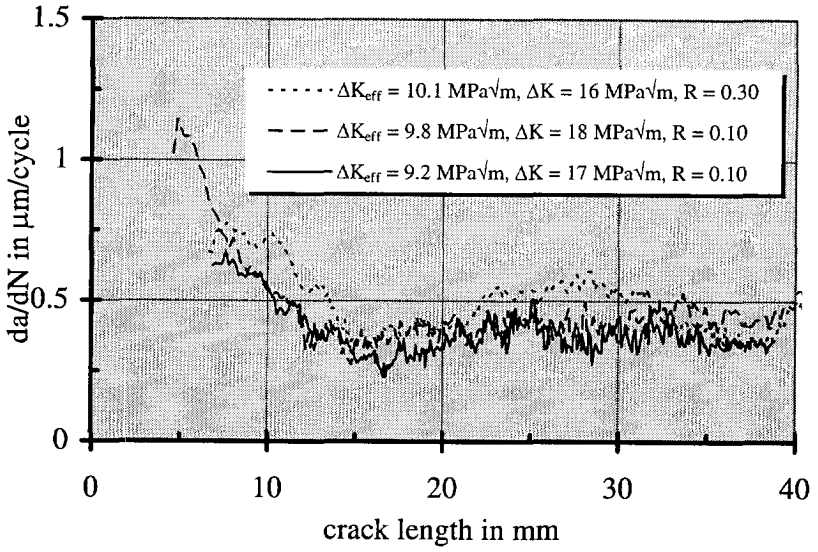

Figure 4.25. Some constant ΔK tests at 10 Hz.

The variation of the crack growth rate da/dN during shear lip development, starting at $a = a_0$ and $t_s = 0$, can be given as:

$$\frac{da}{dN} = \left(\frac{da}{dN}\right)_{tens} - \int_{a_0}^{a} \frac{d}{da}\left(\frac{da}{dN}\right) da \qquad 4.27$$

$\left(\frac{da}{dN}\right)_{tens}$ is the crack growth rate at the beginning of crack growth under a constant ΔK_{eff}, i.e. when the crack surface is still completely in the tensile mode. For $t_s = t_{s,eq}$, the crack growth rate is indicated as $\left(\frac{da}{dN}\right)_{eq}$. With t_s according to equation 4.4 this leads to:

$$\frac{da}{dN} = \left(\frac{da}{dN}\right)_{tens} - \left(\left(\frac{da}{dN}\right)_{tens} - \left(\frac{da}{dN}\right)_{eq}\right)\left(1 - e^{-c(a-a_0)}\right) \qquad 4.28$$

This formula gives an estimate of the curve to be expected, but it cannot describe the waviness in the crack growth rate observed in figures 4.25 and 4.26, i.e. the process of a large decrease followed by small increases and decreases in the crack velocity during the remainder of the shear lip development.

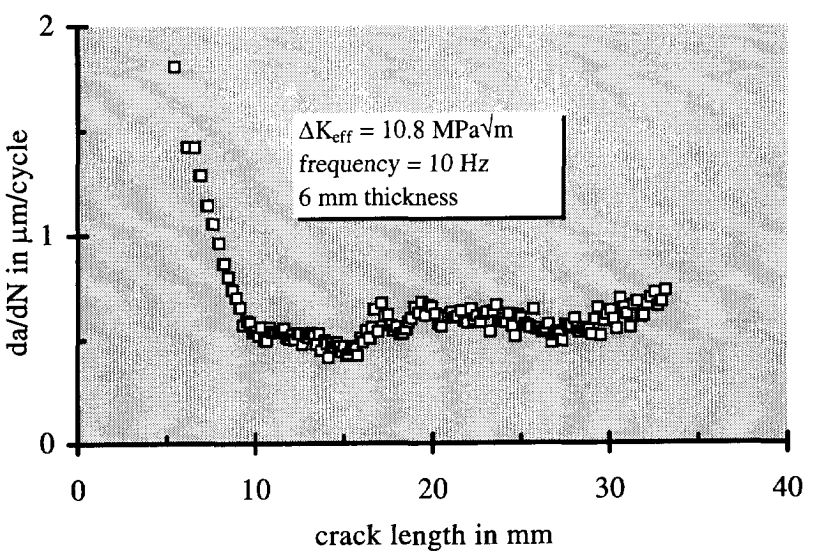

Figure 4.26. da/dN decrease during a constant ΔK_{eff} test.

One characteristic test (the da/dN result is shown in figure 4.26 and the fracture surface in figure 4.27) will be described in detail, the other tests at 10 Hz showed analogous behaviour. First a few related topics will be discussed.

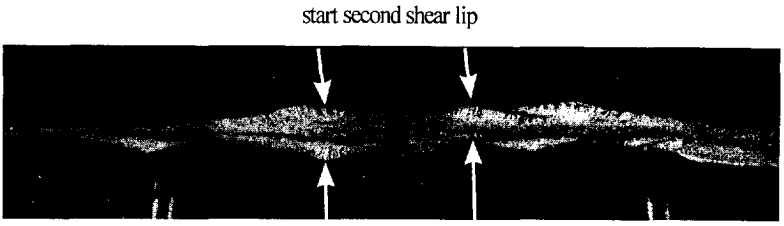

Figure 4.27. Fracture surface of the test shown in figure 4.26.

Asymmetry of plastic zones

It was found earlier [15] that asymmetry in the plastic zone might be associated with the presence of shear lips. To investigate this question two tests were performed. In the first specimen two 18.5 mm long notches were made by spark erosion. Next a small fatigue crack was grown with a low amplitude. The crack now was in the tensile mode, i.e. the plane of the crack was normal to the loading direction. In the second specimen notches at 45° with the surface were made.

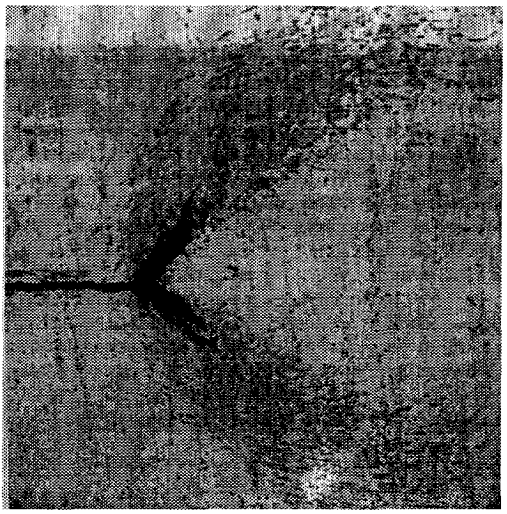

Figure 4.28. Symmetric plastic zone of a crack in tensile mode.

The fatigue crack was grown here with higher loads so that the crack remained slant. After polishing the specimens were treated with a photographic lacquer. Both specimens were loaded to 85 kN. After loading they were immersed in warm water (70°C) for about 2.5 minutes. This procedure caused small cracks in

the lacquer on places where the material had been strongly plastically deformed. With a microscope (magnification about 24x) the photographs shown as figures 4.28 and 4.29 were made. A model of the plastic zone shapes for single and double shear is shown schematically in figure 4.30.

Explanation of crack growth deviation

Because of this asymmetry in the plastic zone, intense plastic deformation builds up in the direction in which the crack grows when a shear lip develops. If a large shear lip develops this plastic deformation is probably intense enough (much strain hardening) to stop crack growth in that direction. Crack growth then starts (reinitiates) again with shear lip growth on another plane at 45° to the plate surface making an angle of about 90° with the first shear lip.

Another reason for crack growth stopping in a particular direction might be the closure behaviour of the large shear lip. Crack growth continues in another direction that lowers the amount of closure.

Probably both reasons will apply (see also section 4.8, page 88).

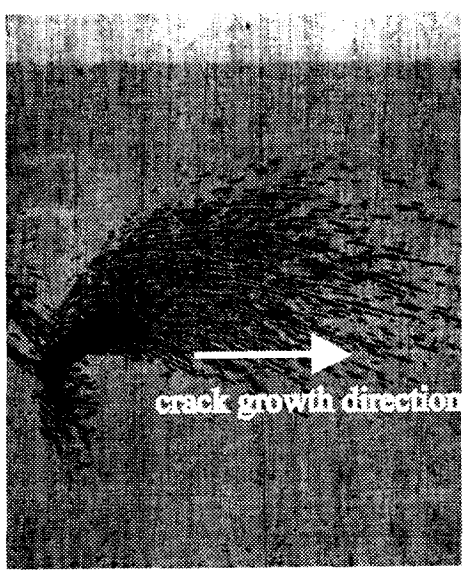

Figure 4.29. Asymmetric plastic zone of a crack in shear mode.

As shown in figure 4.27 a reinitiation on another shear lip plane (under about an angle of 90° with the first one, if shear lips are assumed to make 45° with the loading direction) occurs. In most specimens multiple reinitiations are observed and a zig-zag growth of the crack is then found.

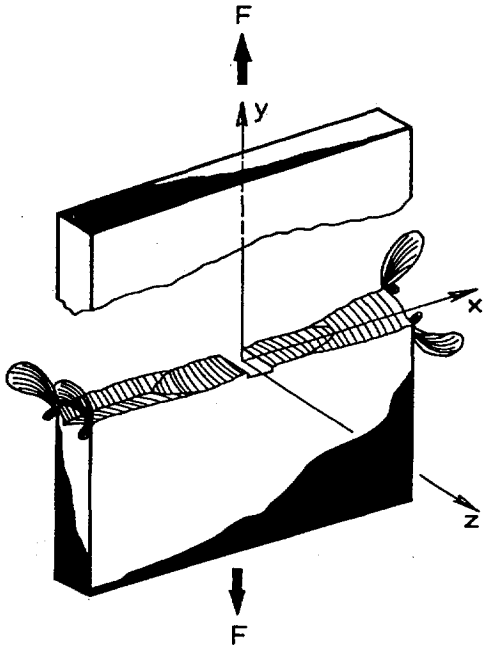

Figure 4.30. A sketch of asymmetric plastic zone development in single and double shear.

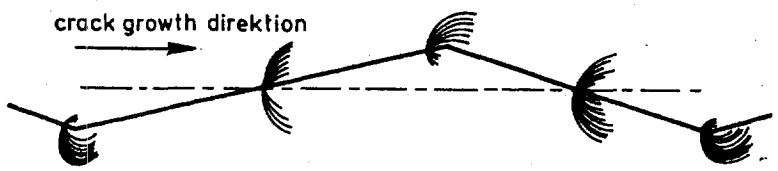

Figure 4.31. A possible explanation of the changes in direction of crack growth by growing asymmetry in the plastic zones.

The process is shown schematically in figure 4.31. In figure 4.32 an example is shown of the change in direction of the crack growth at the start of a new shear lip.

There is a difference in the change of the crack growth direction for single and double shear lips. Cracks growing in fully developed double shear, i.e. $t_{s,eq} \geq t/2$, are no longer growing in a direction perpendicular to the loading direction. The roof type double shear crack grows in a downwards direction (see figure 4.33, an

explanation follows in section 4.6). If a fully slant crack is in the single shear mode the deviation does not occur and the crack growth direction remains perpendicular to the loading direction.

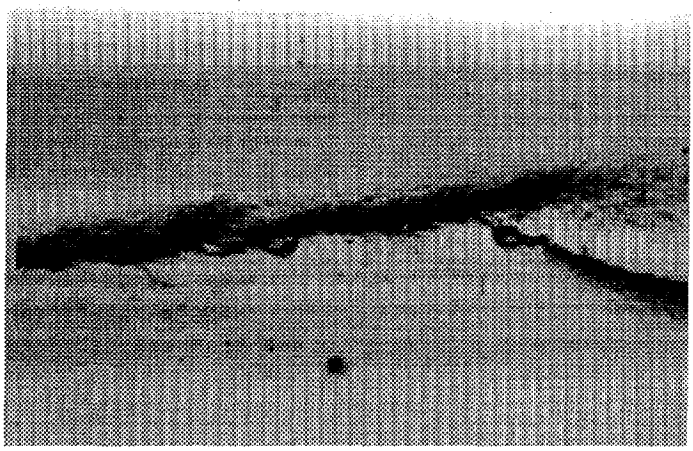

Figure 4.32. Change in crack growth direction.

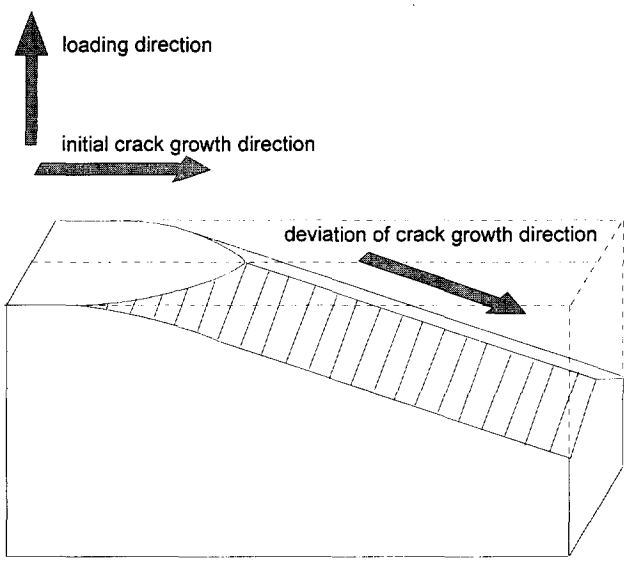

Figure 4.33. The deviation crack growth direction of a double shear fracture surface.

For single shear lips the crack path remains straight, with the crack growth direction perpendicularly to the loading direction, as the shear lips are now at both sides of the fracture. A similar behaviour of the growth direction in case of single and double shear lips was also observed in reference [17].

Discussion of the da/dN behaviour in a constant ΔK test with developing shear lips

We will discuss a test for which the da/dN behaviour is shown in figure 4.26 and the fracture surface in figure 4.27. The t_s variation was shown earlier in figure 4.7. For this test a steep decrease in da/dN until a crack length of about 9 mm is found. Hereafter the decrease of the growth rate is far less until about 15 mm, followed by a small increase until a crack length of about 18 mm.

From the shear lip width results given in figure 4.7 it is not clear what causes the change of the growth rate gradient at 9 mm crack length. However, the beginning of a more or less stationary crack growth rate at a = 18 mm seems to be confirmed in figure 4.7, because at a = 18 mm the shear lip width t_s is about 3 mm. This means that in the 6 mm plate complete shear is achieved.

Macroscopic examination of the fracture surface (see figure 4.27) shows that from 6 to about 9 mm shear lips are growing from the surfaces of the specimen to the middle. One side of the specimen fracture surface is in double shear, the other side is in single shear. At a = 9 mm a little shear lip is developing into the already existing shear lip from the surface of the specimen.

The two shear lips make an angle of about 90°. This phenomenon was discovered at both sides of the specimen with respect to the central hole, thus on the single shear and on the double shear side. (Note that in reality shear lip angles were found to vary between about 20° to 42° depending on ΔK_{eff} [20]. Deviations of shear lip angles from 45° are neglected in this work. Only "ideal" shear lips with 45° angles are considered.)

A deviation of the crack growth direction was clear at the side surface of the specimen, in the area of the developing shear lip [10].

At a = 9 mm a sudden change in the deviation was noticed, due to initiation of the second shear lip. This effect can be explained by the growing asymmetry of the plastic zone sizes in the case of growing shear lips, as was already discussed.

If equation 4.28 is used to predict the da/dN versus the crack length, figure 4.34 is obtained. For $\left(\frac{da}{dN}\right)_{tens}$ the beginning of da/dN in tensile mode is used. For $\left(\frac{da}{dN}\right)_{eq}$ a value of 0.45 μm/cycle is estimated. This is an approximation as $t_{s,eq} >$ t/2 in this case.

It is seen from figure 4.34 that the growth rate prediction is poor. A number of possible explanations of the crack growth rate behaviour will be discussed. The decrease in da/dN as observed from 6 to 9 mm is ascribed to the growing of the shear lip from the surface leading to a longer transverse crack front length and thus to more resistance against crack growth.

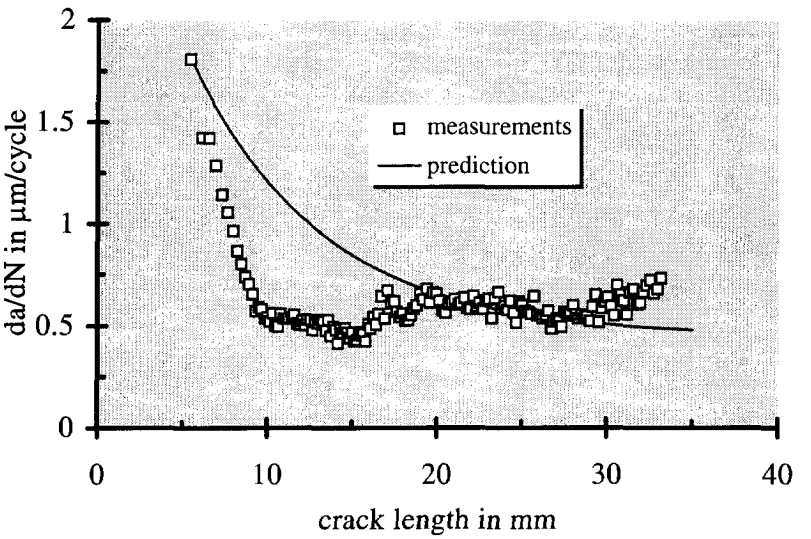

Figure 4.34. Application of equation 4.28 for prediction of fatigue crack growth rate.

From 9 to 18 mm crack length the (total) shear lip width is still increasing, so the first reason still holds. However the second shear lip, starting to grow into first one, at first flattens the crack front leading to a little lower transverse crack front length. Hereafter the transverse crack front length remains more or less the same. Other test specimens from fatigue tests at 10 Hz showed an analogous behaviour.

Another explanation of the da/dN behaviour is based on the increasing closure due to shear lips. The principle of it is shown in figure 4.35.
The extra closure due to shear lips increases with the shear lip width until the shear lip is flattened by the initiation of a new shear lip in the old one. So the closure is expected to increase from 6 to 9 mm and then to slowly decrease when the second shear lip flattens the old one.
The decrease and temporary increase of da/dN suggest a decrease and increase of a local crack closure effect (i.e. ΔK_{eff}), and to add it to the constant applied ΔK_{eff} ,using Elber's crack closure formula, that is responsible for the prediction of da/dN as shown in figure 4.34. The principle of the ΔK_{eff} correction is shown in figure 4.36.

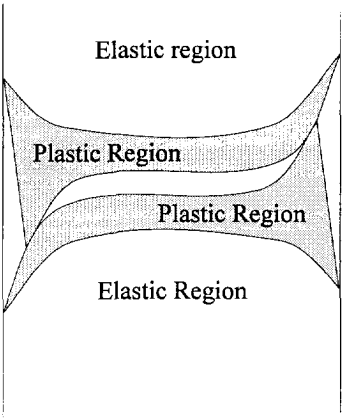

Figure 4.35. Principle of extra closure due to shear lips (from reference [11]).

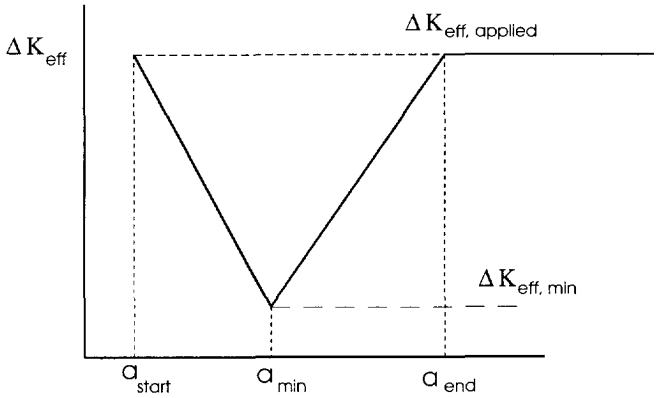

Figure 4.36. ΔK_{eff} varies linearly during the shear lip development with a minimum ΔK_{eff} at the start of a second shear lip.

The resulting da/dN is shown in figure 4.37. Again equation 4.28 was applied, but now the corrected value of ΔK_{eff} was used. A decrease in ΔK_{eff} was necessary to get the fit result shown (from ΔK_{eff} = 10.8 MPa$\sqrt{m}$ (applied value) to ΔK_{eff} is 9.7 MPa$\sqrt{m}$ (minimum value at about 9 mm crack length)). The values taken for a_{start} and a_{end} (see figure 4.36) were 6 mm and 18 mm respectively.

The results of the test discussed seem to point to the fact that crack growth stops in one direction, after the start of a new shear lip growing into the old one. The reasons for the decrease in da/dN at growing shear lip widths will be further discussed in chapter 5.

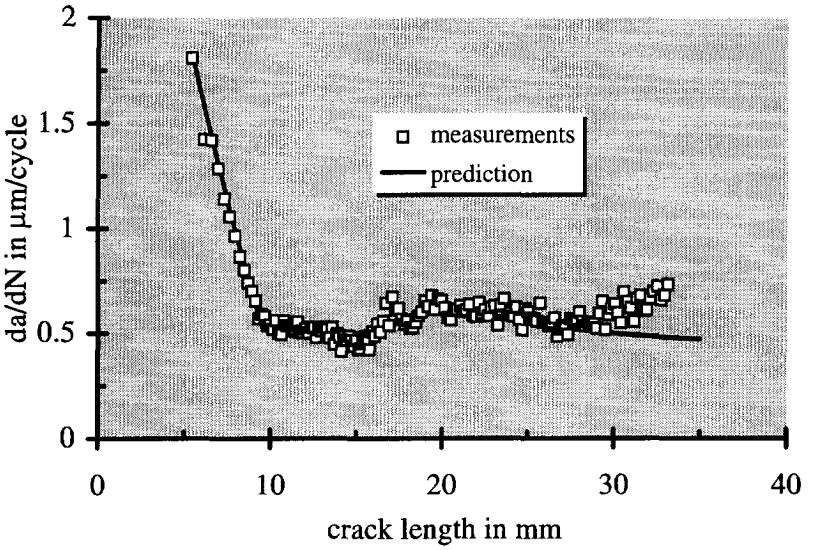

Figure 4.37. Crack growth rate prediction using equation 4.28 and a ΔK_{eff} versus crack length function as shown in figure 4.36.

4.5. Frequency Effects and Slant Fatigue Crack Growth

4.5.1. Effect on shear lip width

The $t_{s,eq}$ results in table 4.1 were obtained in tests performed at 10 Hz. The analysis has led to equation 4.7 which gives $t_{s,eq}$ as function of ΔK_{eff} (Elber). In the present section some tests at other frequencies are discussed. The results of these tests together with that at 10 Hz will be combined to present a more general $t_{s,eq}$ formula. The tests at other frequencies all were performed at a constant value of $\Delta K = 18$ MPa$\sqrt{m}$ and $R = 0.1$ ($\Delta K_{eff} = 9.72$ MPa$\sqrt{m}$), thus the mechanical parameters are kept constant in these tests. The frequencies varied from 17.5 Hz to a frequency as low as 0.05 Hz. The results are given in table 4.2. The results of $t_{s,eq}$ in figure 4.38 show that smaller equilibrium shear lips are found at lower frequencies. The results suggest a linear relation between $t_{s,eq}$ and log(frequency):

$$t_{s,eq} = 0.67\log(f) + 2.19 \qquad 4.29$$

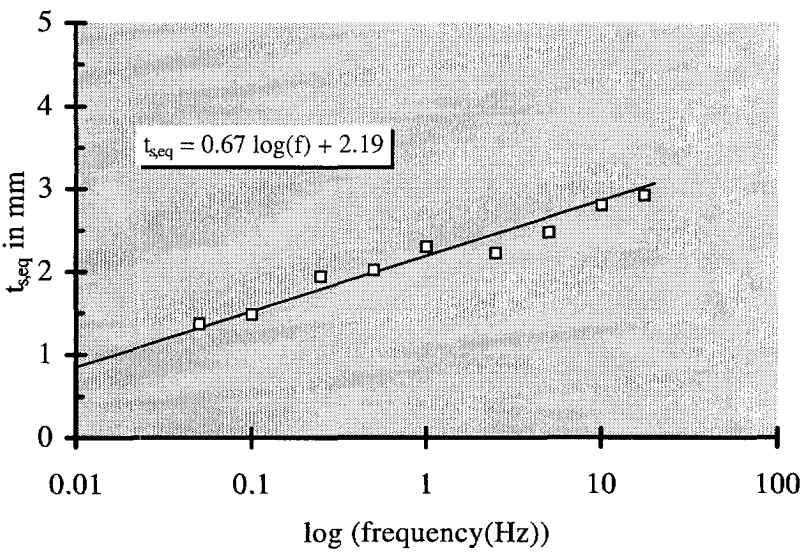

Figure 4.38. $t_{s,eq}$ results at different frequencies.

This linear dependence implies that $\frac{\partial t_{s,eq}}{\partial(\log(f))}$ = constant for constant ΔK_{eff}.

Earlier it was shown (equation 4.7)) that $\frac{\partial t_{s,eq}}{\partial(\Delta K_{eff})}$ = constant for a constant frequency of 10 Hz . Both results suggest that $t_{s,eq}$ should be described as a function of two independent variables, ΔK_{eff} and log(f):

$$t_{s,eq} = c_1 \Delta K_{eff} + c_2 \log(f) + c_3 \qquad 4.30$$

where c_1, c_2 and c_3 are constants. A computer program for a three parameter fit was written and applied on the first 23 test results of table 4.1, the test results that were found by the fitting procedure described earlier, at 10 Hz, and on the test results of table 4.2 at ΔK_{eff} = 9.72 MPa$\sqrt{m}$ and different frequencies. The best correlation was found for:

$$t_{s,eq} = 0.67 \Delta K_{eff} + 0.64 \log(f) - 4.35 \ \text{(mm)} \qquad 4.31$$

Note that we do not find exactly the same equations, 4.31 and 4.7, by substituting ΔK_{eff} = 9.72 MPa$\sqrt{m}$ or f = 10 Hz respectively. The reason is that the 3 dimensional fitting is based on more data then the separate procedures.

Another test was done later outside the range of test conditions covered by equations 4.7 and 4.29. This test was carried out with ΔK = 22.2 MPa$\sqrt{m}$ and R = 0.1 at 0.1 Hz; ΔK_{eff} = 10.8 MPa$\sqrt{m}$ in this case. The same test had already been done for 10 Hz. The $t_{s,eq}$ value at 10 Hz was 3.55 mm. At f = 0.1 Hz $t_{s,eq}$ = 2.16 mm was measured. Equation 4.31 gives $t_{s,eq}$ = 2.23 mm in this case, which is a deviation of about 3% with respect to the measured value, which is quite a good agreement. Of course more tests should be done for a more accurate version of equation 4.31.

4.5.2. Effect on da/dN

During most tests (table 4.1 and table 4.2) da/dN data as a function of the crack length were also obtained. An example for a constant ΔK test at 2.5 Hz is shown in figure 4.39. It is obvious from the figure that da/dN decreases after the start of the constant ΔK and R test. During this process the shear lip width t_s increases. The prefatigue period was performed with a low ΔK_{eff} to keep t_s = 0 mm.
In figure 4.39 a $(da/dN)_{tensile}$ is defined. This $(da/dN)_{tens}$ is an unstable da/dN value found at ΔK_{eff} = 9.72 MPa$\sqrt{m}$ and t_s = 0 mm (tensile mode). The value is found by a linear extrapolation as shown in the figure. In figure 4.40 the frequency effect is illustrated by showing crack growth rate results for 2 different frequencies for ΔK_{eff} 9.72 MPa$\sqrt{m}$. It appears that the same da/dN in tensile mode is indicated by the two tests.

For all tests mentioned in Table 4.2, the crack growth rate $(da/dN)_{tens}$ was determined at the beginning of the constant ΔK test. Secondly, the da/dN found after 10 mm of crack growth, $(da/dN)_{10}$, was also measured. The 10 mm crack extension has been chosen since in all tests the decrease in da/dN had ended (or da/dN showed a (relative) minimum) after this period of crack growth. See for example the results given in figures 4.25, 4.26, 4.39 and 4.40. However not in all tests had the shear lip width stabilized at the minimum value of da/dN, i.e. $t_{s,eq}$ using equation 4.4 had not been reached yet.

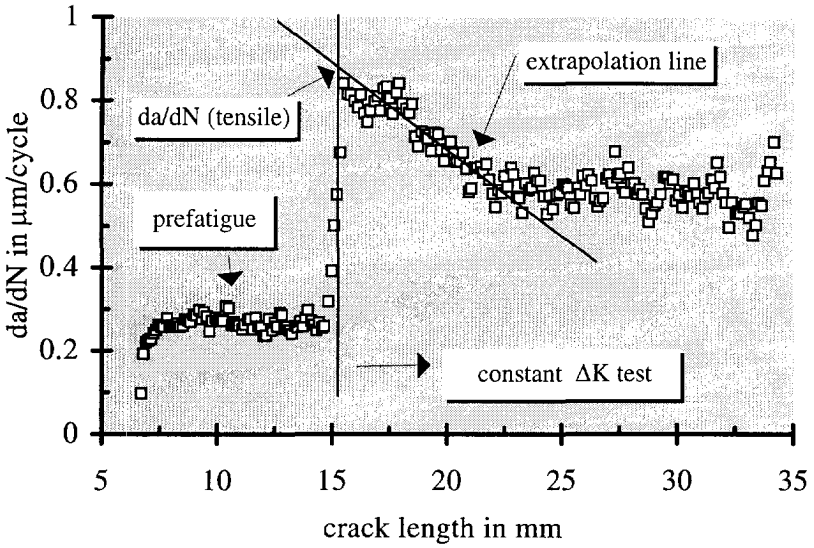

Figure 4.39. da/dN versus a for ΔK_{eff} = 9.72 MPa$\sqrt{m}$, ΔK = 18 MPa$\sqrt{m}$, R = 0.10 and frequency = 2.5 Hz, specimen thickness t = 6 mm.

In figure 4.41 $(da/dN)_{tens}$ and $(da/dN)_{10}$ are plotted against the frequency. A noteworthy observation is that the tensile crack velocity seems to be independent of the frequency, whereas the shear crack growth rate, $(da/dN)_{10}$, is not.
The results indicate that for the present material/environment combination the frequency influence on the crack growth rate must be associated with shear lip development, i.e. when ΔK_{eff} is too low for shear lips, there is no frequency effect. To check the observation that tensile mode cracking is frequency independent, three additional tests were performed at 0.1, 1 and 10 Hz at ΔK_{eff} = 5 MPa$\sqrt{m}$ in which case the fracture surface was expected to remain tensile. The latter was indeed the case. The crack velocities were nearly the same which confirmed the conclusion.

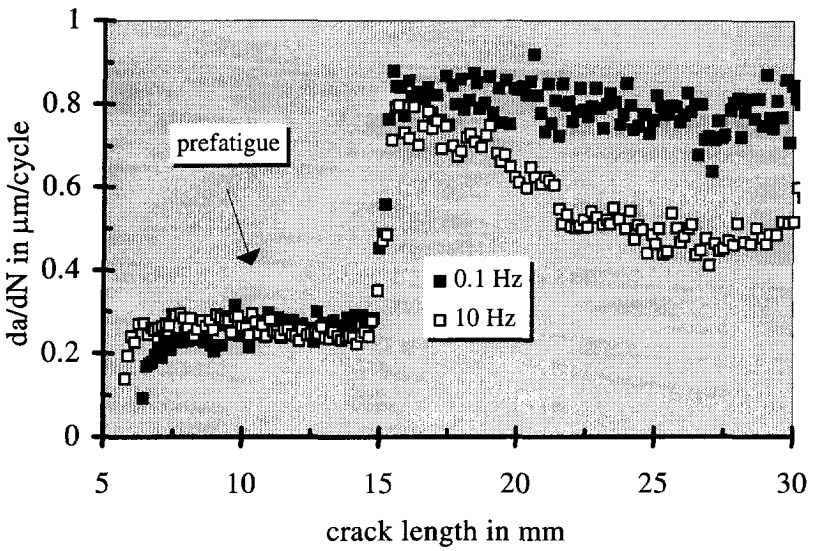

Figure 4.40. da/dN versus a at two frequencies at ΔK = 18 MPa$\sqrt{m}$ and R=0.10, specimen thickness t = 6 mm.

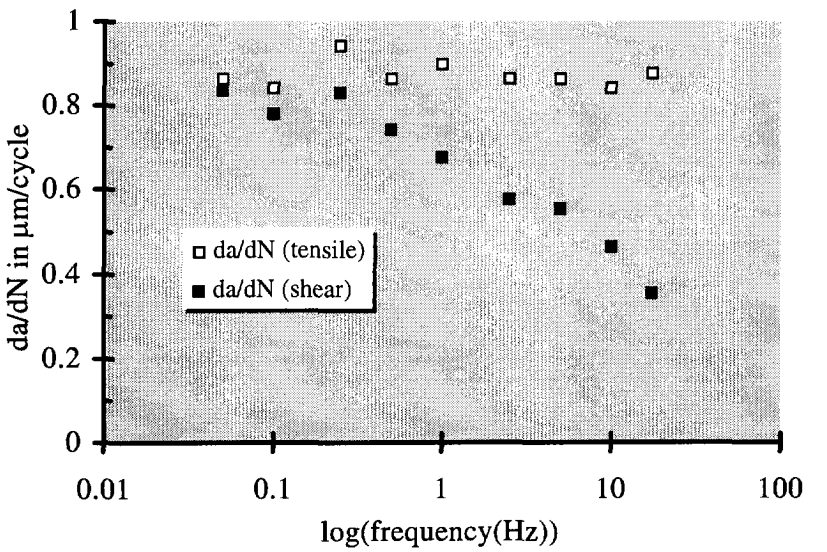

Figure 4.41. da/dN versus log(frequency) at ΔK_{eff} = 9.72 MPa$\sqrt{m}$.

Independence of the start of shear lips on K_{max}

In order to test equation 4.31 still further, five tests at increasing values of K_{max} and a constant $\Delta K_{eff} = 5$ MPa$\sqrt{m}$ have been performed at 10 Hz. No shear lips were expected or found. The tests are shown in table 4.3. The K_{max} range is from about 10 to 50 MPa$\sqrt{m}$. This is a further proof that shear lips do not depend on a plane stress situation only. Nor do they depend on the plastic zone size (in fatigue). For higher K_{max} more plane stress and a larger plastic zone size are expected, but the development of shear lips seems to be independent of K_{max} .It is a very strange result that development of shear lips is not dependent on K_{max} or on the (forward) plastic zone size (as it is in "static" tests). The plane stress situation may be a necessary condition for a shear lip to start but it is certainly not a sufficient condition, not even at very high K_{max}. Shear lip development depends mostly on ΔK_{eff} .

Shear lips and the frequency effect

It is a remarkable observation that our results indicate no frequency effect for crack growth in the tensile mode, whereas a systematic frequency effect appears to occur if shear lips are present. In figure 4.40 two tests with frequencies of 0.1 and 10 Hz are shown, i.e. the frequency changes over 2 decades, while da/dN is then reduced by approximately a factor of 2. It implies that the decrease cannot simply be a matter of "time under load". The crack growth rate da/dt (= da/dN*frequency), in terms of μm/second, is much more affected by the frequency than da/dN. Nevertheless, if there is a frequency effect, there must be a time dependent phenomenon with some influence on the crack extension per cycle. Possibly, there is a time dependent environmental contribution to crack growth, but we will not further speculate on this issue here.

4.6. Shear Lips on Fracture Surfaces Created During (Static) Tensile Tests

In this section shear lips on fracture surfaces as obtained in tensile tests will be discussed. The shear lip width of fatigue tests is frequency dependent as was shown in section 4.5. Using equation 4.31 it can be found that higher frequencies lead to higher $t_{s,eq}$ values at the start of shear lip growth and thus in general to higher da/dt values. Thus higher $t_{s,eq}$ values can be correlated with higher da/dt values. In order to find an upperbound behaviour for shear lips it was decided to perform tensile tests. A tensile test is considered to represent a (very short, ½ cycle) fatigue test resulting in a very high da/dt. The "frequency" is considered high due to the very short crack growth time and the corresponding high crack growth rate and high crack length increase.
Thus the tensile test results in a very high da/dt (or "da/dN") and thus in principle in a very high shear lip width value. It is believed that when no shear lips are found in a tensile test, it will also not be found in a fatigue test, with a much lower da/dt value. Tests initiated by the author on a few different metals (Zn, Brass, Low-Carbon Steel, Al alloys (2024 and 7075), Stainless Steel) confirmed this trend [see reference [27]).

Already for a long time shear lips on static fracture surfaces are considered to be a measure for the toughness of the material. The larger the shear lip width, the tougher the material. In this investigation it was decided to do tensile tests on the same kind of specimen as used in the fatigue tests.

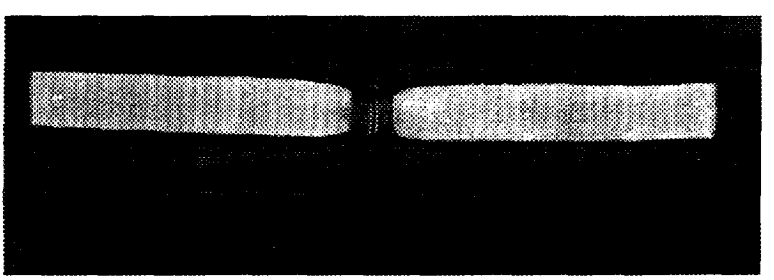

Figure 4.42. Fracture surface in single shear in a tensile test.

A number of tensile tests were performed on Al 2024 6 mm thick specimens with a central saw cut. Some of the fracture surfaces are shown in figures 4.42 to 4.44.
In figure 4.42 a single shear fracture surface is shown. The direction of the initial

"static" failure extension is still perpendicular to the loading direction, while a fully slant fracture occurred. There is no evident deviation of the direction of the fracture path from a plane transverse to the loading direction (= a symmetry plane).

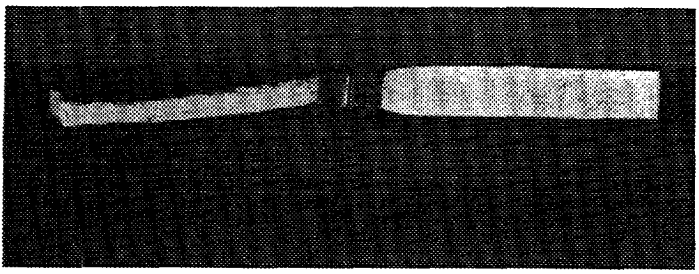

Figure 4.43. Fracture surface in single shear (right) and double shear (left).

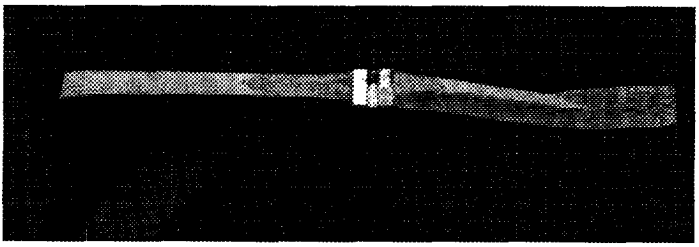

Figure 4.44. A transition from double to single shear on the right side.

In figure 4.43 the right half of the specimen is in single shear, while the other part is in double shear. The "static" double shear fracture occurred in a direction, which significantly deviates from being perpendicular to the loading direction, as found previously for fatigue cracks as well, see figure 4.33.
In figure 4.44 a transition from double to single shear is shown. The single shear part resumes the original crack growth direction transverse to the loading direction.

The zig-zag movement of the crack, as discussed in section 4.4 for fatigue cracks with large shear lips, is absent. The reason probably can be found in the time of crack growth: da/dt can theoretically be as high as the Rayleigh Wave velocity (about 3 km/s for Aluminium) [12]. However, in practice much lower values for da/dt are found, although da/dt values of several hundreds of meters per second are no exception.

A simple geometric model to explain the deviation crack growth direction in double shear mode and no deviation in single shear mode

In figure 4.45 a simple geometric model is shown to explain why a double shear crack deviates from the symmetry plane and a single shear crack does not. The crack extension direction is perpendicular to the paper and is assumed to start in the tensile mode, situation 1. The shear lip situation for a few discrete increasing crack lengths is shown.

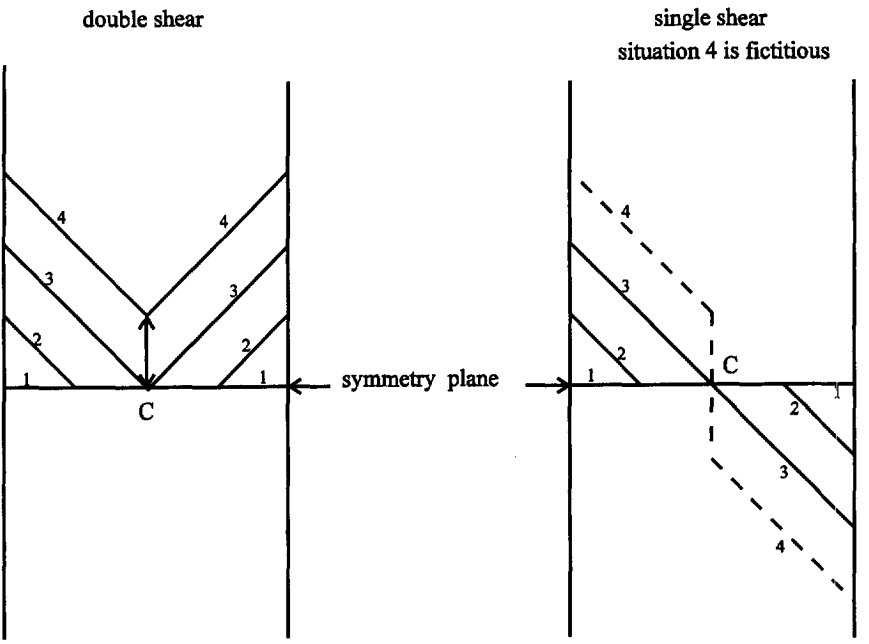

Figure 4.45. A geometric model to explain crack deviation in double shear and no crack deviation in single shear.

First the double shear situation will be discussed. A few crack growth situations have been shown in the figure. Situation 1 is in tensile mode, situation 2, at a larger crack length, is partial shear. In this situation the tensile part of the crack is still in the symmetry plane. Situation 3 shows the transverse section at a crack length with the first attainment of complete shear. The shear lips cannot become wider. There is a large asymmetry in the plastic zone size now as discussed in section 4.4. Unlike a fatigue crack, there will be in general no reinitiation (i.e. no zigzag growth) of another shear lip in most cases (one exception, however, has been chosen to show in figure 4.44, almost at the end of crack growth, as a good example that the single shear resumes the original crack growth direction).

Probably a lot of kinetic energy, due to the very fast crack growth, is also involved in the vertical (shear) crack flank movement. This energy is sufficient to avoid another crack growth direction and to overcome the resistance due to the asymmetry (another possible explanation is given in section 4.8).
The attempt for both parts of the double shear lip to become larger than half the plate thickness causes a deviation from the symmetry plane as in situation 4. See also figure 4.15. The model explains that the roof of the double shear surface always points in a direction opposite to the deviation direction. Because shear lip width in Al 2024 has a maximum size of about 5 to 6 mm [20] there should be no deviation of the crack growth direction for double shear lips in a plate with $t_{s,eq} < t/2$. This was experimentally checked in a tensile test on a center cracked tension specimen of 25 mm thickness. A situation as in figure 4.45 number 2 was found without any other deviation of the main crack growth direction.

In single shear, situations 1, 2 and 3 are comparable to the double shear case. In situation 4 a *very unlikely* situation would occur with a vertical crack surface in the middle of the specimen. This is never observed. Probably the (kinetic) energy is not enough to reach such a high energy consuming situation, as this vertical plane is parallel with the loading direction and there are no shear stresses along this plane. Thus situation 3 is the utmost of shear lip development in single shear. This means that the center C of the crack always stays in the symmetry plane, perpendicular to the loading direction, irrespective of the crack length.
Theoretically the shear lip angle can increase after the single shear situation 3. This also is not observed.

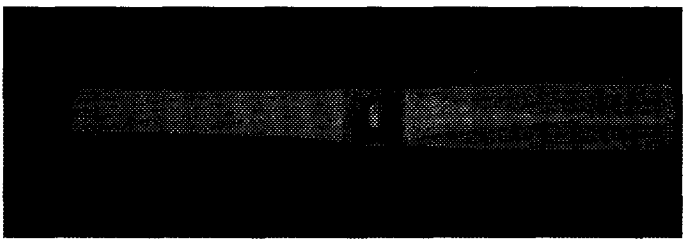

Figure 4.46. Single shear lip width development on the fracture surface of a plate with 10 mm thickness

A good example of a developing (single) shear lip width in a tensile test on a 10 mm thick specimen is shown in figure 4.46. In this 10 mm specimen a shear lip width development is clearly visible extending over several mm of crack

growth. The maximum shear lip width is smaller than 5 mm or the plate width is to low.

4.7. Effects of (Initial) Fracture Mode on Fracture Toughness and/or Stress Intensity

Throughout this work a competition is indicated between the effects of shear lips on the crack driving force (K or ΔK) and on the crack growth resistance (K_c or da/dN). In order to shed some more light on the relation between crack driving force and crack growth resistance, the influence of the fracture mode on the fracture toughness and/or stress intensity is studied in a few exploratory tests. Two kinds of "static" tensile tests have been performed.
First the critical K (= K_c) found in fatigue tests on 10.3 mm thick center cracked tension specimens of Al-2024 is discussed.
Secondly K_c (or K_{Ic}) found in a tensile test on a 12.3 mm thick compact tension specimen of Al-7075 is considered. The latter specimen normally is used for K_{Ic} tests according to the ASTM E-399 procedure [13], but the specimens have been modified here in order to compare different extremes of the fracture mode. The fatigue tests were performed in "lab air" at 10 Hz.

Fatigue tests on Al 2024 T351 specimens
A survey of the tests on the center cracked tension specimens of 2024 T351 is given in the table below. The specimens had a length of 300 mm and a width of 100 mm.

Fatigue loading parameters			Results at instability failure		
type of load	R	Number of tests	a (mm)	shear fraction	K_{max} (MPa$\sqrt{m}$)
CA	0.10	2	36.0/36.0	complete	61.8
S_{max} = 120 MPa	0.70	1	34.0	partial	56.5
S_{max} = 120 MPa	variable	1	33.5	very small	55.3
ΔK_{eff} = 5 MPa$\sqrt{m}$					

Two constant amplitude tests were performed with S_{max} = 120 MPa at R = 0.10 and R = 0.70 respectively. In these tests K_{max} increases with increasing crack length. The specimen fails when $K_{max} \geq K_c$. Also ΔK_{eff} increases as the crack grows. Complete shear (single) was found in the tests at R = 0.10, while for R = 0.70 the shear lip width was much smaller at the point of instability. The crack lengths at the onset of instability were 36.0 mm, 36.0 mm and 34.0 mm for

R = 0.10 (2 tests) and R = 0.70 (1 test) respectively.
Another test was performed with ΔK_{eff} = 5 MPa$\sqrt{m}$ and S_{max} = 120 MPa, which implies that R must increase during the growth of the crack. This was achieved by computer control of the minimum load using a potential drop signal for the crack length measurement. The applied stresses S_{max} and S_{min} , and S_{op} (using Elber's formula 4.6) are shown in figure 4.47. The fracture surface remained in the tensile mode almost until the beginning of instability. Slightly before instability occurred, the crack probably moved so fast that the pulsed direct current potential drop method was not fast enough to enable full control of the required cycle load. That means that just before instability ΔK_{eff} could increase. Very small shear lips were observed in this area.
The resulting crack length at instability for this specimen was 33.5 mm. In all tests the stress S_{max} was held at 120 MPa. This led to K_{max} values at the point of instability that are shown in the last column of the above table.
The results show that smaller shear lips and thus more tensile mode failure, has led to a smaller crack length at the moment of final failure, and thus to a lower K_{max} value at failure.

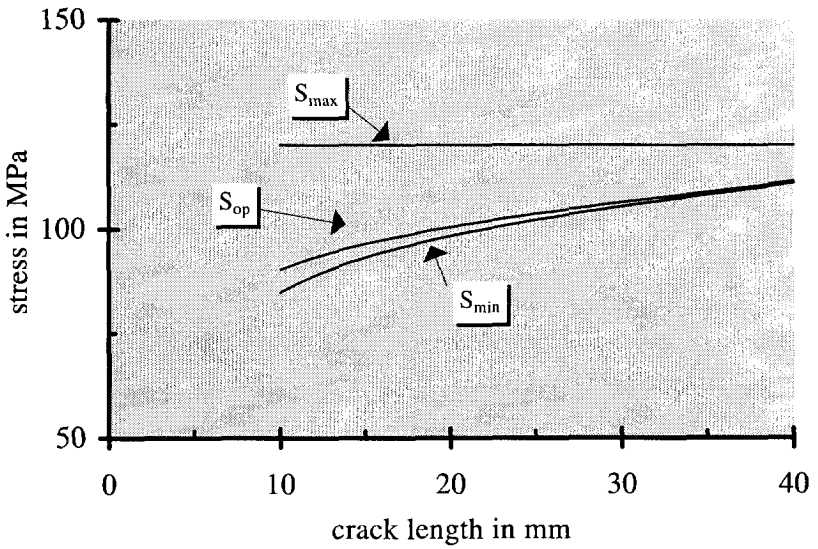

Figure 4.47. Values of S_{max}, S_{op} and S_{min} in a test with S_{max} = 120 MPa and ΔK_{eff} = 5 MPa$\sqrt{m}$.

However, the effect on the failure strength (K_{max} at fracture) is still fairly small. Note that for the ductile 2024 T351 alloy the K_{max} values are well above the valid K_{Ic}, which for 2024-T3 is about 40 MPa$\sqrt{m}$ (see the table above). That is

not surprising, because the specimen thickness has to be more than twice as much for obtaining a plane strain situation needed for a valid K_{Ic}.
The results indicate that the ratio of K_{max} (at the fracture instability) for a crack, which is completely in the shear mode, and a crack in the tensile mode (with small shear lips) is 1.12. If K_{max} at fracture instability is defined as K_c then the conclusion is that the crack has to grow longer before K_c is reached in a shear mode situation. This suggests that K in the shear mode is *at least* 12% lower than K for the tensile mode.
In theory K and thus K_c is assumed to be only valid for tensile mode cracks, thus $K_c = 55.3$ MPa$\sqrt{m}$ for this thickness of the material.

Tests on 7075-T6 specimens
In order to study the effect of shear lips on the critical value of K in plane strain (K_{Ic}) , tests were carried out on compact tension specimens of the high strength 7075-T6 Al alloy. The experimental procedure was as close as possible to the ASTM E-399 standard, except for the initial slit and initial fatigue crack. The material thickness was 12.3 mm, which is sufficiently large to find a valid K_{Ic} value for this material using the standard compact tension specimen with a chevron notch. The aim was to compare specimens with a tensile mode prefatigue crack, with specimens with single shear and double shear cracks. In order to obtain this, some of the specimens had to be modified. As shown in figure 4.48 a slotted hole was made in these specimens to allow the spark erosion apparatus to make the necessary notches of about 3 mm length. A prefatigue crack was grown in the specimens afterwards. The prefatigue zone could not be too large because the effect of the slant cracks diminished by the growing of tensile mode zones in the shear lips. A too short notch led in some cases to a prefatigue crack in a corner of the slotted hole, instead of in the notched middle of the specimen. The chosen 3 mm notch length appeared to be a good compromise. The length of the prefatigue zone was about 2 mm. A survey of the tests is given in the table below. Detailed results are given in table 4.4.

Six tests were carried out for each type of specimen shown in figure 4.48. The standard specimen was used to get a calibration for the K-factor of the specimens with a slotted hole and to have the possibility to compare results with results from the literature. The critical K-factors found for test specimens of type a and b, using in both cases the K solution for a compact tension specimen of type a, are the basis for the correction factor.
The nominal K_c (i.e. calculated with the K-equation for a compact tension

specimen) rose from 25.8 for the standard compact tension specimen to 29.8 for the slotted hole compact tension specimen , an increase by a factor of 1.16 (see table below). This factor was then applied to the specimens with slant cracks.

The corrected values in the last column of the table below indicate a large effect of the fracture mode, much larger than found from the previous (fatigue) tests on 2024 T351 specimens. The explanation may be that linear elastic fracture mechanics is more relevant to the high strength 7075-T6 alloy.
This is confirmed by the K_c value of 25.8 MPa$\sqrt{m}$ obtained for this material, which agrees very well with the valid K_{Ic} of about 25 MPa$\sqrt{m}$, usually found for this material in the literature. For all test results it was checked whether they satisfied the ASTM 399 standard (as far as possible for the test specimens with a slotted hole). The tests of specimens of type a satisfied the conditions for a valid K_{Ic} test. Results of two tests of the type c specimen and one of the type d specimen could not be used since an unsuitable prefatigue crack grew in the specimen.
The corrected K_c results in table 4.4 or in the table below, indicate that the highest K_c is found for specimens with an initial single shear crack. The ratios of $K_{c,slant}$ and $K_{c,tensile}$ are about 1.5 and 2 respectively for the double shear and single shear cases. Thus single shear cracks show the largest effect.

specimen	type of crack	Number of tests	Nominal K_c (MPa$\sqrt{m}$)	Corrected K_c (MPa$\sqrt{m}$)	Ratio of K_c
CT	tensile mode	6	25.8		
CT with slotted hole 7075-T6 t = 12.3 mm	tensile mode	6	29.8	25.8	1
	single shear	4	59.2	51.0	2
	double shear	5	44.4	38.3	1.5

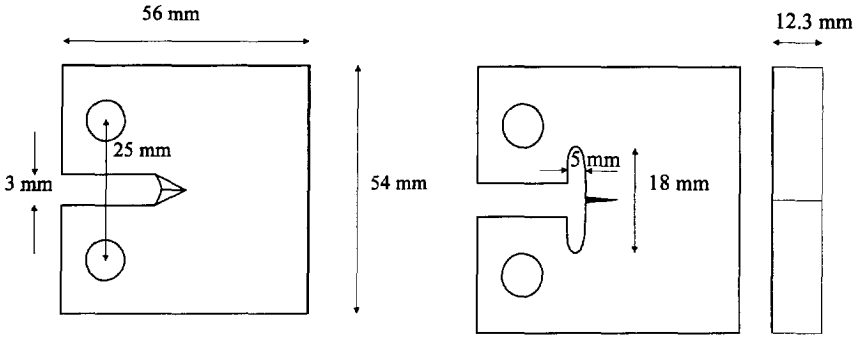

a) standard specimen with chevron notch.

b) initial tensile mode fatigue crack.

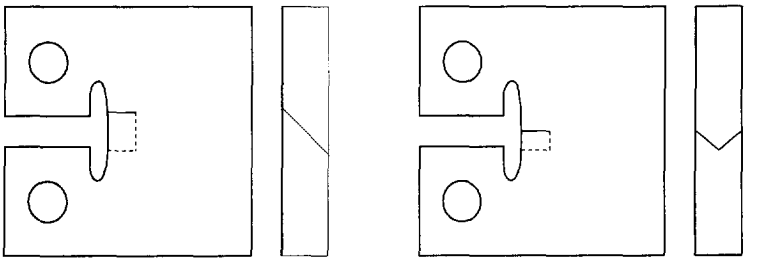

c) initial single shear fatigue crack.

d) initial double shear fatigue crack.

Figure 4.48. Compact tension specimens used for K_c evaluation.

Qualitatively the same trend was observed in fatigue tests. After overloads with an overload factor of about 2 on center cracked tension specimens, fatigue crack arrest occurred. However, when after many cycles the crack growth started again, the growth always reinitiated from a crack tip which was in double shear. A single shear crack did not grow any further [15].

It is remarkable that the results found in the "static" tensile tests differ much from the results found in the fatigue tests described earlier in this section. In the fatigue test the single shear case found resulted in a 12% higher K_{max} at instability, in the tensile test in a 100% higher K_c compared with the K_c found for a flat (tensile mode) crack. A satisfactory explanation cannot be given at the moment. The slant mode, apart from leading to a lower crack driving force for our specimen with slotted holes, might also be associated with a higher crack

growth resistance for static crack extension in the shear mode. Further different materials were used in both cases. The maximum shear lip width in 2024 is estimated to be about 5 to 6 mm [20], in 7075 it is about 1 mm. This latter effect was clearly visible on the fracture surfaces of the slant specimens. The large initial shear lip width decreases rapidly during crack growth until a width of about 1 mm.

This means that for the Al 7075 specimens an initial very unstable situation with a five times too high shear lip width is created. The instability can also be seen on the fracture surfaces in the area of the fatigue zone, where small tensile parts grow in the big slant notch made by spark erosion.

Both initially double and single shear fracture surfaces transform to flat tensile surfaces during the unstable growth with a resulting shear lip width of about 1 mm on the edges.

Of course it might also be assumed that for the "static" tensile tests K_c is a material property (dependent on the thickness) that is independent of the initial fracture mode. The results then indicate that K for a single shear slant crack is 100% lower than for a flat tensile mode crack. Both considerations, a higher K_c or a lower K, give mathematically the same result. At this moment it is not possible to choose between both descriptions that lead to a similar trend.

In a recent paper Bakker [16] shows, using finite element calculations, that the difference in K_I for a fully single shear slant crack and a flat crack is about 40% at the utmost. The difference found here is lower (12%), as found from the fatigue tests on Al 2024, or higher (100%), as found from static tensile tests on Al 7075. For the latter case it might be possible that the method used to find the K-factor for the specimen with a slotted hole is not accurate enough, although very recent finite element calculations show the same result within 1% accuracy [23]. Another difficulty lies in the fact that a slow test (fatigue) is compared with a fast test (K_c).

Anyhow, the effect is large enough to be relevant for cracks in aircraft components of the 7075-T6 alloy. Although the valid K_{Ic} for mode I cracks probably implies conservative residual strength predictions, a further study seems to be of practical interest.

4.8 Some Physical Explanations of Shear Lip Behavior

Based on the following facts a few answers have to be found.

Observed facts

* no shear lips are found on fracture surfaces of materials with a hexagonal structure (Mg,Zn) or in materials where it is to be expected that slip on planes at 45° with the plate surface will consume much energy.
* in a constant amplitude test on Al 2024 in vacuum we always immediately detect shear lips, independent of ΔK.
* in air in a constant amplitude test first tensile mode crack growth is found at lower ΔK, followed by shear lips at higher ΔK.
* at lower frequencies in air more tensile mode area is found and a higher ΔK is needed to get shear lips than at higher frequencies.
* at a fixed frequency the shear lips start to grow at a ΔK_{eff} given by equation 4.31. There is no dependence on K_{max}.
* in a constant ΔK test the shear lip width increases during crack growth until an equilibrium value is reached.
* the frequency has influence on the fracture surface appearance. Smooth shear lips are found at lower frequencies, rough shear lips at higher frequencies.
* at a fixed ΔK the tensile mode crack growth rate is frequency independent.

Related questions

* Why do shear lips develop?
* Why is there a dependence of the start of shear lip width development on ΔK_{eff} and *not* on K_{max} (i.e. on plane stress)?
* Why is there an effect of the environment and/or the frequency on the shear lip width development?
* Why is the tensile mode crack growth rate independent of the frequency in a constant ΔK fatigue test?
* Why does the shear lip width growth result in an equilibrium value $t_{s,eq}$ in a constant ΔK fatigue test?
* Why is there an upperbound shear lip width development in a "static" tensile test?
* Why is there a continuous out-of-plane growth for a double shear lip fracture surface in a "static" tensile test, and often a zigzag growth in a fatigue test?
* Why does the frequency affect the fracture appearance?

Why shear lips develop

The reason why shear lips develop in some materials and not in other materials probably has its origin in the material structure and the type and amount of texture. It is well-known that the stress situation near a through-crack on the plate surface is plane stress [12]. Therefore a simple mechanical explanation is that the process is induced by a situation of plane stress at the specimen surface, which leads to maximum shear stresses on planes inclined at 45° to the specimen surface. A situation of plane stress is considered a necessary condition for the initiation and growth of shear lips, necessary but not sufficient. Materials with a face centered cubic or a body centered cubic structure have many possible slip systems. There will always be a slip possibility near the direction of maximum shear stress (except in a theoretically extreme texture case). Shear lips will form easily in these materials. An exception was found for austenitic stainless steel, a material with a face centered cubic structure, where no shear lips were found in tensile and fatigue tests. The reason probably is a martensitic transformation in this material near the crack tip. The tetragonal structure of the martensite probably has no easy slip systems near the directions of maximum shear stress. For hexagonal closed packed materials the situation is analogous because there are only three slip systems composed of three closed packed directions <1000> and the closest packed {0001} planes. Quite often the texture in plate geometries of hexagonal materials is such that {0001} is parallel to the plate surface. There is thus no easy slip system near the maximum shear stress direction. Shear lips are not detected for these materials. The conclusion is that shear lips will form always unless there is a hindrance of the necessary slip under 45° with the plate surface.

Why shear lip start depends on ΔK_{eff} and not on K_{max}

In this chapter a satisfactory mathematical description of shear lip width behavior under constant stress intensity loading could be given. It was found that the equilibrium shear lip width depended on ΔK_{eff} (equation 4.7), and that the start of shear lips did not depend on K_{max} .

This is a remarkable result, because shear lips are present both on fracture surfaces made in fatigue tests and on fracture surfaces made in static tests. In section 2.5 it was concluded that a situation of plane stress was a necessary condition for the forming of a shear lip.

The amount of plane stress is influenced by K_{max} , at higher K_{max} there is more plane stress. Why thus should the shear lip width be dependent on the fatigue crack driving force ΔK_{eff} and not on K_{max} ?

An answer to that question might be found using a time dependent description of

the fatigue crack growth process with growing shear lips. We will assume that the initiation of shear lips needs some crack growth. In fatigue (in the Paris regime) we have some crack growth in every cycle. It is generally thought that crack extension is not a continuous process during one cycle. There is only crack growth during the increasing part of K. The crack growth rate increases with K during this process. Somewhere near the maximum value of K the crack growth rate will start to decrease and is assumed to become zero when K is decreasing. The process of crack growth during the increasing part of the K cycle and no crack growth and resharpening of the blunted crack during the decreasing part is repeated for the next cycles.
Suppose that we have a tensile mode situation of crack growth in a constant ΔK test. In every cycle we have the same (discontinuous) crack length increment. When will shear lips develop? It may be clear that the shear lip growth has to occur (start) during this small period of crack increment in one cycle, thus during the increasing K period. If the crack length increment in one cycle is too low for the initiation of shear lips, this will also be the case in the next cycles.
Apparently there is no "history" effect for shear lip initiation as long as the crack surface is in the tensile mode. The reason for this is that in every cycle the crack grows a certain amount, making a new fresh (sharpened) crack tip area for the shear lip to try to initiate in the next cycle. Moreover, initial dislocation movements, needed for the start of shear lip growth, are (partly) reversed during the unloading K period of the fatigue cycle. Thus we need a certain continuous crack length increment (which is equivalent to a certain da/dN or ΔK_{eff}) to initiate a shear lip. Below this value initiation of shear lips will not occur even after a large number of cycles. This is in agreement with equation 4.31.
When at a higher ΔK the crack increment is sufficient for initiation of shear lips in a cycle, then it will also be sufficient in the following cycles.

From this model we learn that we need a certain amount of crack growth in a cycle (i.e. da/dN) to get shear lips. Therefore the initiation of shear lips depends on ΔK_{eff} and not on K_{max} , because da/dN does not depend on K_{max} .
This reasoning also explains that in a constant amplitude test we first find tensile mode crack growth followed by shear lip development at higher ΔK, because da/dN increases during a constant amplitude test.
For 10 Hz we found that shear lips develop in a constant ΔK test above ΔK_{eff} = 5.5 MPa$\sqrt{m}$, irrespective of the value of K_{max} . The (tensile mode) crack growth rate for ΔK_{eff} = 5.5 MPa$\sqrt{m}$ is 0.16 μm/cycle. Thus at 10 Hz there seems to be a "delay" of 0.16 μm/cycle between normal (2 dimensional) fatigue crack growth and shear lip crack growth. For a shear lip to develop a (continuous) crack

growth above 0.16 μm is needed. The tests performed in this work were all done with sinusoidal loading. It would be interesting to also do tests with a positive sawtooth (i.e. with a short increasing period and long decreasing period) and a negative sawtooth (i.e. with a long increasing period and short decreasing period) loading to find its effects on shear lips.

Effect of frequency and/or environment on the start of shear lips
For materials that form shear lips a dependence of the forming of shear lips on the frequency (environment) was found. When the loading frequency is lowered (or the environment is made more agressive, e.g. by change from from air to salt water), it was found for Al 2024 that start of shear lip width development is shifted to higher values of ΔK. Flat tensile mode crack growth is favored when the frequency is lower (or the environment is more aggressive).
What can be the explanation for this phenomenon? Remembering the foregoing discussion about the necessity of a slip possibility in the directions of maximum shear stress a *possible* explanation can be that the more aggressive environment has an impeding effect on (the start of) dislocation movement along the slip systems near the plate surface.
There are two possible causes for the impeding effect. First the effect can be thought to result from foreign atoms or ions, products of a corrosion reaction near the surface, diffusing into the matrix. They settle near dislocation lines where the lattice spacing is higher than elsewhere. The settlement of foreign elements (substitutional or interstitional) near the dislocation lines has a lowering effect on the total internal energy , i.e. it costs energy to move the dislocation lines out of this environment. The (start of the) movement of dislocation lines has become more difficult. When a dislocation line has freed itself from its environment of foreign elements it can move very fast.

Another *possibility* might be that dislocation lines near the crack tip surface are pinned by the oxide layer on the surface, for example they are lying slant through the oxide layer surface [24]. This oxide layer will have more "pinning" effect when the frequency is lower, because the oxide layer will have more time to grow. Thus the hindrance of initiation of dislocation motion probably is a surface effect. The environment is not directly important in the interior of the material, but it is indirectly, because the situation at the material surface is also of great importance for the material interior as shear lips always grow from the surface inwards. There probably has to be a little initial slant growth at the surface before shear lips can grow to a larger width. If this initial shear lip growth is prevented by hindrance of dislocation movements near the surface shear lips will only start

to grow at higher ΔK .
I will not further speculate on this issue here and assume that there is a frequency dependent prevention of initiation of dislocation motion, i.e. a lower frequency is assumed to prevent initiation of dislocation movements needed for shear lip forming more than a higher frequency.

Besides the foregoing discussion, Vogelesang and Schijve [19] postulated that tensile decohesion is promoted by foreign ions near the crack tip. The reason for this is probably a lowering of the surface tension for the atomic layer at the crack tip surface.

Thus the effect of a corrosive environment consists of two parts:
1. a promotion of tensile decohesion.
2. an impeding of dislocation movement needed for shear lip growth.

The result of these assumptions is that the delay between continuous crack increase and shear lip growth is found to be frequency (and environmentally) dependent. The delay results from a competition between a tensile rupture (or other tensile promoting) mechanism and a shear decohesion mechanism. An aggressive environment lowers the surface tension at the crack tip and promotes tensile decohesion. At the same time dislocation movement, needed for shear lip formation, is obstructed, because there are more (dislocation) pinning points resulting from foreign atoms and ions made by a corrosion reaction or resulting from the oxide layer near the intersection of the crack tip surface and the edge of the specimen. Thus the delay is higher for a more aggressive environment (and for a lower frequency, because there is more time for the environment to react with the material).
The larger delay for shear lip growth in an aggressive environment (or at lower frequency) means that a larger continuous crack growth increment is needed for the start of a shear lip. Thus da/dN at the start of shear lips is higher and herewith also ΔK_{eff} . The shear lip development will be later and less.

In vacuum there is hardly any delay, because there is no promotion of tensile decohesion by foreign atoms or ions, and because there is also no oxidation of the edge material at the tip. There are no obstacles for dislocation movements needed for the start of the shear lip growth. Shear lips develop almost immediately when the crack grows, even for a very low ΔK_{eff} and for a low frequency.
However there exist conflicting views with some recent corrosion fatigue

theories. A corrosion fatigue theory by Henaff et al.[25] assumes that adsorption of water vapor molecules on fresh crack surfaces is the main mechanism in the increase of the crack growth rate of a stage II fatigue crack (i.e. in the Paris regime) in a corrosive environment. The effect of the adsorption is thought to result from a competition between the transport of active species to the tip, the adsorption consumption rate and the crack advance kinetics. Adsorption may not be viewed as an embrittling process but rather as a mechanism inducing enhanced plasticity of the cyclically strained material at the crack tip.
Lynch [26] assumes that adsorbed hydrogen weakens interatomic bonds at the crack tip and thereby facilitates injection of dislocations from the tip. Crack growth occurs by alternate slip, which promotes coalescence of cracks with small voids nucleated just ahead of the crack tip. These voids have been detected on fatigue crack fracture surfaces at high magnifications.
In both views the environment (lower frequency) leads to more active slip systems. Alternate slip by cooperative slip systems promotes tensile mode crack growth both in the plane strain middle as well as on the plane stress edges of the specimen. At sofar the theories fit with the facts, i.e. more tensile mode crack growth in a more aggressive environment. However a higher ΔK will lead to more slip systems and enhance the activity of systems that already exist, so even more tensile mode crack growth is to be expected at higher ΔK. This expectation is not fulfilled, we now get development of shear lips. Also a higher K_{max} is expected to have an enhanced effect on the activity of (more) slip systems, however shear lip behavior is not found to depend on K_{max} .
We remain in support of the conclusion therefore that shear lips will form always unless there is a mechanism that prevents the necessary dislocation movements on the planes of maximum shear stresses and that the hindrance of the necessary dislocation movements is promoted by a more aggressive environment.
Otherwise it should be expected from these theories that the tensile mode crack growth rate would be frequency dependent even at the applied higher ΔK cycles, which is not the case. In order to find a way out of this dilemma it is possible that these corrosion theories do not apply so much in the (high) ΔK area where the shear lips are active.

Why is the tensile mode crack growth rate independent of the frequency in a constant ΔK fatigue test?
In a lot of papers devoted to corrosion fatigue a large effect of the frequency (environment) is found on the crack growth rate. The investigations described in these papers normally don't describe a situation where shear lips are present. Tensile mode crack growth at a much lower ΔK is described.

The present author found that the tensile mode crack growth rate is not a function of the frequency at a fixed ΔK test for a ΔK as high as 18 MPa$\sqrt{m}$ and R = 0.1, see figures 4.39 and 4.41.
The reason for this behaviour probably can be found in the shape of da/dN-ΔK curves at different frequencies in air and in vacuum. At lower ΔK there exists a large difference in crack growth rates between air and vacuum, while at higher ΔK there is a tendency to convergence of all curves. Probably the applied ΔK of 18 MPa$\sqrt{m}$ (R=0.1) is high enough to be in the area of convergence. The whole difference in constant amplitude crack growth rates can now be explained with difference in shear lip widths in this area, because tensile mode crack growth rates are the same.

Why there is an equilibrium value $t_{s,eq}$ at a constant ΔK test
For higher values of ΔK_{eff} the crack growth increment per cycle is large enough to start shear lip growth. When in a cycle a shear lip is initiated, the stress situation (initiation of mode III stresses) at the tip has changed. Every cycle adds a small shear lip increment to the already present shear lip width. It was shown in section 4.4 that growing shear lips lead to a decrease in da/dN. Suppose that we start fatigue crack growth from a tensile mode prefatigue crack at a high constant ΔK. Already in the first cycle the shear lip growth starts. Then in the next cycle there is an initial shear lip width (very small), which leads to a lower da/dN than in the first cycle. The lower da/dN in the second cycle leads to a lower increase of shear lip width (dt_s) than in the first cycle. In the next cycles, in every single cycle the increase of shear lip width and the decrease in crack growth rate are smaller than in the previous cycle. This process is going on until the changes (per cycle) in t_s and da/dN are very small (about zero), the equilibrium values $t_{s,eq}$ and $(da/dN)_{eq}$ are now reached (see figure 5.1 of chapter 5). The value of $(da/dN)_{eq}$ depends on $t_{s,eq}$ and reverse.

Why there is an upperbound shear lip width behavior in a "static" tensile test compared with fatigue tests?
In a "static" tensile test we have a very large continuous crack growth increment. The crack growth increment will always be amply sufficient for starting shear lip development and growth. Besides that there is no change in the loading direction, i.e. K keeps increasing when the crack grows. This large continuous crack growth is the reason that the shear lip width found in a static test experiences an upperbound behavior compared with shear lip width results from fatigue tests at all frequencies. With upperbound behavior we mean that if we do not find shear lips in a "static" tensile test, we *certainly* will not find them in

fatigue tests at all frequencies. At this moment we do not exclude that besides the large continuous crack growth increment also the very high K (much larger then K_c) and/or the very high da/dt influence the shear lip behavior.
Displacement controlled tests at different constant displacement rates are planned at this moment to investigate the separate influences of the continuous crack growth increment, the K value and the crack growth rate da/dt.

Why is there a deviating growth direction of a double shear lip fracture in "static" tensile tests and fatigue tests, and why are there smooth and rough shear lips?

Another phenomenon that has yet to be discussed is the deviating crack growth direction of cracks with double shear lips, and why there is (sometimes) a reinitiation of shear lips in fatigue tests (zigzag growth) and not in "static" tensile tests. Possible explanations are based on the asymmetric plastic zone when shear lips are present.
Recently Schijve [21] suggested that the deviating crack growth direction of the "static" double shear failure indicates a preference to grow in the direction of the larger plastic zone. This is a consequence of the asymmetry in plastic zone of a crack with shear lips. The large plasticity in the asymmetric zone leads to voids around inclusions, followed by coalescence of voids during crack extension. The crack path follows the coalescence of the voids. This explanation seems valid for (double) shear lip deviations in "static" tensile tests.
During fatigue crack growth a *similar* void formation (i.e. in the direction of the large asymmetric plastic zone) probably does not occur, but the asymmetric plastic zones remain a valid argument. The zigzag pattern of fatigue crack growth (at higher frequencies) still has to be explained.
The cause of the difference in out-of-plane growth of "static" tensile and fatigue cracks will again be explained with a time dependent behavior. Dislocation movements, i.e. start of movement and movement itself, needed for the creation of voids around inclusions and for coalescence of voids are time dependent. In "static" tensile tests we have to do with a large crack growth increase at a very large value of K. During the crack growth the K value will probably not (much) decrease. Voids will have ample possibilities to grow (high stresses) even for fast crack growth after instability, because dislocations start easily (high stresses) and dislocation velocities are high.
In fatigue crack growth the continuous crack growth increment is very short compared with a "static" tensile test. Crack growth only occurs when K increases. Crack growth stops when the K will start to decrease. The dislocations will have more difficulties to start in fatigue and make voids because the stresses

are lower and reverse soon (i.e. dislocation movements will also be reversed if possible).
For higher fatigue frequencies there is probably no time enough for the making of large voids, needed for further crack growth, during the increase of K. Thus in fatigue crack growth at higher frequencies there are no such large weak sites with coalesced voids that promote crack growth as in a fast "static" test . Now a modest plasticity, with its dislocation network, will be probably sufficient to stop ("pin") further dislocation movements that accompany plastic deformation and crack growth and lead to crack arrest. The crack growth has to reinitiate then in another direction with less plasticity.
For lower frequencies there is more time to make voids and for coalescence of voids. Now the zigzag pattern of crack growth is not observed. The shear lip appearance is smooth as in a "static" test. Probably crack stop does not occur in this case, the shear lip can grow further as in the "static" case.

Thus the time dependence of the dislocation processes involved (i.e. mainly the time needed for initiation of dislocation motion, the making of voids and next coalescence of voids), and the reversing of the stresses in fatigue (much lower stresses than for "static" tensile tests), make that for a "static" tensile test and a fatigue test at lower frequency the crack grows in the direction where the plasticity has a maximum. For the fatigue crack growth at higher frequency the crack growth stops on the large asymmetric plastic zone, and has to reiniate in another crack growth direction for continuing its growth. The zigzag growth is often adressed as a rough fracture surface.

4.9. Chapter 4 in summary

In the present chapter various aspects of shear lips on fatigue fracture surfaces have been analyzed, based on a large number of test series, mainly on 2024 T3 center cracked tension specimens. In view of the present status of understanding, it is useful to summarize the major findings, both experimental observations and mathematical correlation's.

1. Although shear lips were recognized long ago, only limited systematic empirical investigations were reported in the literature. The present investigation clearly shows that constant ΔK tests are essential to describe fully the shear lip development, and to realize that an equilibrium shear lip width is obtained in such tests. At the same time, it became evident that under constant ΔS loading, shear lips will have a non-equilibrium size depending on the ΔK history of the growing fatigue crack. This aspect was largely overlooked previously.

2. In the past shear lips were often ignored in investigations of certain influences on fatigue crack growth, although it is quite obvious that fatigue cracks growing in the tensile mode (no shear lips) and fatigue cracks growing (partly) in the shear mode (i.e. with shear lips) should not necessarily be affected in the same quantitative way by certain fatigue load conditions. Even qualitatively, different phenomena might be active. This point of view is supported by crack growth results from the present investigation. They show that under nominally identical loading conditions the growth rate of a crack growing in the tensile mode may be about three times larger than the growth rate of a crack in the shear mode.

3. The results of extensive shear lip width measurements have revealed a number of interesting observations:

a Under constant ΔK loading the shear lip width increases until an equilibrium width ($t_{s,eq}$) . For different R-ratios $t_{s,eq}$ shows a good correlation with ΔK_{eff} , and not with ΔK or K_{max} .

b The equilibrium shear lip width $t_{s,eq}$ is independent of the sheet thickness. Obviously, it can only directly be measured if $t_{s,eq} < t/2$ (t = sheet thickness).

c For the initiation of shear lips on a fatigue fracture surface which is still in the tensile mode a critical ΔK_{eff} value is required. This value accounts for the effect of the stress ratio R, but it is sensitive to the environment and the test frequency.

d If the fatigue fracture is still in the tensile mode (no shear lips), the crack growth rate is independent of the cycle frequency. However, if there are shear lips, a higher crack growth rate is found for a lower frequency. It appears that the frequency effect and the occurrence of shear lips are interrelated.

4. Although shear lips are a complication of the fatigue crack growth phenomenon, it turned out that the shear lip width development shows certain systematic trends during constant ΔK tests. This allows a mathematical description. Based on the assumption that dt_s/da is proportional to ($t_{s,eq} - t_s$) (t_s is the current shear lip width), a linear equation was obtained for $t_{s,eq}$ as a function of ΔK_{eff} . Also a satisfactory relation was obtained for the frequency effect showing that $t_{s,eq}$ is a linear function of log(frequency).

5. The equation obtained for t_s as a function of ΔK_{eff} , based on constant ΔK test results, could predict the shear lip width development during constant ΔS experiments.

6. Observations were made on the so-called zigzag crack growth phenomenon as well as on the deviating crack growth direction for double shear fatigue cracks. It appears that asymmetric plastic zones, introduced by shear lips, play a significant part for these phenomena.

The above summary gives a kind of inventory of shear lip behavior. Apart from a further analysis the observations are already relevant to technical problems in order to see which kind of influences are associated with or affected by the presence of shear lips. However, the question arises whether our observations can be modeled in terms of fracture mechanics parameters, also in view of prediction procedures. An inherent difficulty is present, which is associated with the following consideration. All observations are related to fatigue crack extension, which is a consequence of some crack driving force on one hand (e.g. a ΔK_{eff}), and a material resistance to crack growth on the other hand. The present analysis of our results indicate that ΔK_{eff} is an important parameter. Probably this should not be considered to be surprising, since cyclic plastic deformation around the crack tip should be controlled by ΔK_{eff}.
The material resistance with respect to crack growth resistance is usually characterized by da/dN- ΔK_{eff} graphs. Our problem now is how the shear lips affect the crack driving force and how they affect the material resistance. This is a most intriguing question, especially because the two concepts can not be measured separately. In experiments we always find the combined result of both. From finite element calculations, we know that K depends on shear lips, as would be expected. Our static K_c tests indicate quite significant effects of shear lips on K. The frequency effect should be associated with some time dependent mechanism in the material, and thus with the material resistance. It seems to be plausible that crack growth is faster at low frequencies, but this was found for shear mode cracking only, and not for crack growth in the tensile mode.

4.10 References

1. J. Schijve, Engng Fracture Mech. 14, 789-800 (1981).
2. R.A.H. Edwards, E.M. de Jong and J. Zuidema . The Fracture Mode Transition and its Effect on Crack Growth Retardation. *Proc. Fatigue 84.* University of Birmingham, UK, pp 463-478.(1984)
3. .W. Elber, Fatigue crack closure under cyclic tension, ASTM STP 486, 230-242 (1971).
4. D. Broek and J. Schijve, Aircraft Engineering , November 1966, pp 31-33.
5. D. Broek and J. Schijve, The effect of sheet thickness on the fatigue crack propagation in 2024-T3 Alclad sheet material, NLR report TR M.2129, April 1963.
6. J. Schijve, Engng Fracture Mech. 14, 467-475 (1981).
7. J.C. Newman Jr, A Crack-Closure Model for Predicting Fatigue Crack Growth under Aircraft Spectrum Loading, ASTM STP 748, 1981, pp

55-83.

8. J.C. Newman Jr, Prediction of Fatigue Crack Growth under Variable Amplitude and Spectrum Loading Using a Closure Model, ASTM STP 761, 1982, pp 255-277.
9. J.C. Newman Jr, A Non-linear Fracture Mechanics Approach to the Growth of Small Cracks, Proc. of the 55th Agard Meeting on Behaviour of Short Cracks in Airframe Components, Toronto, 1982
10. J. Zuidema and H.S. Blaauw, Engng Fracture Mech. 29, 401-413 (1988)
11. G. Marci and P.F. Packman, Int Journal of Fract., Vol. 16, No 2, 1980, pp 133-153.
12. H.L. Ewalds and R.J.H. Wanhill, Fracture Mechanics, Delftse Uitgevers Maatschappij and Edward Arnold, ISBN 90 6562 024 9, London 1984.
13. Standard test method for Plane-Strain Fracture Toughness of Metallic Materials E399-90, Annual Book of ASTM Standards, vol. 03.01, 1993, ASTM, Philadelphia.
14. J. Zuidema, A Calculation of the Effective Delta K under Various Fatigue Loading Conditions. In Proceed. of the 9th European Conference on Fracture, ECF-9, Varna, Bulgaria, 1992.
15. J. Zuidema, P.J.M. Mense and R.A.H. Edwards (1987) . Engng Fracture Mech. **26**, 349-356.
16. 16. A.Bakker, Fatigue Fract. Engng Mater. Struct., Vol 15, No 11, pp 1051-1069, 1992.
17. S. R. Swanson, F. Cicci and W. Hoppe, Crack Propagation in Clad 7079-T6 Aluminium Alloy Sheet Under Constant and Random Amplitude Fatigue Loading, ASTM STP 415, American Society for Testing and Materials, 1967, pp. 312 - 362.
18. D. Broek, P de Rijk and P.J. Sevenhuijsen, The Transition of Fatigue Cracks in Alclad Sheet, Report NLR-TR M.2100, Nationaal Lucht- en Ruimtevaart Laboratorium, 1962, Amsterdam.
19. L.B. Vogelesang and J. Schijve, Fatigue Engng Mater. Struct., Vol. 3, pp. 85 - 98, 1980.
20. J. Zuidema and M. Mannesse, Engng Fracture Mech.40, 105-117 (1991)
21. J. Schijve, personal communication.
22. J. Schijve, Engng Fracture Mech., Vol. 11, 1979, pp. 167-221.
23. A. Krom, private communication, june 1995.
24. C.J. van der Wekken and B. Lichter, personal communication.
25. G. Henaff, K. Marchal and J. Petit, Acta metall. mater. Vol. 43, No 8, pp. 2931-2942, 1995.
26. S. P. Lynch, Environmentally Induced Cleavage-like Cracking in Aluminium

Alloys, Int. Conf. on Corrosion-Deformation Interactions CDI'92, Fontainebleau, France, oct. 5-7, 1992.

27.F.A. Veer, Doctor Thesis T.U. Delft, October 1993.

Table 4.1. Results of constant ΔK and R tests on 6 and 10.3 mm thick plates (c.c.t. specimens); a (*) indicates that only c has been fitted; a (-) indicates that $t_{s,eq}$ is estimated directly from the broken specimens; frequency = 10 Hz.

plate thickness (mm)	ΔK (MPa√m)	R	K_{max} (MPa√m)	ΔK_{eff} (Elber) (MPa√m)	$t_{s,eq}$ (mm)	c (1/mm)
10.3	9.43	0.64	26.00	7.12	1.01	0.263
10.3	11.95	0.54	26.00	8.56	2.12	0.157
10.3	14.87	0.43	26.00	9.98	3.04	0.164
10.3	18.58	0.29	26.00	11.41	3.78	0.098
10.3	24.67	0.05	26.00	12.84	4.90	0.093
10.3	14.40	0.10	16.00	7.78	1.42	0.498
10.3	18.00	0.10	20.00	9.72	2.78	0.184
6.0	12.00	0.10	13.30	6.47	0.55	0.511
6.0	9.74	0.30	14.00	6.06	0.30	0.813
6.0	11.40	0.50	23.00	8.00	1.75	0.187
6.0	15.00	0.10	16.70	8.11	1.83	0.202
6.0	16.00	0.30	23.00	9.95	2.96	0.137
6.0*	23.00	0.08	25.00	12.24	4.48	0.105
6.0	20.00	0.10	22.20	10.80	3.55	0.156
6.0	18.00	0.10	20.00	9.72	2.74	0.245
6.0	17.00	0.10	18.90	9.18	2.42	0.164
6.0	12.65	0.56	29.00	9.18	2.40	0.198
6.0*	24.38	0.39	40.00	16.00	7.00	0.080
6.0*	15.83	0.68	50.00	12.24	4.48	0.152
6.0	11.73	0.71	40.00	9.18	2.42	0.189
6.0	12.41	0.65	35.00	9.41	2.60	0.169
6.0	19.64	0.05	20.64	10.20	3.04	0.156
6.0	18.00	0.10	20.00	9.72	2.80	0.163
6.0_	10.00	0.10	11.10	5.40	0	-
6.0_	9.74	0.30	14.00	6.05	0.15	-
6.0_	12.00	0.10	13.30	6.48	0.60	-
6.0_	8.70	0.62	23.00	6.50	0.60	-
6.0_	14.00	0.10	15.60	7.56	1.20	-
6.0_	11.40	0.50	23.00	8.00	1.50	-
6.0_	11.50	0.50	23.00	8.05	1.50	-
6.0_	15.00	0.10	16.70	8.10	1.50	-
6.0_	17.00	0.10	18.90	9.18	2.10	-
6.0_	18.00	0.10	20.00	9.72	3.00	-

Table 4.2. Results of constant $\Delta K = 18$ (MPa$\sqrt{m}$) and $R = 0.1$ tests on 6 mm thick plates at different frequencies: $\Delta K_{eff} = 9.72$ (MPa$\sqrt{m}$).

frequency (Hz)	$t_{s,eq}$ (mm)	c (1/mm)	$c\ t_{s,eq}$
17.50	2.92	0.170	0.49
10.00	2.80	0.163	0.45
5.00	2.47	0.203	0.50
2.50	2.22	0.188	0.42
1.00	2.30	0.209	0.48
0.50	2.02	0.209	0.42
0.25	1.94	0.188	0.36
0.10	1.48	0.190	0.28
0.05	1.37	0.177	0.24

Table 4.3. Five constant ΔK tests at $\Delta K_{eff} = 5$ MPa$\sqrt{m}$ and increasing K_{max}, 6 mm plate. No shear lips were detected.

ΔK (MPa$\sqrt{m}$)	R	K_{max} (MPa$\sqrt{m}$)	ΔK_{eff} (Elber) (MPa$\sqrt{m}$)	ΔK_{eff} (Schijve) (MPa$\sqrt{m}$)
9.28	0.10	10.28	5.0	5.4
6.61	0.64	18.33	5.0	5.4
6.20	0.77	26.67	5.0	5.5
6.01	0.83	35.00	5.0	5.5
5.86	0.88	50.00	5.0	5.5

Table 4.4. Results of K_C tests.

type	prefatigue a(mm)	K_C (MPa$\sqrt{m}$)	$K_{C,corrected}$ mean value (MPa$\sqrt{m}$)
a	22.9	26.3	
a	22.6	25.9	
a	22.6	25.5	25.8
a	22.4	25.1	
a	22.5	26.2	
a	22.5	25.5	
b	22.5	27.7	
b	21.3	30.4	
b	21.1	30.1	25.8
b	22.2	28.9	
b	20.8	31.7	
b	20.9	30.2	
c	23.0	58.7	
c	22.8	64.5	51.0
c	22.5	63.4	
c	23.3	50.0	
d	23.4	47.2	
d	23.8	40.5	
d	23.2	44.0	38.3
d	23.1	45.1	
d	23.3	45.2	

5. A Model for Predicting Slant Fatigue Crack Growth in Al 2024

5.1. Introduction

The development of shear lips during fatigue crack growth was the subject of the previous chapter. Various constant ΔK tests were carried out in order to obtain such results as qualitatively presented in the graphs of figure 5.1. The results of numerous shear lip width measurements on 2024 T351 specimens have led to equations 5.1 to 5.3, being equations 4.4, 4.7 and 4.9 in chapter 4. It was shown that for constant ΔK test results:

$$t_s = t_{s,eq} (1 - e^{-c(a-a_o)}) \qquad 5.1$$

The constants c and $t_{s,eq}$ were found to be functions of ΔK_{eff} :

$$t_{s,eq} = 0.67\ \Delta K_{eff} - 3.72 \qquad 5.2$$

$$c = 0.22/t_{s,eq} + 0.08 \qquad 5.3$$

where $t_{s,eq}$ is in mm , ΔK_{eff} in MPa$\sqrt{m}$ and c in mm^{-1}; a is the crack length and a_o the crack length at the beginning of shear lip development.

In this chapter a simple model will be presented to predict the crack growth rate under mixed tensile/shear or complete shear circumstances using the flat, tensile mode crack growth data. First the equilibrium relations for da/dN and shear lip width will be described. Later in this chapter the theory will be applied to predict non-equilibrium constant amplitude crack growth. Thickness effects and

frequency effects will be considered too.
Also in this chapter the crack closure formula found by Elber [1] is used for ΔK_{eff}:

$$\Delta K_{eff} = (0.5 + 0.4\ R)\Delta K \qquad 5.4$$

where the validity is restricted to $-0.1 \leq R \leq 0.7$.

5.2. Experimental procedure

Constant ΔK tests were performed on center cracked plate specimens of Al 2024 T351 at 10 Hz. Two thicknesses, 6 and 10.3 mm, were used. The center cracked specimens were 100 mm wide and 300 mm long. The direction of crack growth was perpendicular to the rolling direction. All specimens were prefatigued at such a low ΔK that the fracture surface was in the tensile mode at the start of the constant ΔK test.

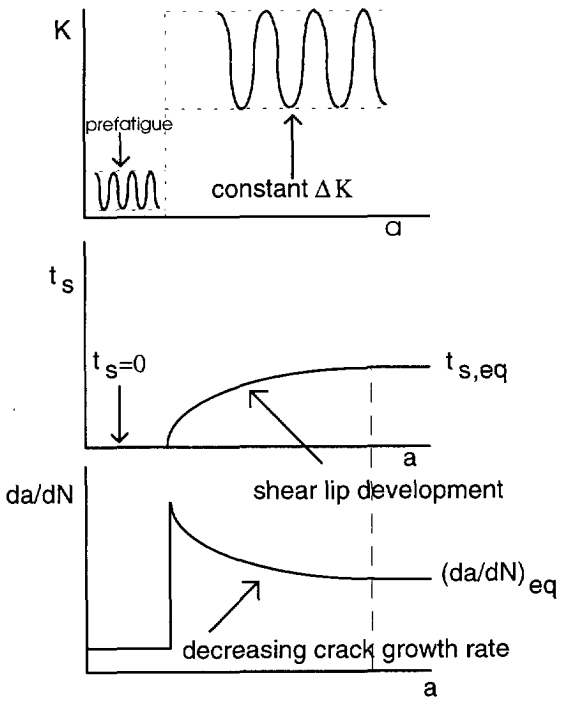

Figure 5.1. Schematic figure of shear lip width increase and crack growth rate decrease in a constant ΔK test.

In table 5.1 a survey is given of the tests performed. Some of these tests were already presented in figure 4.2 of chapter 4. For these tests the measured shear lip width is also given.

5.3 Tensile mode crack growth rate

When shear lips are not yet present the fracture surface is flat (tensile mode). In all constant ΔK tests we started in the tensile mode. The crack growth rate at first decreases almost linearly with the crack length when shear lips develop. This linear decrease enables us to find da/dN in the tensile mode even when the applied ΔK_{eff} is too high for a stable tensile mode situation of crack growth. We define the tensile mode crack growth rate $(da/dN)_{tensile}$ as the rate that is found by extrapolating the linear decreasing part of da/dN back to the start of the constant ΔK test (see figure 5.2).

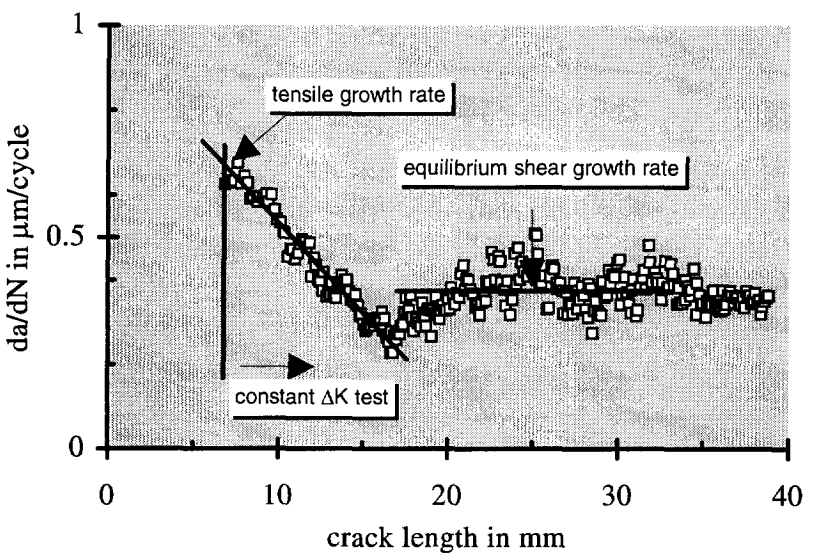

Figure 5.2. Definition of the extrapolated tensile da/dN and the equilibrium shear mode da/dN.

This procedure was already adopted in chapter 4, see figure 4.38. A reliable extrapolation was not possible in all tests (in Table 5.1 this is shown by indicating no value for $(da/dN)_{tensile}$). The $(da/dN)_{tensile}$ plotted against ΔK showed a large amount of scatter probably owing to the different R values(see figure 5.3). Results of Petit [5] on 10 mm thick compact tension specimens of Al 2024-T351 have also been plotted in figures 5.3, 5.4 and 5.5 for comparison. A much better result was obtained by plotting against ΔK_{eff} using Elber's equation 5.4., see figure 5.4.

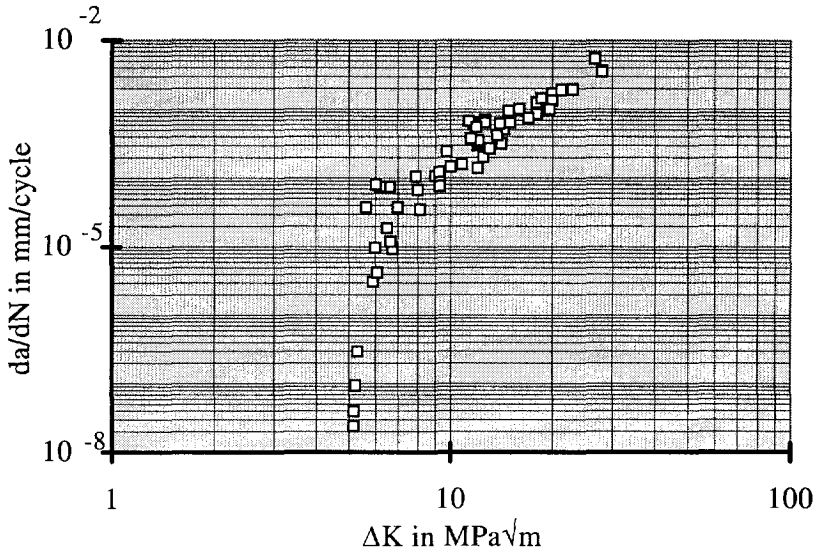

Figure 5.3. Tensile da/dN versus ΔK.

In references [2,3] it is assumed that the crack growth rate is proportional to the plastic zone size. This plastic zone size is in turn proportional to ΔK^2. We adopt here an analogous procedure for $(da/dN)_{tensile}$.The tensile mode crack growth rate will be plotted as a function of $(\Delta K - \Delta K_{threshold})$ instead of ΔK in order to incorporate threshold effects too [4]. However scatter was large again, probably due to the different R - values used.

A reasonably good fit is achieved for the log-log plot results shown in figure 5.5 by adopting ΔK_{eff} minus a constant (= $\Delta K_{eff,threshold}$) as a variable. With a quadratic function, equation 5.5 is obtained:

$$(da/dN)_{tensile} = 1.88x\ 10^{-5}\ (\Delta K_{eff} - \Delta K_{eff,th})^2 \qquad 5.5$$

The value for $\Delta K_{eff,th}$ = 2.6 MPa√m was found by linear regression. Equation 5.5 has been plotted in figures 5.4 and 5.5. The value of 2.6 MPa√m means physically an effective threshold ΔK value at da/dN = 0. This is a remarkable result as it implies that an effective threshold ΔK can be found from extrapolated tensile mode da/dN data.

However, it should be noted that also other fits with an exponent unequal to 2 are possible instead of equation 5.5. Equation 5.5 is just the best fit with an exponent of 2.

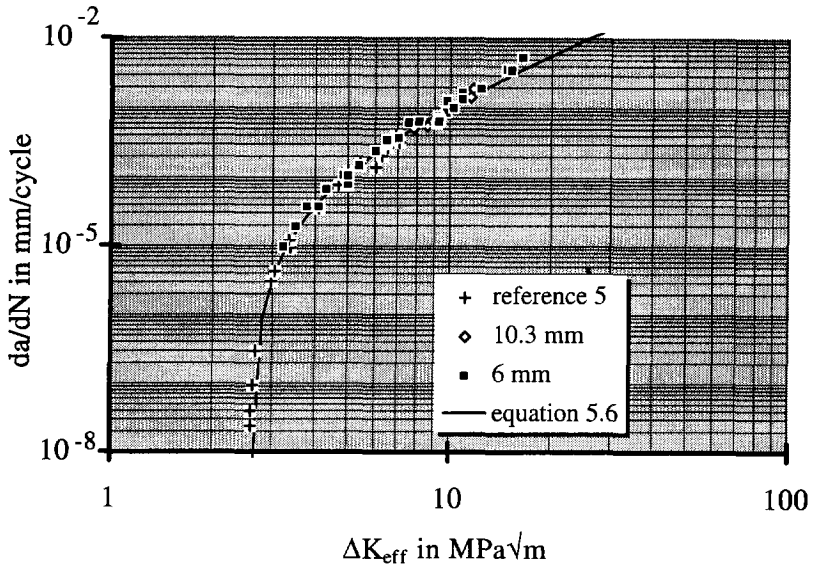

Figure 5.4. Tensile da/dN versus ΔK_{eff}.

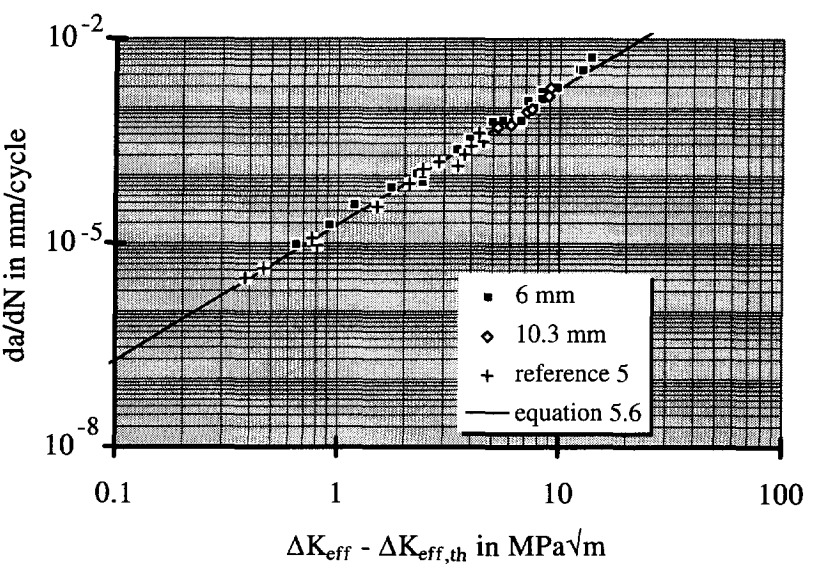

Figure 5.5. Tensile da/dN versus ΔK_{eff} - $\Delta K_{eff,th}$.

Another question that should be answered is the problem of closure build up after a transition in the loading. We cannot expect that directly after the start of the constant ΔK test the closure situation is stable. It will probably take some mm of crack growth at the applied constant ΔK before we reach a stable situation. Thus at first sight it is not correct to plot the $(da/dN)_{tensile}$ versus ΔK_{eff}

because Elber performed his measurements in a "more or less stable" situation. Elber's formula is not valid for such startup effects. Nevertheless the present author decided to plot $(da/dN)_{tensile}$ against ΔK_{eff} using Elbers crack closure relation without a correction. There were two reasons to do this.
At first the plasticity induced crack closure is assumed to be small compared with shear lip induced crack closure [29,30,31]. Secondly the tensile mode da/dN is found by an extrapolation procedure. Most of the experimental results used in the extrapolation procedure probably have reached a stabilized plasticity induced crack closure situation, because these measurements are made several mm of crack growth after the loading transition (see also chapter 7, section 7.4). The closure situation for the shear lip will not be a stable one, but that is one of the topics of this chapter.

In both figures 5.4 and 5.5 results of 6 mm and 10.3 mm thickness are given. There is no obvious thickness effect on $(da/dN)_{tensile}$. Apparently, if the fatigue crack grows fully in the tensile mode a thickness effect is not observed or it is very small. As will be discussed later this is no longer true if there are shear lips.

5.4. A model for predicting the crack growth rate in a mixed square/slant mode

As was already mentioned the tests were performed with constant ΔK and R. The formula used for K is:

$$K = \frac{P}{wt}\sqrt{\pi a}\sqrt{\sec\frac{\pi a}{w}} \qquad 5.6$$

where P is the load and w the plate width. If no shear lips develop the crack growth rate da/dN (= $(da/dN)_{tensile}$) should stay the same under these circumstances. However, when ΔK is high enough shear lips will develop. A decrease in da/dN is then observed (see figures 5.1 and 5.2). Eventually, both the shear lip width and the crack growth rate reach an equilibrium value, which we denote as $t_{s,eq}$ and $(da/dN)_{eq}$ respectively.

Causes of the decrease in da/dN with increasing shear lip width
One could think of several causes to explain the phenomenon of the decrease of da/dN. Four possible reasons for a reduction in the crack growth rate will be discussed. Two are based on the influence that shear lips might have on the crack driving force. The other two are based on the possible influence of shear lips on the crack growth resistance.

- Factors that are assumed to affect the crack driving force are:
    1. A direct influence of the slant crack on K leading to a decrease in ΔK , i.e. equation 5.6 is not valid for a slant crack, K is lower then.
    2. A different crack closure behavior of the shear lip parts compared with tensile parts, i.e. the crack closure stress level is higher in the shear lip parts leading to a lower overall ΔK_{eff} .
- Factors that are assumed to affect the crack growth resistance are:
    3. A different crack growth mechanism is active in the shear lip parts compared to the tensile parts, which can lead to different resistance to crack growth in both modes.
    4. The total crack growth resistance increases due to a longer crack front line in the case of shear lips, implying that *more* fresh surface will be made when shear lips are present, leading to more resistance.

Of course combinations of these factors are also possible.

Cause 1, a direct influence of the fracture mode on K, is based on the fact that the mode I K for a slant crack is lower than the mode I K for a tensile crack, which follows from Finite Element calculations [6,7].
A lower ΔK for a slant crack also can be based on the following considerations. In a constant ΔK test, the energy release rate ΔG, which means the energy that is available for crack extension per unit thickness and per crack length increment, is assumed to be constant and independent of the fracture surface mode. This means that we assume that the amount of energy which is "pumped" into the specimen by the fatigue machine is independent of the fracture mode. In the tensile mode $\Delta G = \Delta G_{I(t)}$. In the shear mode mode II and III components will also arise which will consume part of the available energy:

$$\Delta G = \Delta G_{I(t)} = \Delta G_{I(s)} + \Delta G_{II(s)} + \Delta G_{III(s)} \qquad 5.7$$

This formula implies that $\Delta G_{I(s)} < \Delta G_{I(t)}$ and thus $\Delta K_{I(s)} < \Delta K_{I(t)}$. A complication is that now we can expect mode II and mode III fatigue crack growth too. As we do not expect a high mode II component of crack growth we neglect this. The pure mode III crack growth rate is less than one tenth of the pure mode I crack growth rate at the same crack opening level [12], so it seems that it can be neglected too. However, because we have here a combination of mode I and III, the mode III crack growth rate might be higher than one tenth of the mode I, because the high mode III crack closure will play a less important role when the crack is opened by the mode I loading. At this moment we do not have any data about the crack growth mechanisms under combined mode I/III

loading. We will therefore neglect this and consider only mode I crack growth to be relevant.

Cause 2, a different crack closure behavior, suggests that the amount of crack closure is different for the shear lips and the tensile mode parts. This seems logical because shear lips occur in an area with predominantly plane stress conditions. Therefore the plastic zone sizes will be larger than at mid-thickness. Besides that, it seems logical to assume that shear lips combined with a little mismatch between fracture surfaces will lead to extra crack closure. As a consequence the crack closure stress level will be higher at the shear lips. As a proof of this assumption, black oxide spots on the shear lips are frequently observed, which are supposed to be due to fretting oxidation due to (enhanced) closure.
There is some agreement in the literature that in general shear lips can be associated with more closure [8,9,10,11]. A possible mechanism leading to extra closure due to shear lips was already shown in chapter 4, figure 4.35.
In chapter 7 measurements will be presented about closure with and without shear lips. It will be shown that only certain types of shear lips lead to extra closure. For the moment we do not exclude that there is extra closure in the case of shear lips.

Cause 3, another crack growth mechanism, refers to a possibly different crack growth mechanism in the tensile and the shear mode parts. In the tensile part striations are very often found which do not show up in the shear lips unless higher R-values are used [12]. Probably the shear lips are crunched by the crack closure wedge leading to destruction of the striations. This crunching effect will of course be less at higher R values.
If striations are found in both parts then probably similar basic growth mechanisms, i.e. fatigue crack growth by a striation mechanism in each cycle, might be operative in both tensile and shear mode parts, leading to about the same crack growth resistance.
Striations in shear lip parts have also been found by the present author, which supports the conclusion that the actual crack growth mechanisms (crack growth by striations) in the shear mode parts are the same as in mode I (tensile) fatigue crack growth. This is also confirmed in the literature [13,14,15].

Cause 4, a higher crack growth resistance due to a longer crack front line, was suggested by Schijve [16] and also in reference [17]. They implied that a longer

crack front line results in more resistance to crack growth and thus in a lower apparent stress intensity factor ΔK. Their suggestion forms a mix between crack growth resistance and crack driving force. An increasing resistance is assumed and next translated to a decreasing driving force. Therefore in a situation with shear lips more fresh fracture surface is made then in the tensile mode situation per crack extension unit. Here we assume a higher crack growth resistance owing to the longer crack front line only.

However, note that all causes together lead to less fresh crack surface made per cycle in case of shear lips. In a transition from tensile mode to full (100%) shear mode a decrease in da/dN with a factor of about 3 is observed, whereas the transverse crack front length is about $\sqrt{2}$ times longer. As a consequence, when we compare a situation of tensile growth with a situation of pure shear growth, at the same applied ΔK, in the latter (shear lip) case *less* fresh surface per cycle is made, i.e. :

$$da/dN_{(tensile)} * t > da/dN_{(eq)} * t\sqrt{2}.$$

Thus in reality in the tensile mode area more fresh surface is made per cycle than in the shear mode area.

A connection between ΔK_{eff} and the shear lip width.

The above discussion leads us to the conclusion that the driving force influences, causes 1 and 2, will influence the crack growth rate. The discussion of resistance, causes 3 and 4, eliminates different mechanisms being operative (cause 3), but does not exclude that the longer slant crack has a different resistance compared with a tensile crack (cause 4). Causes 1 and 4 connect ΔK and the transverse crack length ℓ.

Because we observe a decrease in da/dN for larger ℓ, we try a very simple formula, connecting both quantities, $\Delta K.\ell$ = constant. This formula is of course only allowed if the same crack growth mechanisms apply to the tensile mode and the shear mode parts, as pointed out in the discussion of cause 3. It is a simplification, because extra closure in the shear lip parts (cause 2) is not included.

The effects of shear lips on ΔK and crack growth resistance (causes 1 and 4) and on the amount of closure (cause 2) probably are the reasons for the observed decrease of da/dN. That suggests to use an effective ΔK as a characterizing parameter instead of ΔK. This parameter contains elements of both K and crack closure. Of course it is difficult to estimate the relative amounts of both contributions. The following simple assumption is adopted:

$$\Delta K_{eff} \cdot \ell = \text{constant} \qquad 5.8$$

where ℓ is the transverse crack front line length. All three causes discussed earlier, K, closure and resistance, the latter due only to crack front length and *not* to a different mechanism, are combined in equation 5.8. Equation 5.8 predicts the dependence of ΔK_{eff} on the transverse crack front length and thus on the shear lip width. For ℓ = t (no shear lips) ΔK_{eff} has the normal Elber value. When shear lips develop ℓ is larger and a correction on ΔK_{eff} is needed according to equation 5.8.

We will compare the situation at the beginning of the constant ΔK test, when the crack front is still in the tensile mode, with the equilibrium situation when the shear lip width $t_{s,eq}$ and the corresponding equilibrium crack growth rate in the shear mode, $(da/dN)_{eq}$, have reached a steady state value. Although we have the same applied ΔK in both cases, the real ΔK_{eff}, "as felt by the tip", will be lower in the slant case. From equation 5.8 it follows that:

$$\frac{\Delta K_{eff,\,tensile}}{\Delta K_{eff,\,eq}} = \frac{\text{transverse length slant crack}}{\text{transverse length tensile crack}} = \frac{\ell}{t} \qquad 5.9$$

When it is assumed that the shear lips make 45° with the loading direction then:

$$\frac{\ell}{t} = 1 + 2(\sqrt{2} - 1)\frac{t_{s,eq}}{t} \qquad 5.10$$

$\Delta K_{eff,tensile}$ is the ΔK_{eff} at the beginning of the test, where the surface is in tensile mode. It is equal to the applied ΔK_{eff} ,using equations 5.6 and 5.4, thus equal to the normal Elber value. $\Delta K_{eff,eq}$ is the ΔK_{eff} at the end of the test, when shear lips have reached their equilibrium value. $\Delta K_{eff,eq}$ thus depends on $t_{s,eq}$. We define $\Delta K_{eff,eq}$ with equation 5.9.

(Reversed) Similarity

In the previous discussion it was assumed that besides an influence on K (cause 1) shear lips also have an influence on the amount of crack closure (cause 2) and on the crack growth resistance by the longer crack front length (cause 4). These arguments led us to adopt equation 5.8.

In order to be able to predict da/dN in a situation of shear lips, an approach is followed using a sort of similarity (= similitude, see chapter 2) concept. The similarity concept states that similar crack driving forces (ΔK or ΔK_{eff}) lead to the same da/dN. Here the reversed argument is also thought to be true, equal crack growth rates are a consequence of equal values of ΔK_{eff} irrespective of the

fracture mode.

At the start of the constant ΔK test there are no shear lips and the ΔK can be described with equation 5.6. After some crack growth shear lips will develop. In general ΔK can not be found now from equation 5.6 as this formula is valid only for a tensile mode crack. It may be obvious also that for a crack with shear lips, standard relations of ΔK_{eff} can not be used, because normally in these standard relations the fracture mode situation is not a variable, except for the tensile mode case where ΔK is defined with equation 5.6.

The ΔK_{eff} relation of Elber, equation 5.4, led to a reasonable result for the tensile mode crack growth rate as was shown in figures 5.4 and 5.5. Therefore it will be assumed that ΔK_{eff} for the tensile mode situation can be defined using equation 5.6 for ΔK and using equation 5.4 for the crack closure correction.

The reversed similarity concept states that when a crack in shear mode has the same da/dN as a crack in tensile mode for both cases the same ΔK_{eff} will apply. This gives an opportunity to define ΔK_{eff} for a slant crack and to use it in a crack growth law.

Application of the model

The similarity approach enables us to use equation 5.5 as a calibration equation to find da/dN from ΔK_{eff} and vice versa. It enables a *quantitative* prediction of da/dN in a shear mode situation, i.e. it means that we can substitute $\Delta K_{eff,eq}$ in the tensile mode equation 5.5 to find da/dN = $(da/dN)_{eq}$.

The principle yields:

$$(da/dN)_{eq} = 1.88\ 10^{-5}\ (\Delta K_{eff,eq} - 2.6)^2 \qquad 5.11$$

with $\Delta K_{eff,eq}$ according to equation 5.9.

The calculation procedure is explained in figure 5.6. The problem is to predict da/dN in a situation with shear lips, when $(da/dN)_{tensile}$ is known. We start at a given crack length (a) and calculate $\Delta K_{eff,tensile}$ (= the normal Elber value) and $(da/dN)_{tensile}$,using equation 5.5

Using equation 5.9 we find the effective ΔK in the presence of shear lips, $\Delta K_{eff,eq}$. Then using equation 5.5 again we find point 3, representing the da/dN based on a tensile crack front geometry. Next point 2 can be constructed, being the predicted $(da/dN)_{eq}$.

Note that we applied (reversed) similarity in the last step, by assuming that for points 3 and 2, at the same da/dN values, we will have the same ΔK_{eff} values.

Next the crack length is increased with Δa and the calculation is repeated for the new crack length. The value of $t_{s,eq}$, which we need to calculate $\Delta K_{eff,eq}$,

follows from equation 5.2 using $\Delta K_{eff} = \Delta K_{eff,tensile}$.

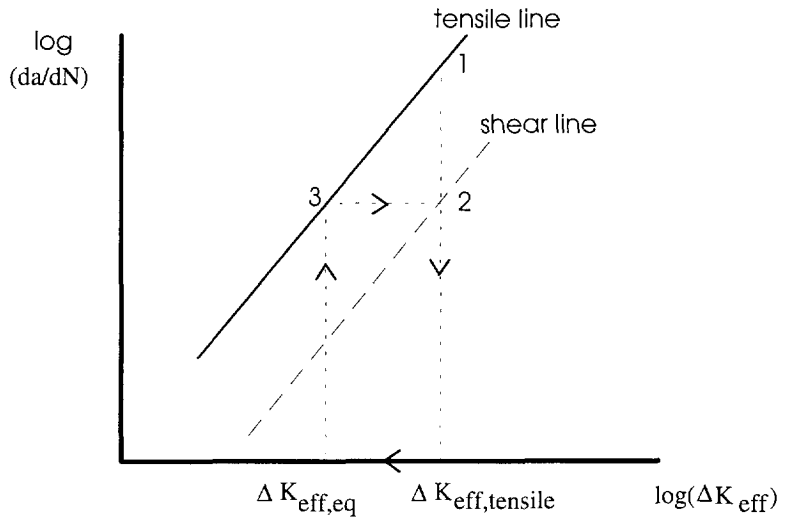

Figure 5.6. Graphical presentation of the calculation procedure.

This is allowed because equation 5.2 is found in chapter 4 using only the standard Elber function for ΔK_{eff} .

Lagging behind of shear lip parts

We assumed ΔK_{eff} to be inversely proportional to the transverse crack front length, equation 5.8. In practice it is often found that the shear lips on the edges of the specimen lag behind the tensile middle during crack growth. The crack front line length is longer now than the value of ℓ calculated in equation 5.10. In the calculation of ℓ we do not correct for this effect, because ℓ is found from $t_{s,eq}$ (equation 5.10) and because the shear lip width measurements were made perpendicular to the crack extension direction.

However, note that the crack growth resistance will not be a function of the crack front line length, but of the fresh crack surface area (plus the accompanying plastic deformation zone) that is created per unit crack extension. This means that we assume that ΔK_{eff} is inversely proportional to a crack area that is formed per unit crack extension, thus:

$$\Delta K_{eff} * \text{the cracked area per unit crack extension} = \text{constant} \qquad 5.12$$

With this interpretation, which is physically more acceptable than the association of the crack growth resistance with a one dimensional quantity such as the crack

front line length, the cracked area is not dependent on the amount of lagging behind of shear lip parts.

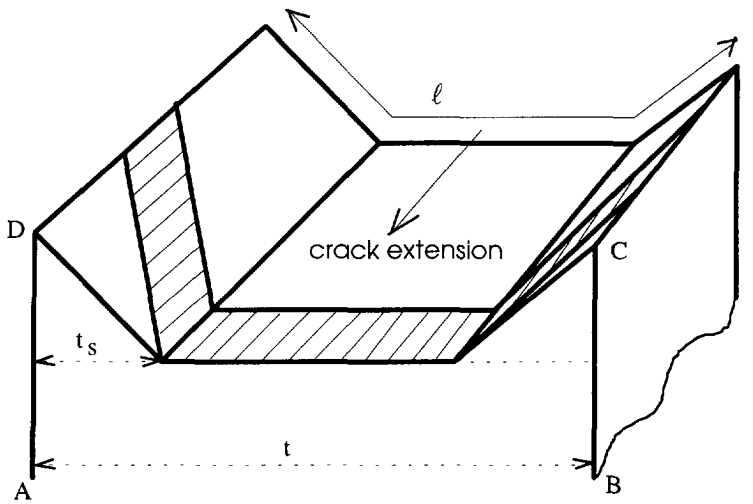

Figure 5.7. Crack resistance area in case of shear lips.

The same fresh crack surface is made for a situation with tunneling due to shear lips and for a situation where the crack front lies in a plane perpendicular to the side surface of the plate.

The conclusion thus is that with this considerations it remains possible to use equation 5.8 also in the case of tunneling due to shear lips. As a necessary consequence of this the transverse crack front length, ℓ in equation 5.8, has to be interpreted as the projection of the transverse crack front line on a plane perpendicular to the crack extension direction (plane ABCD), i.e. length ℓ in figure 5.7.

Thickness effects

Our simple model predicts a ratio $\Delta K_{eff,tensile} / \Delta K_{eff,eq}$ that is only dependent on the ratio $t_{s,eq}/t$ (equation 5.10). Thus at the *same percentage* shear there is no dependency of the plate thickness. For pure tensile mode $\ell/t = 1$ and there is no thickness effect. For pure shear, where $t_{s,eq} = 0.5\ t$, the ratio $\ell/t = \sqrt{2}$ and thus also:

$$\frac{\Delta K_{eff,\,tensile}}{\Delta K_{eff,\,eq}} = \sqrt{2} \qquad 5.13$$

There is again no thickness effect, and ΔK_{eff} in the tensile mode is about 40%

higher than in the shear mode.

During the transition from pure tension to full shear ℓ /t varies from 1 to $\sqrt{2}$ and the effect on ΔK_{eff} and da/dN can now be calculated. In this transitional area there is a thickness effect, because ℓ /t depends on t now.

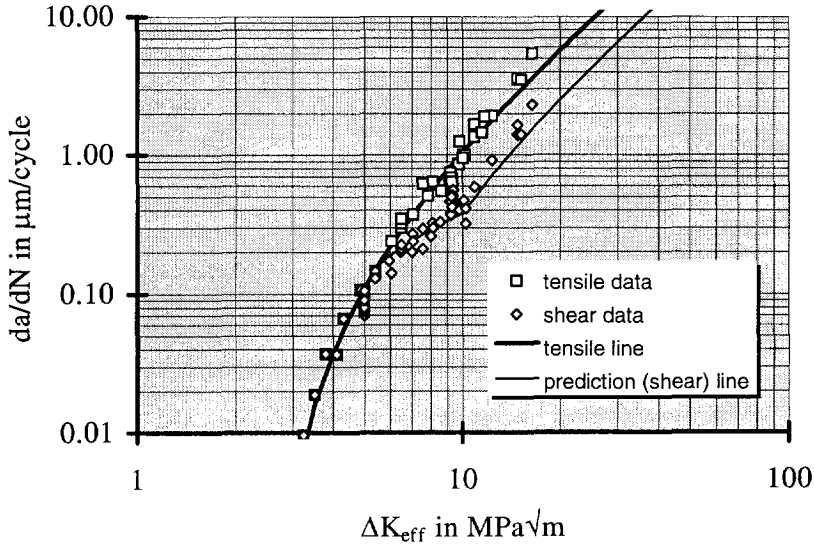

Figure 5.8 Prediction of da/dN versus ΔK_{eff} for t = 6 mm.

In figures 5.8 - 5.10 the results of the calculation are shown. $(da/dN)_{eq}$ is calculated for small steps of Δa. The experimental crack growth rates , in the tensile mode and in the equilibrium shear mode, are also shown, in figure 5.8 for 6 mm plate thickness and in figure 5.9 for 10.3 mm thickness. Note that the shear line is the predicted equilibrium da/dN line. Note also that for complete shear the shear line is parallel to the tensile line. The line for complete shear is shifted by a ΔK_{eff} increase of $\sqrt{2}$ as compared to the tensile line.

Two slopes can be observed in the shear data, one for the intermediate tensile/shear range and a larger one for the complete shear range. The latter slope is equal to the slope of the tensile data. This change in slope is often found and reported in the literature, see also the discussion in section 5.5.

In a normal constant amplitude test we will find three slopes, one for the tensile mode situation, a lower one in the transition range and next a higher one in the complete shear lip range. The model is capable to predict these slopes (figure 5.8).

In figure 5.10 only the lines of the calculations are plotted for three plate thicknesses: 2, 6 and 10.3 mm, to illustrate the thickness effect of the calculation in the transitional area.

It should be recalled that each data point in figures 5.8 and 5.9 is the mean crack growth rate in the "stable" shear lip situation, i.e. where $t_{s,eq}$ is reached (i.e. $(da/dN)_{eq}$ in figure 5.1). Every measured $(da/dN)_{eq}$ point is the result of a complete test on a center cracked tension specimen. The results cannot be fully compared to the results of a constant amplitude test in which ΔK increases, because the real shear lip width lags behind the equilibrium width in such tests.

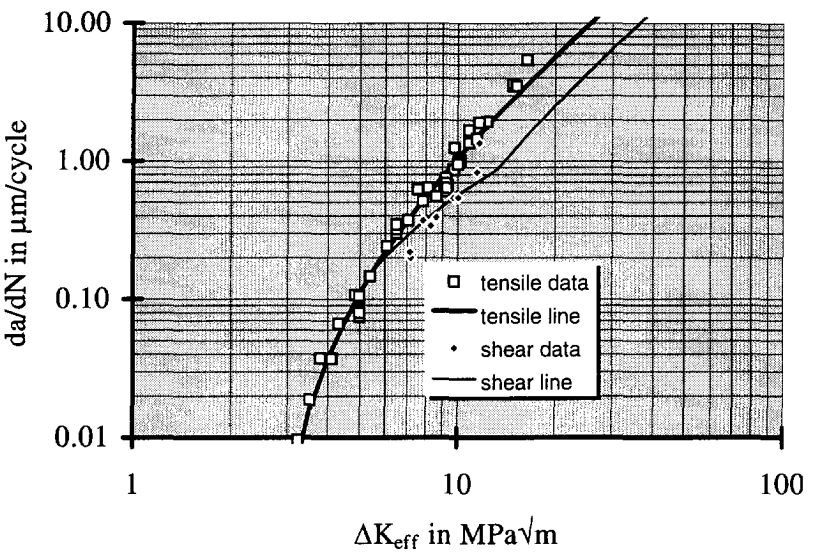

Figure 5.9. Prediction of da/dN versus ΔK_{eff} for t = 10.3 mm.

The general trends, however, that are found here, are expected to be valid for constant amplitude loading too. The greater the thickness, the more the tensile crack growth rate line will be approached. In the case of constant amplitude loading the shear line will lie somewhat above the shear line at constant ΔK loading because in the constant amplitude case the shear lips are smaller.

Thus the shear line is the real line, which represent the results in a situation of stable shear lips as found in tests. The tensile line is a more theoretical line, which in principle describes a non-stable situation (see figure 5.2). However, the tensile line is not unimportant. In a lot of practical variable amplitude situations flat tensile fatigue fracture surfaces are found. In these cases it is recommended to use the tensile line for fatigue crack growth predictions.
Especially for very high load excursions a larger Δa will then predicted, which is correct in view of the absence of shear lips. Constant amplitude test results that refer to a situation of complete or partial shear, are not to be recommended because of the difference in fracture mode.

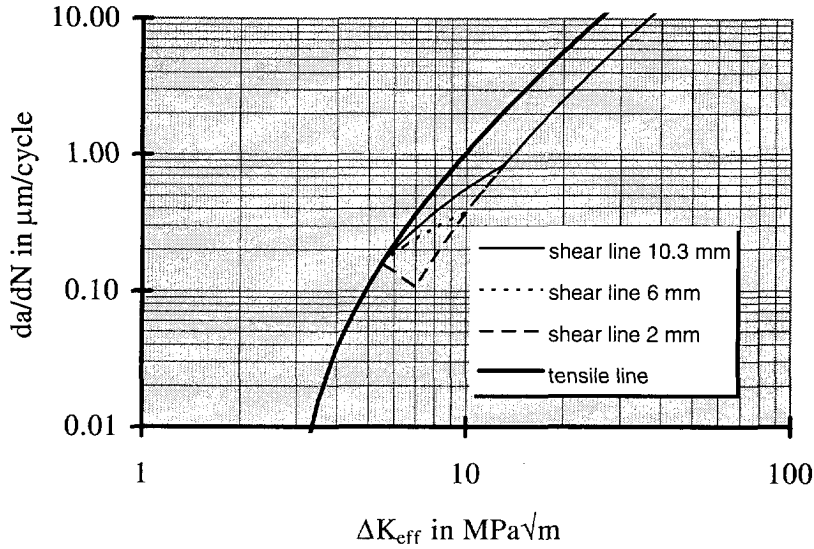

Figure 5.10. Calculated results for 2, 6 and 10.3 mm.

5.5 Implications for Mode I, II and III crack growth

At present it is generally assumed that (part of) fatigue crack growth can be described by the equation of Paris:

$$\frac{da}{dN} = c\,(\Delta K_{eff})^{m} \qquad 5.14$$

In this equation ΔK_{eff} is the nominally effective ΔK , corrected for crack closure using standard relations like the Elber equation. In this chapter we use $\Delta K_{eff,tensile}$ (introduced in the previous section) to denote the nominal ΔK_{eff} .

For the experimental results (tensile data) in the normal Paris regime, i.e. for ΔK_{eff} values between 5 and 10 MPa$\sqrt{m}$, the slope m of the da/dN - ΔK_{eff} data on a log-log scale is about 3 (see figure 5.8).
Note that the value of m for the tensile line, equation 5.5, (which is the same as the value for the shear line with complete shear lips) varies from 3.5 for ΔK_{eff} = 5 Mpa$\sqrt{m}$ to 2.7 for ΔK_{eff} = 10 Mpa$\sqrt{m}$, as follows from differentiating the tensile curve equation 5.5.

The da/dN decrease, going from the tensile line to the complete shear line at the same ΔK_{eff} is found by:

$$\frac{(\frac{da}{dN})_{tensile}}{(\frac{da}{dN})_{eq}} = (\frac{\Delta K_{eff,tensile} - 2.6}{\Delta K_{eff,eq} - 2.6})^2$$

It varies from 2.74 for ΔK_{eff} = 10 MPa$\sqrt{m}$ to 2.36 for ΔK_{eff} = 16 MPa$\sqrt{m}$.
Bakker [6] calculated the influence of the slant mode on K by performing finite element calculations for situations without shear lips and with double and single shear lips. He calculated the effect of shear lips on the mean (i.e. mean through the plate thickness) equivalent stress intensity and on the mean of the mode I stress intensity factor, $K_{eq,m}$ and $K_{I,m}$ respectively. The equivalent stress intensity is defined as the mode I stress intensity which has the same energy release rate as the actual combined mode I, II and III loading.
The results of the calculations for *complete* shear are summarized in the next table ($K_{tensile}$ is the K_I value for a situation without shear lips):

shear lip type	$K_{eq,m}$ / $K_{tensile}$	$K_{I,m}$ / $K_{tensile}$
double	0.839	0.601
single	0.838	0.624

When $K_{eq,m}$ is responsible for the crack growth rate, and when the 3 modes have the same da/dN for equal ΔK, the results from the table predict a decrease in da/dN by a factor of about 1.7, when a Paris exponent m = 3 is taken. However, when only $K_{I,m}$ is responsible for the crack growth rate the decrease is by a factor 4.1 for single shear and 4.6 for double shear. The real value of about 3, as found in this work (see also the discussion, section 5.7), lies between these limits (1.7 for $K_{eq,m}$ and larger than 4 for $K_{I,m}$ alone), indicating that K_{II} and/or K_{III} also have a contribution to the crack growth rate. This contribution is lower than the contribution of K_I for equal values of ΔK.
The causes of the lower contributions of ΔK_{II} and ΔK_{III} can be the lower crack growth rates of these modes and/or the higher sensitivity of these modes for crack closure due to (irregular) shear lips.
The results of $K_{eq,m}$ / $K_{tensile}$ in the table are about equivalent with $\Delta K . \sqrt{\ell}$ = constant (i.e. $\Delta G . \ell$ = constant). The results of $K_{I,m}$ / $K_{tensile}$ in the table are about equivalent with $\Delta K . \sqrt{\ell^3}$ = constant.
Fracture mechanics terms are not well defined for a situation of complete shear. Thus when we compare a tensile mode situation with a situation of complete shear in a "constant ΔK" test the only quantity that remains the same is the load P (at the same crack length). To be able to attack the slant crack problem with

fracture mechanics parameters we load two center cracked tension plates, with thicknesses ℓ_A and $\ell_B = x\ \ell_A$ with the same load P. For this situation with the same load $\Delta K\ .\ell$ = constant is valid, independent of the value of x. When a value of the Paris exponent m = 3 is assumed we get a ratio of the crack growth rates in both plates of:

$$\frac{(da/dN)_A}{(da/dN)_B} = x^3$$

For a "pseudo" shear lip configuration with $x = \sqrt{2}$ this leads to a decrease in da/dN with a factor $2\sqrt{2}$, which is about 2.74 as found above. Thus this very simple consideration can predict the da/dN decrease that is found in practice, when the "pseudo, two-dimensional" shear lip configuration with $x = \sqrt{2}$ is considered equal to the three-dimensional real shear lip situation.

The conclusion is thus that we can explain the experimental result in two ways. One with $\Delta G\ .\ell$ = constant (i.e. $\Delta K\ .\sqrt{\ell}$ = constant), when the modes II and/or III have a contribution to the crack growth (however with a lower (unknown) growth rate than mode I) or we can explain the result with $\Delta K\ .\ell$ = constant, when only mode I contributes to crack growth, where ΔK is the mode I stress intensity cycle.

For many tests performed on Al 2024 by various authors m values of about 3 are found. The slope in the transitional part is thickness dependent. For 6 mm it is about 1.4 and for 10.3 mm thickness it is about 1.8.
It should be noticed that for constant amplitude loading the values in the transitional area will be somewhat higher. The change in slope for constant amplitude loading is reported in many papers, references [18,19,20,21]. In some references [22,23,24,9] the increase in slope after the transitional area is considered to be a proof that shear lips have an accelerating effect on fatigue crack growth. From the foregoing it may be clear that this conclusion is not correct. The first lower slope is due to shear lip development in the transitional area. It is followed by the normal, higher slope after completion of the transition.

5.6. Application of the model to constant amplitude fatigue crack growth

In references [25] and [26] in a constant load amplitude test a temporary decrease in fatigue crack growth rate was found while ΔK was increasing. The effect was attributed to shear lip development. We will apply the model to test its capability to predict such a decrease in da/dN, at increasing ΔK, and to determine

the conditions relevant to such a situation. In chapter 4, section 4.3, a method is described to calculate the actual shear lip width during a constant stress amplitude fatigue test. The shear lip width t_s lags behind the equilibrium value $t_{s,eq}$. The amount of delay is determined by the rate $d(\Delta K_{eff})/da$.
The da/dN calculation procedure is the same as described for constant ΔK except that now the momentary shear lip width t_s is used instead of the equilibrium value $t_{s,eq}$. We assume that the model can also be applied for the non-stationary situation of constant amplitude growth. Of course the closure behavior in a constant amplitude test will be slightly different from that in a constant ΔK test due to the continually changing ΔK with increasing crack length. This effect is expected to be small and it will be neglected. Lagging behind of the shear lip width under constant amplitude circumstances will lead to a slightly higher ΔK_{eff} as found from equation 5.7 because ℓ is lower now.

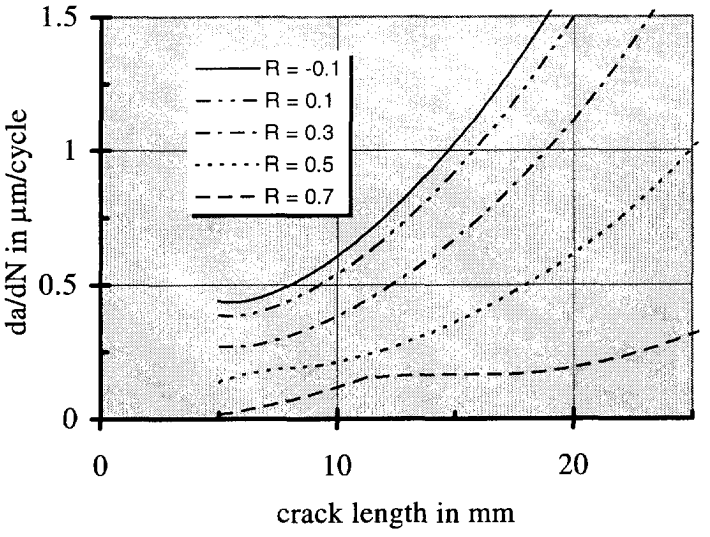

Figure 5.11. Calculated results for 5 R-values; t = 2 mm, S_{max} = 120 Mpa.

Calculations are shown in figures 5.11, 5.12 and 5.13 to show thickness and frequency trends without comparison with experimental results.
In figure 5.11 the constant amplitude calculation results are shown for da/dN versus crack length (a) for 5 different values of R for a 2 mm thick plate. The calculation starts with a crack of 5 mm in the tensile mode.
In figure 5.12 the results of similar calculations are given for a 10.3 mm thick plate. Figure 5.11 shows that a change in slope is possible. The change in slope is not present in the 10.3 mm thick specimens.

Effect of frequency on the calculation

In chapter 4, section 4.5 , the effect of frequency on $t_{s,eq}$ and da/dN has been shown. The equilibrium value $t_{s,eq}$ was found to be a function of ΔK_{eff} and frequency f:

$$t_{s,eq} = 0.67\ \Delta K_{eff} + 0.64 \log f - 4.35 \text{ (mm)} \qquad 5.15$$

f in Hz, ΔK_{eff} in MPa$\sqrt{m}$.

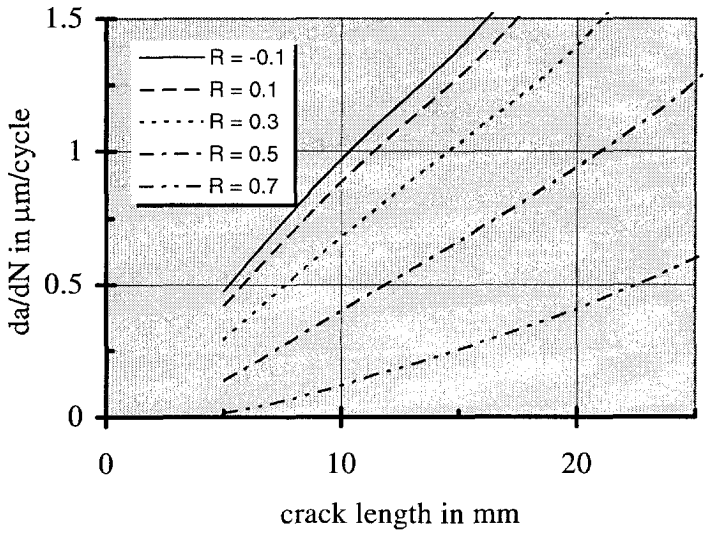

Figure 5.12. Calculated results for 5 R-values; t = 10.3 mm, S_{max} = 120 MPa.

With this $t_{s,eq}$ formula and the equation for c (equation 5.3) we are able to predict constant amplitude fatigue crack growth rate results at different frequencies. The tensile crack growth curve (equation 5.5) was assumed to be frequency independent as substantiated in chapter 4, section 4.5. In figure 5.13 calculated values of da/dN for 5 different frequencies are plotted to show the frequency effect. A decrease in da/dN is possible. For thicker specimens the calculated frequency effect is less pronounced.

Two constant amplitude tests on 160 mm wide specimens of 2 mm thickness were carried out to verify the frequency effect (see figure 5.14). The specimen length was 300 mm. Two frequencies were used, 25 Hz and 0.1 Hz. Both constant amplitude tests started in the tensile mode, made by a prefatigue

procedure at low ΔK. For the test at 25Hz a decrease in da/dN is observed in the beginning. This is not observed in the test at 0.1 Hz.

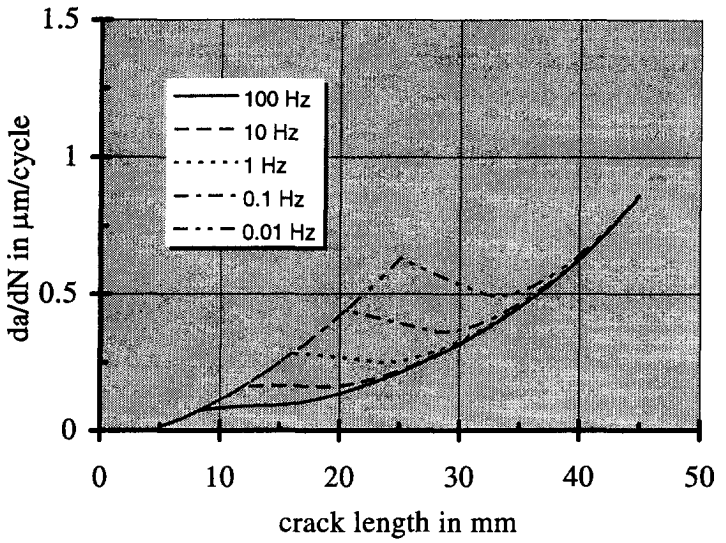

Figure 5.13 Calculated results for 5 frequencies; t = 2 mm, R = 0.70, S_{max} = 120 MPa.

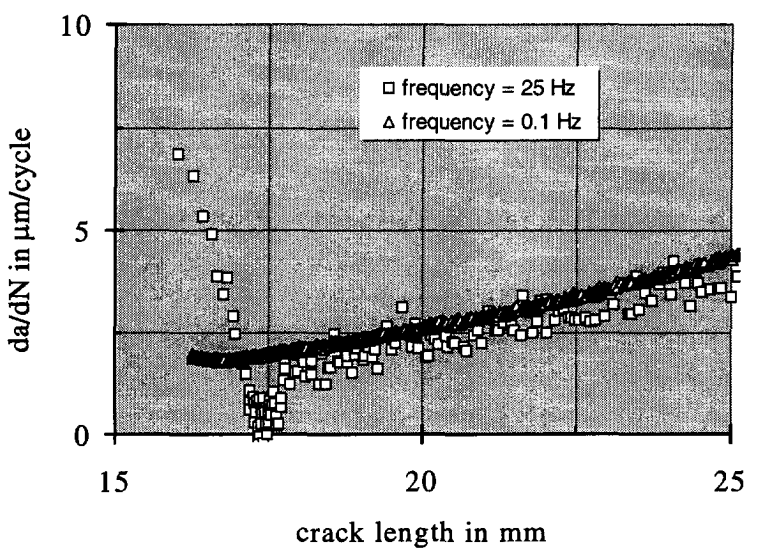

Figure 5.14. Results of two c.a. tests; R = 0.10; S_{max} = 120 Mpa; t = 2 mm.

For 25 Hz the shear lip development is much faster than for 0.1 Hz which can

explain this result.
Apparently for the former case ΔK_{eff} drops faster due to the increasing shear lip width than it is increasing due to the constant amplitude loading. When the increase of the shear lip width becomes less the constant amplitude increase of ΔK_{eff} will begin to dominate, leading to an increasing da/dN.

5.7. Discussion

In section 5.4 we have mentioned several possible causes for the reduction in crack growth rate during shear lip development. It was suggested that the amount of crack closure is different for shear and tensile parts. As was discussed it seems logical to assume that shear lips will have another crack closure behavior than a tensile mode crack.
It was shown that the crack growth rate in the shear mode could be reasonably predicted by a sort of similarity approach and by the assumption $\Delta K_{eff} . \ell$ = constant. If however $\Delta K . \ell$ = constant is also adopted, then both assumptions lead to the conclusion that the crack closure behavior is the same in the tensile and shear parts (i.e. U is not a function of ℓ). If alongside of $\Delta K_{eff} . \ell$ = constant also $\Delta G . \ell$ = constant is adopted (as resulted approximately from the finite element calculations by Bakker[6]), a different crack closure behavior in tensile and shear parts is implied. For this case U is a function of ℓ with $U . \sqrt{\ell}$ = constant.
This leads to $U_{shear} = \frac{1}{\sqrt{\sqrt{2}}} U_{tensile}$. When this result is applied to the crack closure function of Schijve, assuming that this closure formula is valid in the tensile mode, we get $U_{shear} = 0.46 + 0.28R + 0.10 R^2$ (see also chapter 7, equation 7.6).

Over a limited range of ΔK_{eff} values it is possible to find a Paris type equation for the tensile line, as defined in equation 5.14. For the ratio of $(da/dN)_{tensile}/(da/dN)_{eq}$ the model ($\Delta K_{eff} . \ell$ = constant) predicts a value of $2\sqrt{2}$ for m = 3, which was about confirmed by the measurement results. Thus the effect of shear lips on K (mode I) is 41% *at the utmost*, when extra closure due to shear lips is neglected. Compare this result with the results of Finite Element calculations from the literature. In reference [6] a decrease in K_I of about 40 % was predicted for the transition from tensile mode to complete shear.
The change in slope for constant amplitude loading is reported in a lot of papers. In reference [27] slope values of 4 or higher are found for low and high ΔK regions. For intermediate ΔK values a slope between 2 and 3 was found. The specimen thickness was 0.25 inch. In reference [28] a slope m=4 is found for

higher ΔK values. Also in chapter 7 of this work an m value of 4 or higher is found for higher ΔK.

Most tests have been performed on 6 mm plate, so figure 5.5 is our most important figure to test the model. As we did not use a fit factor in the model the results are good at low ΔK_{eff}. For high ΔK_{eff} , where complete shear is reached, the prediction does not fit the results so well. Examination of the fracture surface reveals that the shear lip often reinitiates on another 45° plane at high ΔK_{eff} (see chapter 4, figure 4.27). The direction of the crack growth now is not along a straight line, but it fluctuates above and below it. Examination of transverse sections of the specimens reveals that reinitiating has a locally flat making effect (see chapter 3, figure 3.8). This will have an influence on the transverse crack length and it also will influence the (extra) closure behavior of shear lips and thus ΔK_{eff} . In the model, however, we assume for high ΔK_{eff} a situation of total shear with a transverse length $\ell = t\sqrt{2}$.
Hence the model will underestimate $(da/dN)_{eq}$ for higher ΔK_{eff}. Measuring of the real transverse length instead of using the shear lip width will improve this deviation. This will also correct for the fact that the shear lip angle is not always 45° as assumed in the model. The differences in transverse length after "completion" of the shear lip, caused by the reinitiating of shear lips mentioned above, are also responsible for the observed changes in the growth rate [32,33].

From figure 5.10 it is clear that the thickness effect found is largely a shear effect. The thicker the specimen is, the less influence a certain shear lip width has and the more the tensile crack growth line is approached. In a situation of pure tensile mode no thickness effect is observed. This is also assumed to be true for complete slant growth.
The calculated results for constant amplitude tests (figures 5.11, 5.12 and 5.13) can be understood from the fact that $t_{s,eq}$ is a function of ΔK_{eff} only (at a constant frequency) and shows no dependence on thickness, whereas da/dN (through $\Delta K_{eff,shear}$) depends on t_s/t . During a constant amplitude test ΔK_{eff} increases, so da/dN will increase. Above a certain ΔK_{eff} level $t_{s,eq}$ also increases and thus t_s/t increases, so da/dN will decrease. Which of these effects will dominate depends on the maximum (constant load) stress amplitude S_{max}, on the R-ratio and the plate thickness t. Frequency has an analogous effect. A higher frequency leads to a higher $t_{s,eq}$ and thus through t_s/t to a lower crack growth rate. When applying this model to other 2024 alloys, or even other materials, one has to check if equation 5.2 and equation 5.3 are valid for these materials.

5.8. Conclusions

The conclusions we draw from this chapter are:

1. An increase of the shear lip width decreases the crack growth rate da/dN.

2. The two slopes in the da/dN versus ΔK curves on log-log scale are due to the impeding action on da/dN of growing shear lips in the transitional area between pure tensile mode and pure shear mode.

3. The formula found for the tensile mode crack growth, equation 5.6, is important for fatigue crack growth prediction under variable amplitude loading where the fracture surface is expected to remain flat.

4. The crack growth rate in the case of shear lips can reasonably be described by $\Delta K_{eff} \cdot \ell$ = constant and by adopting a similarity approach.

5. The thickness effect on da/dN is dependent on the change of the transverse crack front length; for low ΔK_{eff} (pure tensile mode) no thickness effect is observed. It is expected to be true too for high ΔK_{eff} (pure shear mode).

6. The tensile growth rate can be described by Elber's crack closure formula. A good description requires an effective threshold value.

7. An explanation for the observed temporary decrease of da/dN in some constant amplitude tests is given.

5.9. References

1. W. Elber, Fatigue crack closure under cyclic tension, ASTM STP 486, 230-242 (1971).
2. L.P. Pook, The role of crack growth in metal fatigue, 1983, The Metals Society, London.
3. L.P. Pook and A.F. Greenan, Engng Fracture Mech. 5, 935-946 (1973).
4. T.C. Lindley, Near threshold fatigue crack growth: Experimental Methods, Mechanisms and Applications, in Subcritical Crack Growth due to Fatigue, Stress Corrosion and Creep, ed. L.H. Larsson, 167-211, JRC, Ispra, Italy (1981).
5. J. Petit, B. Bouchet, C. Gasc and J. De Fouquet, Proc. ICF4, Waterloo, Canada (1977),pp. 867-872.
6. A.Bakker, Fatigue Fract. Engng Mater. Struct., Vol 15, No 11, pp 1051-1069, 1992.
7. Yoshoika, in Stress Intensity Factors Handbook by Y. Murakami, Vol. 2, Pergamon Press, pp. 833-836, 1987.
8. H.L. Ewalds and R.T. Furnee, Crack Closure along the Fatigue Crack Front of Center Cracked Specimens, Second European Colloquium on Fracture (ECF

2), Darmstadt, October 9 - 11, 1978, pp. 349-360.

9. G. Marci and P.F. Packman, Int. J. Fract, Vol. 16, No 2, 1980, pp. 133-153.
10. J. Schijve, Fatigue Crack Closure: Observations and Technical Significance, Mechanics of Fatigue Crack Closure, ASTM STP 982, American Society for Testing and Materials, Philadelphia,1988, pp. 5-34.
11. W.J.D. Shaw and I. Le May, Crack Closure During Fatigue Crack Propagation, Fracture Mechanics, ASTM STP 677, American Society for Testing and Materials, 1979, pp. 233-246.
12. R.A. Daiuto and B.M. Hillberry, Effect of thickness on fatigue crack propagation in 7475-T731 Aluminium alloy sheet. NASA contractor report 172367. Purdue University, W. Lafayette, USA (1984).
13. R.O. Ritchie, R.F. Smith and J.F. Knott, Met. Sci., 1975, 9,(11),485-492
14. G.G. Garrett, Metallurgical Transactions A, Vol. 10A, may 1979, pp. 648-651.
15. L.P. Pook Met. Sci., 1976,10,(9),334-335.
16. J. Schijve, Engng Fracture Mech. 14, 467-475 (1981).
17. A. W. Bowen and P.J.E. Forsyth, The Effect of Frequency Changes on Fatigue Crack Growth in 7178-T6 Aluminum Alloy, Conf. Proceed. Fracture 1977, Volume 2, ICF4, Waterloo, Canada, june 1977, pp 1217-1222.
18. R.G. Forman, V.E. Kearney and R.H. Engle, Numerical Analysis of Crack Propagation in Cyclic Loaded Structures, Trans. ASME (Ser. D) 69,1967, pp. 459-463.
19. W.D. Dover and N.F. Boutle, Journal of Strain Analysis, Vol. 13, No 3, 1978.
20. J.J. McGowan and H.W. Liu, Journal of Engng Mater. And Techn. Vol. 102, 1980, pp. 341-346.
21. D.G. Rickerby and P. Fenici, Engng Fract. Mech., Vol. 19, No 4, 1984, pp. 585-599.
22. L.P. Pook Met. Sci., 1976,10,(9),334-335
23. R.O. Ritchie, R.F. Smith and J.F. Knott, Metal Science, Vol. 9, 1975, pp. 485-492.
24. L.P. Pook and N.E. Frost, Int. J. Fract, 9, (1), 1973, pp. 53-61.
25. S.R. Swanson, F. Cicci, W. Hoppe, Crack Propagation in Clad 7079-T6 Aluminium Alloy Sheet under Constant and Random Amplitude Fatigue Loading, in Fatigue Crack Propagation, ASTM 415, American Society for Testing and Materials (1967), pp. 312-362.
26. L. Schra, Constant Amplitude Fatigue Crack Growth Data for the Fokker 100 Lower Wing Skin Material, Memorandum SM-85-020U, National Aerospace Laboratory, NLR, The Netherlands (1985).

27.T.S. Kang and H.W. Liu, Int. J. Fract., Vol. 10, No 2, 1974, pp. 201-222.

28.F.A. Veer, The Effect of Shear Lips, Loading Transitions and Test Frequency on Constant ΔK and Constant Load Amplitude Fatigue Tests, Doctor Thesis, Technical University of Delft, october 1993.

29.T.C. Lindley and C.E. Richards, Materials Science and Engineering, 14, 1974, pp. 281-293.

30.H.R. Shercliff and N.A. Fleck, Fatigue Fract. Engng Mater. Struct., Vol. 13, No 3, pp. 287-296, 1990.

31.J. Weertman, Phys. Stat. Sol. (b) 172, 1992, pp. 27-40.

32.J. Zuidema and M. Mannesse, Engng Fracture Mech. 40, 105-117 (1991)

33.J. Zuidema, Int. J. Fatigue 13, 73-78 (1991)

Table 5.1. Results of constant ΔK tests on 6 and 10.3 mm thick plates.

ΔK	R	thickness	da/dN(t)	da/dN(s)	$t_{s,eq}$
(MPa√m)	(mm)	(mm)	(mm/c)	(mm/c)	(mm)
14.4	0.10	10.3	5.10E-04	3.70E-04	1.42
18.0	0.10	10.3	8.70E-04	5.40E-04	2.78
14.0	0.22	10.3		3.40E-04	
16.0	0.25	10.3		2.00E-04	
9.40	0.64	10.3		2.20E-04	1.01
12.0	0.54	10.3	5.50E-04	3.90E-04	2.12
21.3	0.10	10.3	1.90E-03	1.35E-03	
14.9	0.43	10.3	9.50E-04	5.40E-04	3.04
18.6	0.29	10.3	1.45E-03	8.30E-04	3.78
6.0	0.10	6.0	9.60E-06	9.60E-06	
6.5	0.10	6.0	1.88E-05	1.88E-05	
7.0	0.10	6.0	3.73E-05	3.73E-05	
8.0	0.10	6.0	6.67E-05	6.67E-05	
9.0	0.10	6.0	1.07E-04	1.07E-04	
10.0	0.10	6.0	1.46E-04	1.46E-04	
11.0	0.10	6.0		1.72E-04	
12.0	0.10	6.0		2.23E-04	
13.0	0.10	6.0		2.70E-04	
14.0	0.10	6.0		2.94E-04	
15.0	0.10	6.0		3.23E-04	1.83
10.0	0.10	6.0		1.29E-04	
12.0	0.10	6.0		2.00E-04	
23.0	0.08	6.0	1.92E-03	9.20E-04	4.48
12.0	0.10	6.0	3.00E-04	2.12E-04	
28.0	0.07	6.0	3.50E-03	1.65E-03	
9.74	0.30	6.0	2.40E-04	1.40E-04	0.30
14.0	0.10	6.0	6.20E-04	2.10E-04	
11.4	0.50	6.0		2.60E-04	1.75
15.0	0.10	6.0	6.40E-04	3.00E-04	1.83
16.0	0.30	6.0	1.00E-03	4.70E-04	2.96
20.0	0.10	6.0	1.67E-03	5.90E-04	3.55
20.0	0.10	6.0	1.35E-03		

18.0	0.10	6.0	1.25E-03	4.20E-04	2.74
18.0	0.10	6.0	8.60E-04	4.00E-04	2.80
17.0	0.10	6.0	7.20E-04	3.80E-04	2.42
17.0	0.10	6.0	7.50E-04	3.70E-04	
28.0	0.07	6.0	3.60E-03	1.40E-03	
9.28	0.10	6..0	1.00E-04	1.00E-04	
11.5	0.74	6.0		5.60E-04	
6.61	0.64	6.0	7.47E-05	7.00E-05	
6.20	0.77	6.0	7.50E-05	7.50E-05	
6.01	0.83	6.0	8.00E-05	8.00E-05	
11.7	0.71	6.0	6.40E-04	5.10E-04	2.42
12.4	0.65	6.0		4.70E-04	2.60
11.7	0.71	6.0	6.00E-04	4.60E-04	
26.7	0.39	6.0	5.40E-03	2.30E-03	
11.3	0.77	6.0	6.70E-04	5.10E-04	
13.7	0.43	6.0		4.60E-04	
12.7	0.56	6.0	6.90E-04	5.00E-04	2.40
12.7	0.56	6.0	6.40E-04	4.20E-04	
5.90	0.88	6.0		9.00E-05	
28.0	0.07	6.0	3.50E-03	1.40E-03	
19.6	0.05	6.0		4.10E-04	3.04
19.6	0.05	6.0	1.00E-03	3.20E-04	
9.90	0.52	6.0		2.00E-04	
7.90	0.34	6.0	1.05E-04	1.05E-04	
12.1	0.10	6.0	3.20E-04	2.10E-04	
12.1	0.10	6.0	3.45E-04	2.25E-04	
5.64	0.57	6.0	3.70E-05	3.70E-05	
11.5	0.29	6.0	3.70E-04	2.40E-04	
15.8	0.10	6 0		3.30E-04	
9.30	0.10	6.0	1.20E-04		
9.30	0.10	6.0	1.23E-04		

6. Retardation of Fatigue Crack Growth in Al-2024 after Blocks of Underloading

6.1. Introduction

The beneficial effect of overloads on fatigue life has been widely recognized, e.g. [1]. Large retardation's in fatigue crack growth rate occur when cycles with a high stress intensity K_{max} are followed by cycles with a much lower K_{max}. The most well-known explanation is based on the effect of residual plastic deformation, which leads to compressive stresses before the crack tip and increases the crack opening load on subsequent crack growth (crack closure). Sometimes blunting of the crack tip is also held responsible for crack growth retardation after a reduction in K_{max}.
In contrast with overloads it was found that underloads (compressive overloads) tend to accelerate crack growth, e.g. [2]. Moreover, if a tensile overload is followed immediately by an underload the beneficial effect of the overload may be significantly reduced.

Several materials show a transition from fatigue crack growth on a normal (90°) crack surface to a slant (45°) crack surface at increasing ΔK, as discussed in previous chapters. This slant fatigue crack growth surface has been found to have an influence on retardation after load changes [3-7]. The Al 2024 alloy is particularly sensitive to this kind of fracture mode change. In this chapter we will investigate how a change of the fracture mode affects acceleration or retardation after underloads. Tests are carried out with large numbers of underloads because a small number of underloads does not change the fracture mode. Tests with overloads were also performed for comparison purposes.
The type of tests are shown in figures 6.1 and 6.2. Figure 6.1 shows blocks of underloading cycles and overloading cycles that will give rise to shear lips (slant mode) when the number of under(over)loads is high enough. Figure 6.2 shows underloading cycles and overloading cycles that will not give rise to shear lips (slant mode) because the ΔK_{eff} applied is too small. All tests were performed at constant K_{max} and K_{min}. During the low ΔK cycles ΔK_{eff} is sufficiently low to have no shear lip forming (tensile mode only). The underload and overload cycles in figure 6.1 , type a and type b, will both give rise to shear lip formation. Their effects on crack growth in the high cycle block and the subsequent low cycle block can then be observed. All low ΔK cycles have been chosen to have the same effective ΔK using [8]:

$$\Delta K_{eff} = (0.55 + 0.33\,R + 0.12\,R^2)\,\Delta K \qquad 6.1$$

R is the stress ratio K_{min}/K_{max}.

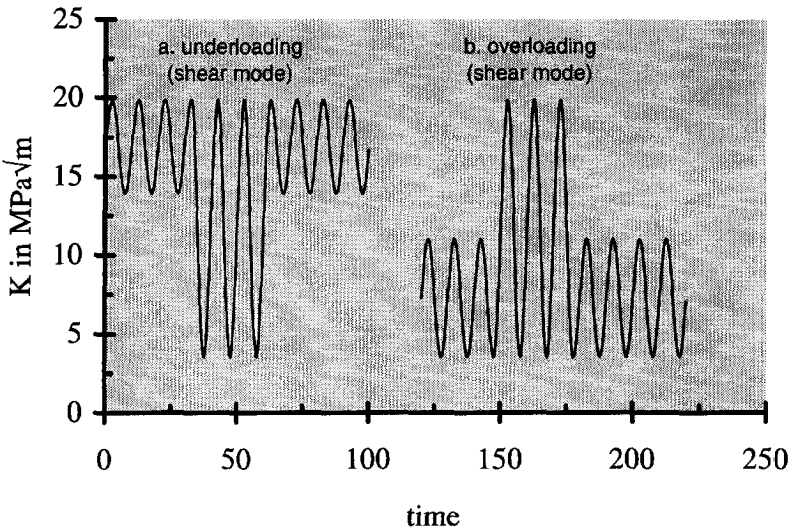

Figure 6.1. Principle of underload and overload tests in shear mode.

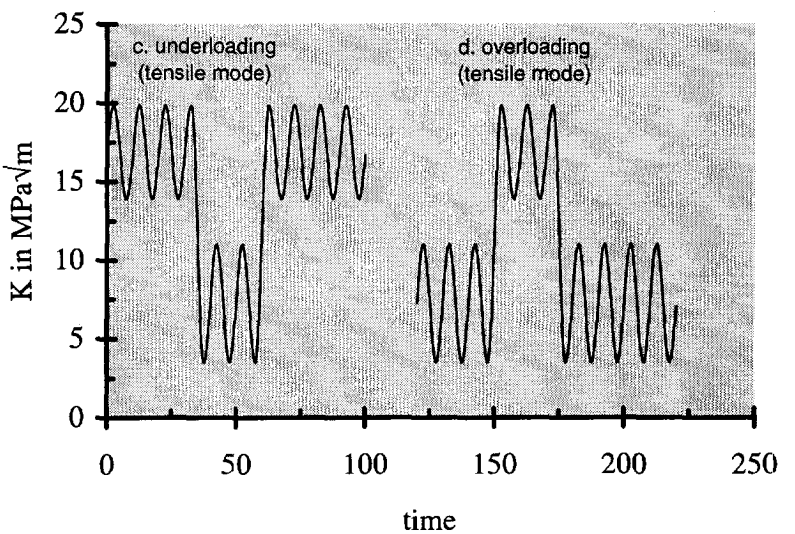

Figure 6.2. Principle of underload and overload tests in tensile mode.

The low (applied) ΔK_{eff} value is 5 MPa$\sqrt{m}$. For the high ΔK_{eff} of the underload and overload cycles different values are used, viz. ΔK_{eff} = 8, 10 and 16 MPa$\sqrt{m}$ respectively.

For ΔK_{eff} = 16 MPa$\sqrt{m}$ only underload tests were performed, since overload tests at this level will immediately result in crack arrest in the subsequent low ΔK block. A survey of the block program tests is given in figure 6.3.
A few tests of the kind shown in figure 6.2, type c and type d, were also performed. All ΔK_{eff} levels in these tests have the same value of 5 MPa$\sqrt{m}$, so that no shear lips are expected, see chapter 4. K_{min} and K_{max} values are the same as in figure 6.1. With the results of tests of types a and c underload situations with and without shear lips can be examined. The same applies for tests of types b and d for overload situations. However, underload tests as shown in figure 6.2 (type c) will probably not show crack growth in the underload period, since K_{max} in this period is smaller than the opening K of the preceding cycles. For the sake of completeness some tests were still performed.
For a test of type a no significant (residual) plastic deformation interaction is expected, since K_{max} is the same for the underload cycles and the preceding and subsequent cycles. A larger reversed plastic zone is, of course, formed during the underloads, but this is more likely to result in acceleration rather than retardation in the subsequent low ΔK cycles. The reversed plasticity will reduce the effect of the monotonic (forward) plastic zone. If there is a retardation effect after the underloads it is probably caused only by the presence of shear lips, which have been formed during the underloads.
For a low number of underloads the fracture mode will not change enough. Now theoretically an acceleration of crack growth rate after the underloads is possible, as the action of the crack closure wedge is reduced by the underloads. For a higher number of underloads there can be a substantial fracture mode change. The retardation due to incompatible crack growth and/or crack closure can outweigh the acceleration due to the reduction of the closure wedge by the underloads. The sum of both processes results in a delayed retardation, as will be shown. For a test of type b we expect both shear lip and overload effects.

6.2. Experimental Methods

The material used in the tests was Al 2024 T351 . The chemical composition (%wt) was: Cu 4.75, Mg 1.18, Mn 0.67, Zn 0.19, Cr 0.004, Ti 0.03, Fe 0.14, Si 0.34, remainder Al. The mechanical properties recorded in the longitudinal direction of the plate were: yield stress 353 MPa, tensile strength 459 MPa, elongation to failure 21% and Young's Modulus 71.9 GPa. The overloads and underloads were applied mostly at the same frequency (10 Hz) as the low amplitude cycles, without stopping the fatigue machine at the load transitions. Some tests were performed at other frequencies. In these cases only the

frequencies of the underloads or overloads were changed. The low amplitude cycles before and after the underloads and overloads were in all cases kept at 10 Hz.

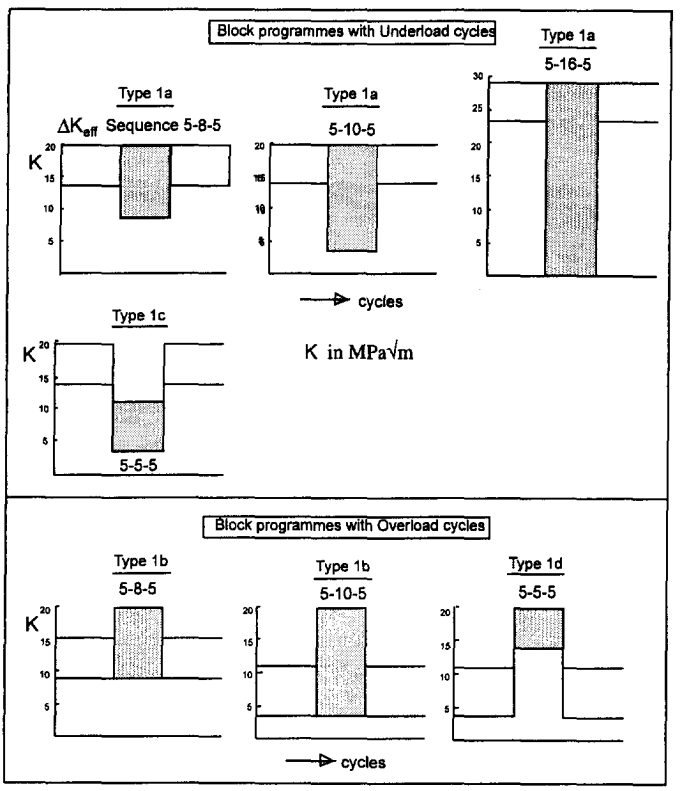

Figure 6.3. Test program of the underload and overload tests.

We did not stop the fatigue machine because an effect could be measured when the fatigue machine was stopped to apply the overload or underload blocks. There was no overshoot or undershoot of the load at the transition points. The cycle numbers for the start and end of the over(under)loads were recorded by the computer. The specimens were center cracked tension specimens, 100 mm wide, 6 mm thick and 300 mm long. The specimens were center notched to 2a = 10 mm using a spark discharge technique.

The tests were performed in lab air conditions at about 20°C. The overall test program for tests at 10 Hz is listed in table 6.1. Results for tests at other frequencies are shown in the appropriate figures. The principle of the measurements is presented in figure 6.4. It shows the result of a test with 12200 underload cycles at ΔK_{eff} = 16 MPa$\sqrt{m}$. Two delay variables, Δa and ΔN, are defined in this graph. Δa and ΔN represent the (delay) effect on crack length and

cycles after the underloading.

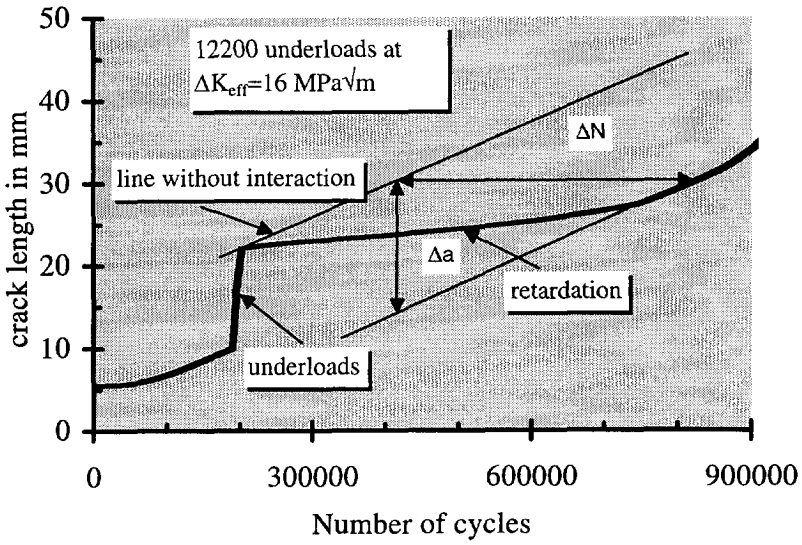

Figure 6.4. Definition of delay variables Δa and ΔN.

6.3. Calculation of Delay Parameters

The calculation procedure will be explained using the test result shown in figure 6.5. In this figure the parts AB and DE represent normal unaffected crack growth at the low ΔK cycles before and after the application of underloads respectively. BC is the crack increment during the underload cycles. CP is a part with delayed crack growth. The number of cycles that is needed for crack growth from C to P is denoted as ΔN_1 . The corresponding crack length increment as Δa_1. These parameters thus represent the number of cycles and the crack length increment that are influenced by the underloads. The problem is now to determine the tangency point P.

The following calculation steps are:

1. Find the equation of DE by a linear regression:

$$a = C_1 N + C_2 \qquad 6.2$$

2. Calculate the standard deviation σ of the linear regression line as:

$$\sigma^2 = \frac{1}{n} \sum_{j=j(D)}^{j(E)} \{a(j) - (C_1 N + C_2)\}^2 \qquad 6.3$$

where n is the total number of data points between D and E.

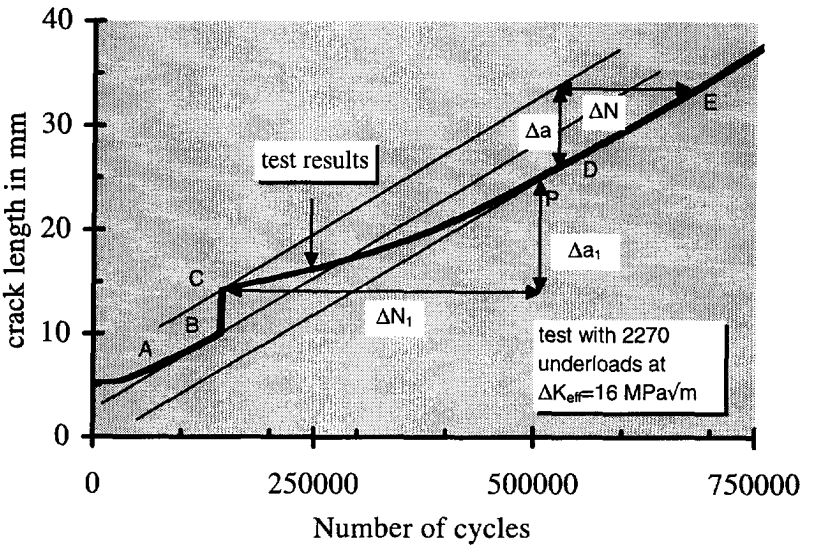

Figure 6.5 A test with 2270 underloads.

3. Find point P. This is achieved by extrapolating line ED until for all subsequent points:

$$\delta a > \sigma \qquad 6.4$$

then point P is found. δa is the difference between the a value of a measurement point and the corresponding a value given by equation 6.2.

4. Calculate ΔN_1 and Δa_1 from:

$$\Delta N_1 = N(P) - N(C) \qquad 6.5$$

$$\Delta a_1 = a(P) - a(C) \qquad 6.6$$

5. Calculate ΔN and Δa from:

$$\Delta N = \frac{a(C) - C_2}{C_1} - N(C) \qquad 6.7$$

$$\Delta a = C_1 \Delta N \qquad 6.8$$

6.4. Results

The calculated delay variables ΔN are shown in figure 6.6 for overload and underload cycles of the test ΔK_{eff} sequence 5/8/5 MPa$\sqrt{m}$. Because the crack length delay factor Δa is linearly proportional to ΔN, similar trends are indicated by Δa, see equation 6.8. The results found for ΔN_1 and Δa_1 show a

large amount of scatter and are not shown. The calculation procedure probably is too sensitive to scatter of the crack length measurements. The values of Δa_1 are listed in table 6.1.

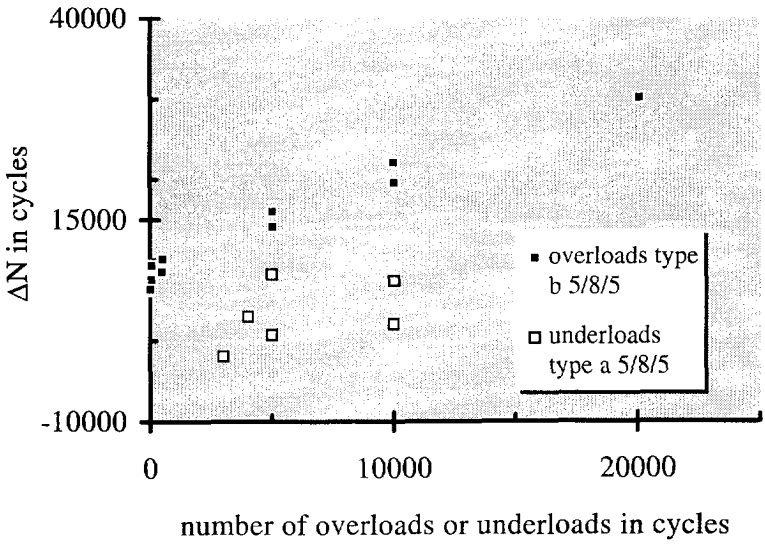

Figure 6.6. Results of number of delay cycles (ΔN) for ΔK_{eff} sequence 5/8/5.

In figure 6.7 ΔN results for the ΔK_{eff} sequences 5/10/5 MPa$\sqrt{m}$ have been plotted for underloading only, because a number of overloads > 100 results in crack arrest for overloads on one side of the specimen, leading to a strongly asymmetric crack growth.
The results cannot be used then any more. Underloading at ΔK_{eff} = 10 MPa$\sqrt{m}$ does not present such a problem for larger numbers of underloads.

For ΔK_{eff} sequence 5-16-5 MPa$\sqrt{m}$ no overload tests were performed. The results of the underloading at this ΔK_{eff} sequence are shown in figure 6.8. Underloading at ΔK_{eff} = 16 MPa$\sqrt{m}$ results in fast-growing shear lips. At higher numbers of underloads the crack surface reaches a situation of complete shear. However, there is a frequency effect as shown in the figure.
For a number of underload cycles (at 10 Hz) larger than about 3000 the crack growth temporarily stopped on one side after the underloading. Only after several mm of crack growth on the other side did the crack growth reinitiate again on the temporarily non-growing side.

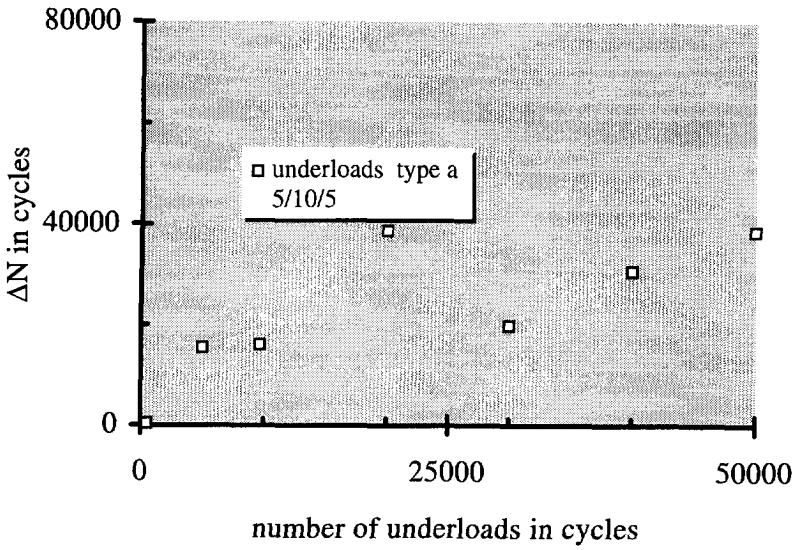

Figure 6.7. Results of number of delay cycles for ΔK_{eff} sequence 5/10/5.

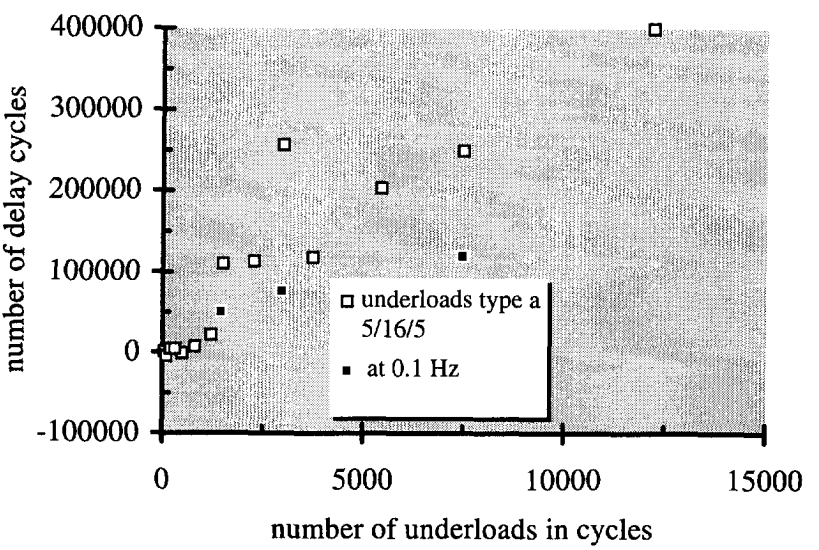

Figure 6.8. Results of number of delay cycles for ΔK_{eff} sequence 5/16/5.

The crack then had become strongly asymmetric. It follows that crack growth becomes asymmetric in the case of *overloading* after more than about 100 cycles at $\Delta K_{eff} = 10$ MPa$\sqrt{m}$, and in the case of *underloading* after more

than about 3000 cycles at ΔK_{eff} = 16 MPa$\sqrt{m}$ (at 10 Hz). It is interesting to note that crack arrest occurred most at a crack tip with a single shear lip. The growing side always showed double shear lips. This is in agreement with earlier findings [9].

The effect of the shear lip can be noticed during the underloading block and afterwards. The results in figures 6.9 and 6.10 show that there is a retardation effect after the application of 12200 underload cycles at ΔK_{eff} =16 MPa$\sqrt{m}$ at 10 Hz. Application of the same number of underloads at 0.1 Hz did not lead to any obvious retardation (figure 6.10). This can be understood from previous chapters.

As discussed in section 4.5, the shear lip width is frequency dependent. A lower frequency results in a lower shear lip width, and according to chapter 5 the lower shear lip width results in less decrease of da/dN. Besides that, the frequency also has an influence on the shear lip fracture appearance and thus on crack closure (see chapter 7). In figure 6.10 the effect of the underloads on da/dN is shown for both frequencies. For underloads at 10 Hz there is a strong decrease in da/dN during the underloads. This is not observed for underloads at 0.1 Hz. Figure 6.11 shows a magnified part of figure 6.10. It shows a delayed retardation that has occurred after the underloading at 10 Hz. For comparison figure 6.12 shows crack growth results before, during and after the application of 3000 underload cycles at ΔK_{eff} =16 MPa$\sqrt{m}$ at 10 Hz and 0.1 Hz. The same trend with respect to the frequency of the underloads can be observed in this figure. The test at 10 Hz shows much more retardation.

In figure 6.13 the effect of frequency is shown on the retardation after the 3000 underloads in more detail by da/dN results. Besides the frequency the retardation is also dependent on the number of underloads as was already shown in figure 6.8 for the underload sequence 5/16/5. The da/dN behavior after the underloads, for a different number of underloads, is shown in figure 6.14. Because da/dN decreases during underloading at 10 Hz it can be expected that the mean da/dN during the underloading period will be dependent on the number of underloads. The mean da/dN of the underloading period was calculated from the a-N results. In order to obtain accurate a values at the beginning and the end of this period, two least square regression lines over 50 data-points just before and just after the underload period were calculated. In the formula of these lines the cycle numbers at the start and the end of the underload period are substituted. This results in accurate values of crack length a at the start and finish of the underloads.

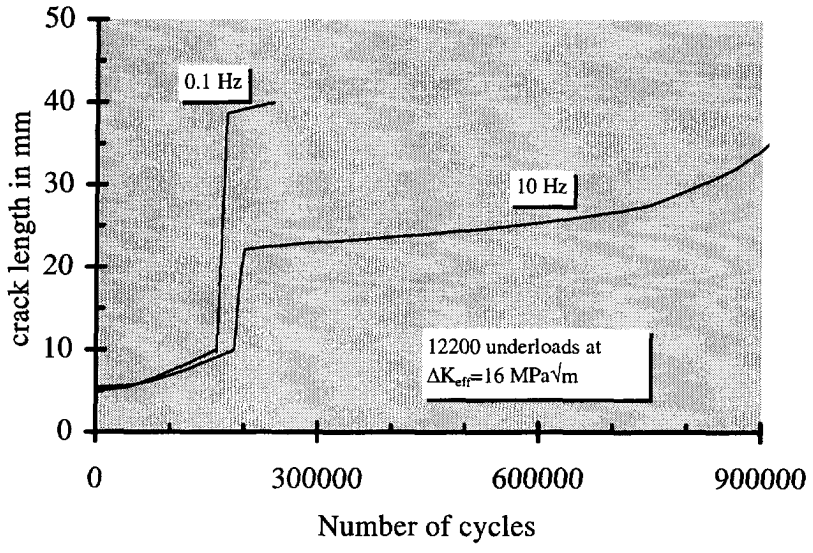

Figure 6.9. Fatigue crack growth during 12200 underloads at ΔK_{eff} = 16 MPa√m.

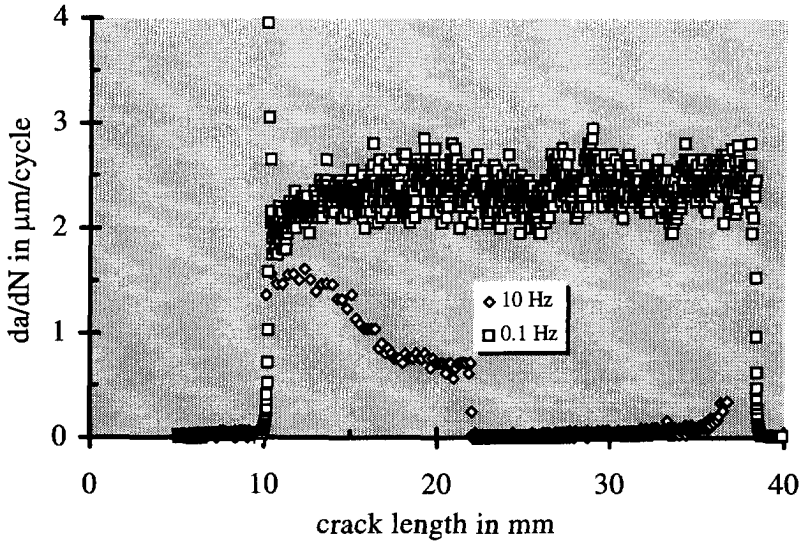

Figure 6.10. Fatigue crack growth rate during 12200 underloads at ΔK_{eff} = 16 MPa√m.

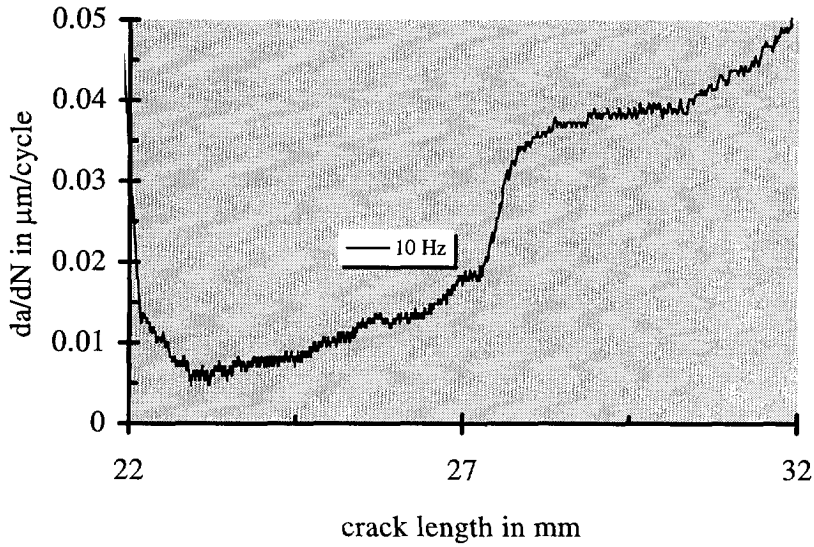

Figure 6.11. Delayed retardation after underloads.

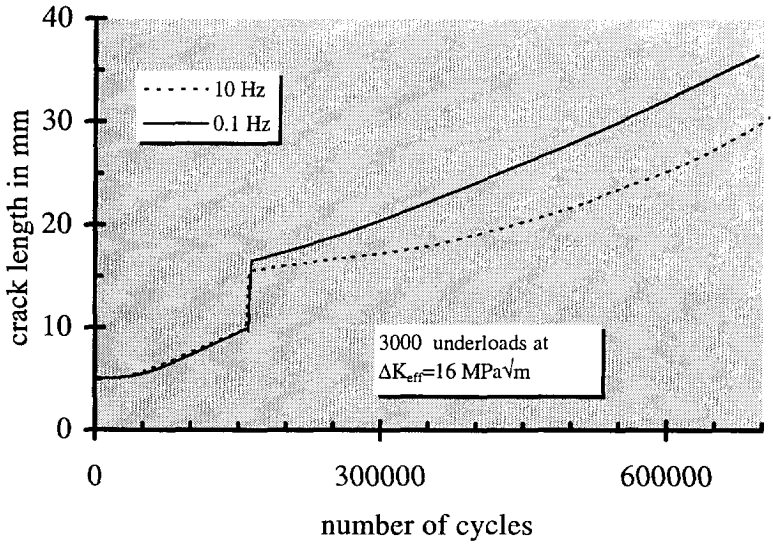

Figure 6.12. Fatigue crack growth before, during and after 3000 underloads at ΔK_{eff} = 16 MPa$\sqrt{m}$ and frequencies of 10 Hz and 0.1 Hz.

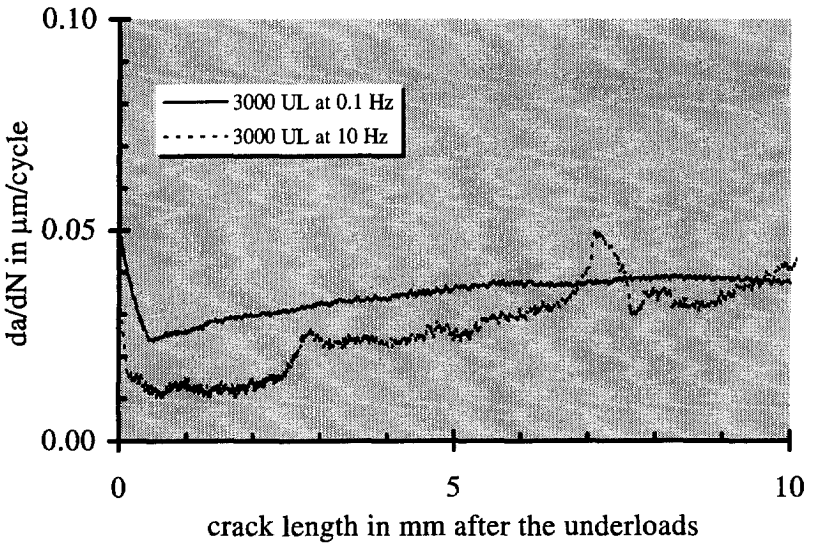

Figure 6.13. Frequency effect on retardation in da/dN after 3000 underloads.

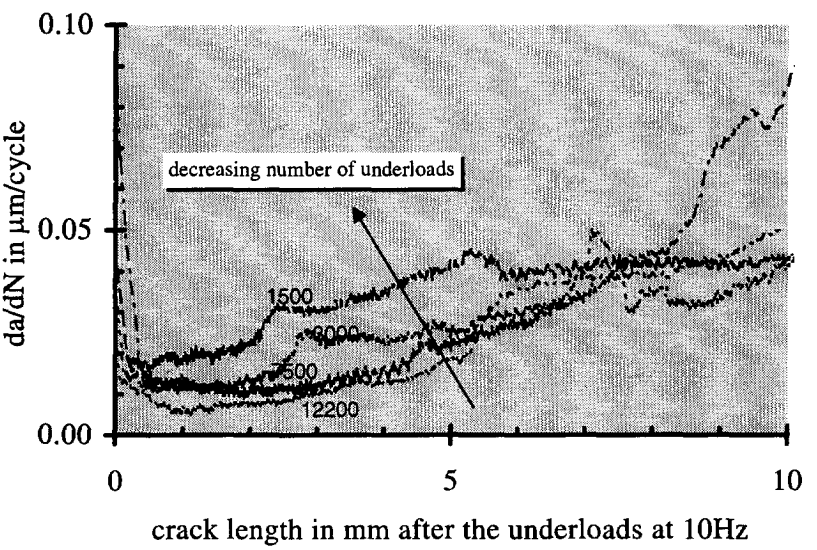

Figure 6.14. Retardation in da/dN as a function of the number of underloads.

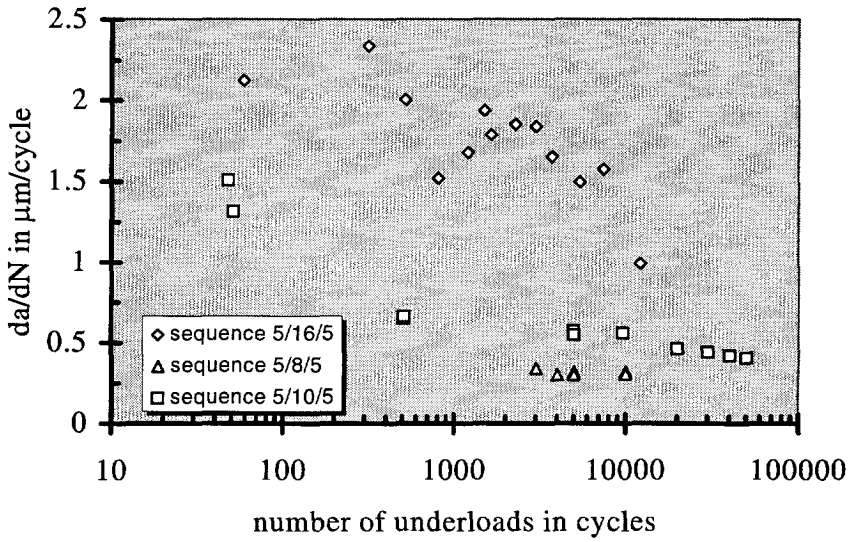

Figure 6.15. Mean crack growth rate during underloads.

The mean da/dN is found by dividing the difference between these two crack lengths and the number of underloads. This procedure was used in order to avoid scatter in individual a values as measured by the potential drop method. The number of 50 data points was chosen to give a reliable result.
In figure 6.15 the results of the mean da/dN values are shown as a function of the number of underloads. It is clear that the mean of da/dN during the underload block decreases more for larger ΔK_{eff} values and an increasing number of underloads. For underloadings at the lowest ΔK_{eff} (= 8 Mpa$\sqrt{m}$) the effect is very small.

6.5. The effect of type of overload and frequency on crack growth retardation

In this section the difference between type b and type d overloads will be discussed, based on tests with ΔK_{eff} sequences 5/10/5 and 5/5/5 of type b and type d respectively. The number of overloads was limited to a maximum of 100, because higher numbers of overloads led to asymmetric growth for the 5/10/5 sequence. The effect of the frequency of the overloads was also measured. In both sequences we have the same value of K_{max} for the cycles before, during and after the overloads. The only difference is the value of K_{min} during the overloads. Type b overloads were chosen to lead to shear lips, whereas for type d

this was not expected. However, no shear lips were detected for either case because of the low number of overload cycles.

The test results are presented in figures 6.16 and 6.17 (these tests are not presented in table 6.1). It is clear that type b overloads lead to much more retardation after the overloads than type d. Moreover, the retardation for type b is more strongly dependent on the number of overloads than for type d. Type d does not show a clear frequency dependence, while for type b a tendency is observed for more retardation at a lower frequency of the overloads. Probably for both types the number of overloads is too small to find a real effect of the frequency.
If both figures (6.16 and 6.17) are compared in more detail, it turns out that the number of delay cycles are about equal for low numbers of overloads. Linear extrapolation to one overload cycle leads for both to about 40000 delay cycles. However, for about 50 overloads the difference is already a factor of 3, about 120000 cycles for type b and 40000 for type d. The number of type d overloads has no effect on the number of delay cycles for overload numbers under about 75. An explanation of the effects will be given in section 6.8.

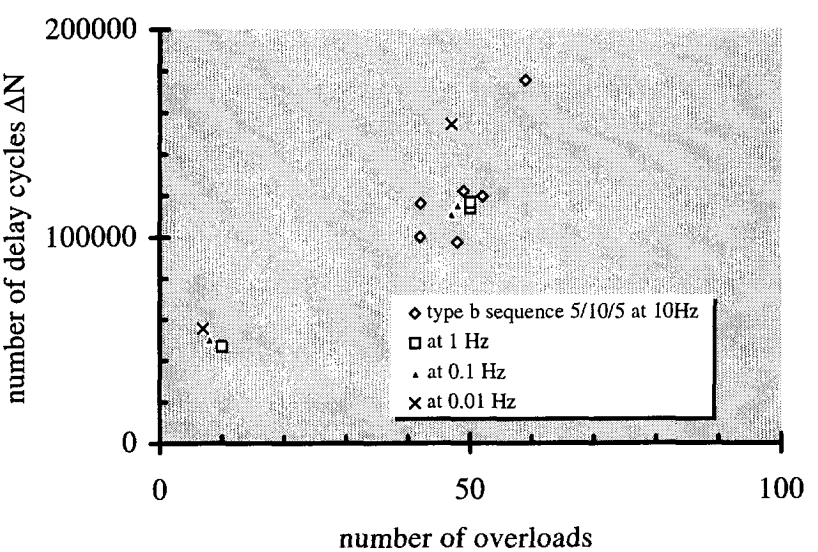

Figure 6.16. Test results from type b overloads.

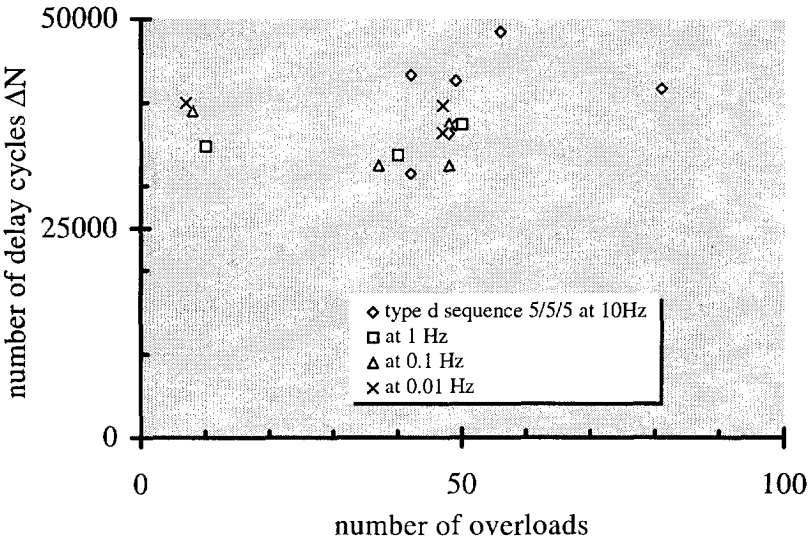

Figure 6.17. Test results from type d overloads.

6.6. Explanation of Crack Growth Retardation after Underloads

It is generally accepted that crack growth retardation after an overload can be explained by the higher crack closure wedge due to the larger plastic zone size formed during the overload cycle. More overload cycles result in a longer crack closure wedge and thus more crack growth retardation. The reason why a large number of underloads can also give retardation is not directly clear. K_{max} , and thus the forward plastic zone size, is the same before, during and after the underloads. Therefore plasticity induced crack closure cannot be held responsible for the retardation. It is suggested here that the shear lips that are formed during the underloads are causing retardation.

As discussed before the effect of shear lips on da/dN can be considered to result from the effect of the slant crack surface on K and/or crack closure and/or crack growth resistance (see chapter 5).

Crack closure in the presence of shear lips is considered to be the sum of plasticity-induced closure and a term due to irregularity and mismatch resulting from the shear lips. Only the latter term is of relevance in the underload situation at constant K_{max} , since in principle the plastic zone size does not change.

In chapter 5 shear lips were assumed to have an effect on the ΔK_{eff} .Using the assumption:

$$\Delta K_{eff} \cdot \ell = \text{constant} \qquad 6.9$$

with ℓ the length of a transverse section of the crack front as found on specimens with shear lips, the da/dN in constant ΔK tests could be very well predicted. Equation 6.9 was sufficient to describe the effect on da/dN. As we will see this mechanism cannot directly explain the results found in underload tests.

We will discuss the results of a test with 40009 type a underloads at ΔK_{eff} = 10 MPa$\sqrt{m}$. At this ΔK_{eff} level of underloading the crack growth remains symmetrical.

The shear lip vanishes very rapidly after the underload period (within 2 mm). The crack length affected, Δa_1, is found to be 5.45 mm, which is much larger. Thus the effect of the shear lip extends beyond its physical presence. This rules out the possibility that the effect on K alone is the major contributing cause. It also rules out the applicability of equation 6.9, because then the crack length affected would be 2 mm at the utmost.

The large crack closure wedge due to mismatch, surface roughness and irregularity of the shear lips, formed during the underloads block, apparently results in an affected crack length of 5.45 mm after the underloads. It may be, however, that in the crack length area, just after the underloads, where the shear lip width decreases (they vanish within 2 mm) there is, besides a closure effect, also a K-effect.

In order to separate the two mechanisms (effect of shear lips on K or effect on crack closure) we also performed underload tests at 0.1 Hz. Here too before and after the underloads (at 0.1 Hz) the same ΔK_{eff} = 5 MPa$\sqrt{m}$ was applied at 10 Hz. At 0.1 Hz shear lips also developed, but they were smoother and more symmetrical than at 10 Hz. An example of da/dN during 12200 underloads at 10 Hz and 0.1 Hz was already shown in figure 6.10. It is clear that the growing shear lips are accompanied by a decreasing da/dN for underloads at 10 Hz, whereas this is not the case for 0.1 Hz. The smooth shear lips occurring at 0.1 Hz did not lead to a decrease in da/dN. After the underloads at 0.1 Hz very little retardation was measured. The conclusion is that only rough and irregular shear lips are responsible for crack growth retardation and that the major retarding mechanism is crack closure due to surface roughness and mismatch of the shear lips.

The fact that a larger number of underloads result in more retardation can be explained by a longer crack closure wedge.

6.7. A simple model to calculate the crack growth rate during and after underloads

The model is qualitative and has no pretension to predict exactly the crack growth rate. Only trends will be shown. The basis of the model is equation 6.9. Further use is made of some results found in chapter 5, equations 5.8 - 5.11. Because use is made of $\Delta K_{eff} \cdot \ell$ = constant, it may be clear that unless a special interpretation is chosen, an affected crack length after the underloads which is larger than the zone of decreasing shear lip width cannot be the result. Because in almost all tests the affected crack length is 2 to 3 times larger than the zone of the decreasing shear lip width we have to adopt a special interpretation of the length ℓ in equation 6.9. The length ℓ is dependent on the shear lip width. For constant amplitude and constant ΔK loading, in which cases the shear lip width always increases or is approximately constant, ℓ is dependent on the momentary shear lip width at the tip.

For the areas of decreasing shear lip widths we follow another approach. As was shown in the previous section, the shear lip effect is largely a crack closure effect, owing to irregular shear lips. The larger the shear lip width, the larger the closure effect will be. This means that for increasing shear lip widths the major crack closure causing shear lip width is the shear lip width at the very crack tip. This will not be the case for decreasing shear lip widths. Here a competition between shear lip width and the higher crack opening further from the tip will exist. The closure behavior of a decreasing shear lip width is therefore more dependent on the crack growth history than the closure behavior of an increasing shear lip width. In fact the whole crack growth history, starting from the initial saw cut, should be incorporated. This is worked out in reference [10] and more in detail in a forthcoming paper. Here we only deal with the shear lip behavior. This consideration is implemented in the model as follows. For increasing shear lip widths or shear lip widths that are more or less constant with crack growth we assume that ℓ is found from the shear lip width at the crack tip. For decreasing shear lip widths we assume that ℓ is found from the mean of the shear lip widths over an area of several mm crack length behind the tip. The length of this crack length area is a parameter that has to be found by comparing with actual results and to match calculations with the experimental results. In figure 6.18 the result of a calculation with 1000, 2000 and 3000 underloads (type a) at ΔK_{eff} = 16 MPa$\sqrt{m}$ is shown. In this calculation example a shear lip crack

closure crack length of 3 mm was adopted, i.e. the mean of the shear lip width was taken over 3 mm behind the tip. The ℓ value found from this shear lip width was substituted in equation 6.9 to calculate da/dN and then a versus N. The qualitative trends are predicted quite well in the example. More underloads lead to more retardation afterwards.

In figure 6.19 both the measurements and the prediction of a test with 5000 underloads with ΔK_{eff} = 16 MPa$\sqrt{m}$ at 10 Hz are shown. Two prediction curves are shown, one with the special treatment of ℓ for decreasing shear lips and one without this treatment.

In the calculations use is made of an experimentally obtained Paris curve for this material, based on only a few constant ΔK_{eff} values and the appropriate da/dN: $da/dN = 0.000082\ (\Delta K_{eff})^{3.9}$,where ΔK_{eff} is measured in MPa$\sqrt{m}$ and da/dN in µm/cycle. The curve is estimated for the tensile mode, i.e. use is made of extrapolated da/dN values as was already done in chapters 4 and 5. The Paris exponent is rather large, i.e. larger than found in chapter 5. It should be noted that the ΔK_{eff} of 16 MPa$\sqrt{m}$ is also much larger than the values used in chapter 5. It may be that already some plasticity effects influence the Paris curve .

The calculation starts at an initial crack length a = 8 mm crack length and an initial number of 120000 cycles, estimated from the actual results.

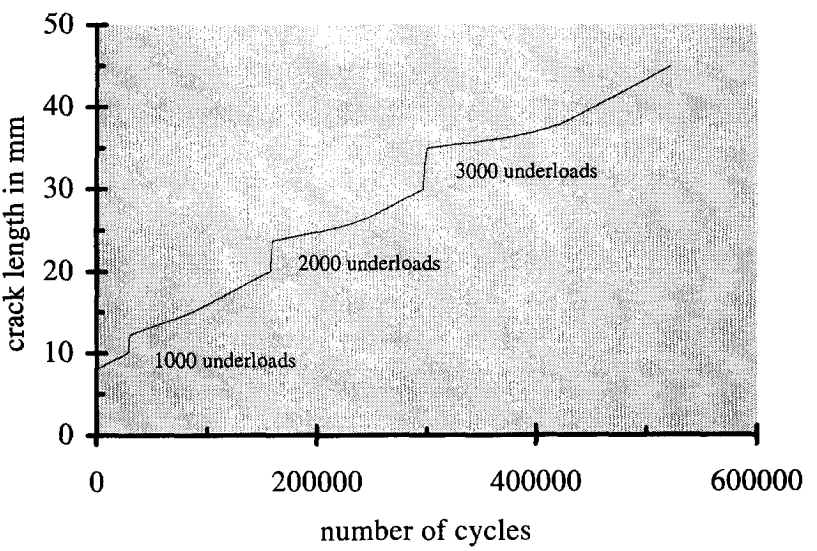

Figure 6.18. Calculation of a versus N using a simple model.

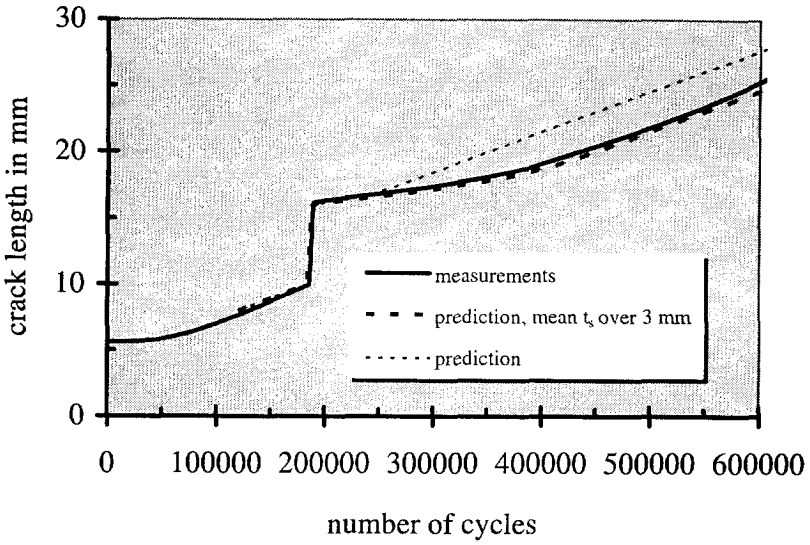

Figure 6.19. Measurement and prediction of the a-N curve with 5000 underloads, underload sequence 5/16/5 at 10 Hz.

6.8. Discussion

As pointed out previously the effect of a shear lip by its closure effect extends over a larger distance than the distance where the shear lip is present. This is specially true for tests at 10 Hz where the shear lips were rough and irregular. At 0.1 Hz the shear lip effect was much less. The shear lips were smooth at this frequency. It seems that only rough shear lips have a noteworthy effect on crack closure, which then leads to an affected crack length significantly larger than the lengths where the shear lips are present. The length of the affected zone (Δa_1 in Table 6.1) is often 2 to 3 times larger than the zone of the decreasing shear lip width. It is also much larger than the monotonic plastic zone size of the underloads.

For the underloads at $\Delta K_{eff} = 8$, 10 and 16 MPa$\sqrt{m}$, the plastic zone size is 1.0, 1.0 and 2.2 mm respectively. Irwin's formula for the plastic zone size was used:

$$2r_p = \frac{1}{\pi}\frac{K_{max}^2}{\sigma_{ys}^2} \qquad 6.10$$

Thus the plastic zone size cannot directly be the cause of the highly affected

In order to separate the combined effect of shear lips and overloads in tests of type b, we also performed some tests with tensile overloads, tests of type d. A remarkable result was obtained in two comparable tests of types b and d. Four overload blocks at $\Delta K_{eff} = 10$ MPa$\sqrt{m}$ (type b) and at $\Delta K_{eff} = 5$ MPa$\sqrt{m}$ (type d) with the same overload ratio $K_{max,high}/K_{max,low} = 1.8$ were applied at crack lengths of 10, 15, 20 and 30 mm respectively. The number of overloads in each block was the same and so low that no shear lips could be detected in the case of test b (with the naked eye). The number of cycles needed for crack growth between 8 and 35 mm crack length was 866231 cycles for test b, and 592523 cycles for test d, i.e. a longer crack growth life for type b.
Because shear lips were absent in both cases, the reverse was expected, i.e. a shorter life (in cycles) for b than d due to the faster growth in b during the overloads. The retardation after the blocks of overloads should have been about the same (or less for the test of type b because the crack closure wedge is more compressed), as the same overload ratio was used. An explanation of this phenomenon, based on plasticity induced crack closure, can be given. The mean crack growth rate of the overloads at $\Delta K_{eff} = 10$ MPa$\sqrt{m}$ is about 10 times higher than the mean crack growth rate of the overloads at $\Delta K_{eff} = 5$ MPa$\sqrt{m}$, This results in a 10 times longer crack closure wedge in the first case. The longer crack closure wedge is probably responsible for the longer life in the test of the type b.
The longer crack closure wedge also explains the different retardation behavior in tests of type b and d with different frequencies as found in section 6.5.

Tests of the type c showed no crack growth during the underload cycles, as was expected. Large numbers of underloads, up to 20000, showed no crack growth for a stress intensity ratio $K_{max,low}/K_{max,high} = 0.55$. Also no delayed crack growth retardation could be measured after the underloads. The crack growth rate before and after the underloads was the same. Thus crack closure models which predict no crack growth after a load transition, where K_{max} is lower than K_{op}, calculated with equation 6.1, indicate the observations quite well.

An interesting phenomenon is the effect of the irregularity in the forming of shear lips in tests with underloads at higher frequencies, viz. 10 Hz. This is in contrast to tests at lower frequencies. At 0.1 Hz the shear lip development was very regular. Very smooth shear lips were formed. The width of the shear

lips was also more symmetrical with respect to the front and rear side of the specimen than for tests at 10 Hz. It was surprising that at 0.1 Hz hardly any reduction in da/dN could be measured, even for high numbers of underloads at $\Delta K_{eff} = 16$ MPa$\sqrt{m}$. There was still a delayed retardation effect after the underloads, but the retardation was much smaller than for tests at 10 Hz. It was also found that asymmetric growth did not occur or hardly occurred after underloads at this frequency. Probably the irregularity of the shear lips is the major crack growth delaying cause. A smooth shear lip has a much smaller effect.

6.9. Conclusions

With respect to retardation in fatigue crack growth in Al 2024 after blocks of overloads and underloads we conclude:

1. The application of overloads always cause delayed retardation on subsequent crack growth. Larger numbers result in more retardation.
2. The application of large numbers of underloads always cause delayed retardation on subsequent crack growth when the applied ΔK of the underloads is so high that shear lips are found on the fracture surface. Larger numbers and a high frequency enhance the retardation.
3. The application of one or a small number of underloads has no effect on subsequent crack growth.
4. The crack length affected by the underloads extends far beyond the physical presence of shear lips, indicating that shear lips not only have an effect on K but certainly also on K_{op}. The affected crack length is significantly larger than the monotonic plastic zone size.
5. Tests with underloads at a lower frequency indicate that the reduction in crack growth rate during application of the underloads and the delayed retardation are largely caused by irregularities of the shear lips. A smooth regular shear lip is found at 0.1 Hz, which has only a slight effect, indicating that crack closure caused by an irregular shear lip is the most important delaying mechanism.

6.10. References

1. W.J. Mills and R.W. Hertzberg (1975) The effect of sheet thickness on fatigue crack retardation in 2024-T3 Aluminium alloy. Engng Fracture Mech. 7, 705-711.
2. R.W. Hertzberg (1989) Deformation and fracture mechanics of engineering materials. Third Edition. John Wiley & Sons, Inc., New York, USA
3. J. Schijve (1974) Fatigue damage accumulation and incompatible crack front orientation. Engng Fracture Mech. 6, 245-252.
4. J. Zuidema and H.S. Blaauw (1988) Slant fatigue crack growth in Al-2024 sheet material. Engng Fracture Mech. 29, 401-413.
5. R.A. Dainto and B.M. Hillberry (1984) Effect of thickness on fatigue crack propagation in 7475-T371 Aluminium alloy sheet. NASA contractor report 172367. Purdue University, W. Lafayette, USA.
6. J. Zuidema and M. Mannesse (1989) A model for predicting slant fatigue crack growth in Al-2024. Engng Fracture Mech. 34 , 445-456.
7. R.A.H. Edwards, E.M. de Jong and J. Zuidema (1984) The fracture mode transition and its effect on crack growth retardation. Proc. Fatigue 84. University of Birmingham, UK, 463-478.
8. J. Schijve (1981) Some formulas for the crack opening stress level. Engng Fracture Mech. 14, 461-465.
9. J. Zuidema, P.J.M. Mense and R.A.H. Edwards (1987) Environmental dependence of fatigue crack growth retardation following a single overload in 2024-Al alloy. Engng Fracture Mech. 26, 349-356.
10. J. Zuidema, A calculation of the effective ΔK under various fatigue loading conditions, in Proceedings of E.C.F-9. conference pp 391 - 396 ,Varna, Bulgaria, 1992.

Table 6.1. Listing of tests performed at 10 Hz.

a. Underload tests (type a)								
baseline			underload				number of	delay crack
K_{max}	K_{min} MPa√m	ΔK_{eff}	K_{max}	K_{min} MPa√m	ΔK_{eff}	Start mm	underloads cycles	length, Δa_1 mm
19.85	13.89	5	19.85	8.71	8	10	10010	0.69
19.85	13.89	5	19.85	8.71	8	20	10020	3.08
19.85	13.89	5	19.85	8.71	8	10	5010	0.66
19.85	13.89	5	19.85	8.71	8	20	5010	4.08
19.85	13.89	5	19.85	8.71	8	10	3010	2.84
19.85	13.89	5	19.85	8.71	8	20	4010	3.91
19.85	13.89	5	19.85	3.52	10	10	51	
19.85	13.89	5	19.85	3.52	10	15	507	0.42
19.85	13.89	5	19.85	3.52	10	25	4991	3.27
19.85	13.89	5	19.85	3.52	10	10	48	0.18
19.85	13.89	5	19.85	3.52	10	15	510	3.97
19.85	13.89	5	19.85	3.52	10	25	4999	2.59
19.85	13.89	5	19.85	3.52	10	10	9649	1.79
19.85	13.89	5	19.85	3.52	10	20	20023	4.32
19.85	13.89	5	19.85	3.52	10	10	40009	5.45
19.85	13.89	5	19.85	3.52	10	10	30013	5.42
19.85	13.89	5	19.85	3.52	10	10	50000	5.16
29.09	23.51	5	29.09	0	16	10	12200	5.22
29.09	23.51	5	29.09	0	16	10	3730	4.20
29.09	23.51	5	29.09	0	16	10	2270	7.25
29.09	23.51	5	29.09	0	16	10	5430	4.75
29.09	23.51	5	29.09	0	16	10	500	0.46
29.09	23.51	5	29.09	0	16	10	59	13.85
29.09	23.51	5	29.09	0	16	10	100	3.95
29.09	23.51	5	29.09	0	16	20	200	2.67
29.09	23.51	5	29.09	0	16	30	315	2.18
29.09	23.51	5	29.09	0	16	10	811	1.22
29.09	23.51	5	29.09	0	16	20	1205	2.45
29.09	23.51	5	29.09	0	16	30	1603	3.13
29.09	23.51	5	29.09	0	16	10	1496	11.73
29.09	23.51	5	29.09	0	16	10	7486	5.25
29.09	23.51	5	29.09	0	16	10	2998	9.04

b. Underload tests (type c)								
19.85	13.89	5	11.01	3.52	5	10	5015	4.49
19.85	13.89	5	11.01	3.52	5	20	10006	4.01
19.85	13.89	5	11.01	3.52	5	30	20002	3.04
c. Overload tests (type b)								
15.13	8.71	5	19.85	8.71	8	10	10013	1.82
15.13	8.71	5	19.85	8.71	8	20	20065	3.30
15.13	8.71	5	19.85	8.71	8	10	60	0.67
15.13	8.71	5	19.85	8.71	8	20	503	0.33
15.13	8.71	5	19.85	8.71	8	10	530	0.83
15.13	8.71	5	19.85	8.71	8	20	5010	2.07
15.13	8.71	5	19.85	8.71	8	10	5020	1.01
15.13	8.71	5	19.85	8.71	8	20	10010	2.97
15.13	8.71	5	19.85	8.71	8	10	60	0.44
15.13	8.71	5	19.85	8.71	8	20	60	0.95
11.01	3.52	5	19.85	3.52	10	10	49	0.93
11.01	3.52	5	19.85	3.52	10	15	52	1.08
11.01	3.52	5	19.85	3.52	10	20	50	2.46
11.01	3.52	5	19.85	3.52	10	30	48	1.79
11.01	3.52	5	19.85	3.52	10	10	42	1.18
11.01	3.52	5	19.85	3.52	10	20	107	2.65
11.01	3.52	5	19.85	3.52	10	30	156	0.82
d. Overload tests (type d)								
11.01	3.52	5	19.85	13.89	5	10	56	1.86
11.01	3.52	5	19.85	13.89	5	15	49	1.64
11.01	3.52	5	19.85	13.89	5	20	49	1.31
11.01	3.52	5	19.85	13.89	5	30	48	2.00
11.01	3.52	5	19.85	13.89	5	10	42	0.74
11.01	3.52	5	19.85	13.89	5	20	81	2.02
11.01	3.52	5	19.85	13.89	5	30	107	1.57

7. Crack Closure Relations of Al 2024 with and without Shear Lips

7.1 Introduction

The objective of this chapter is to investigate the closure behavior of crack flanks with and without shear lips. This is done by performing constant amplitude and constant ΔK fatigue crack growth tests in air and vacuum. The closure behavior of rough and regular shear lips is investigated by doing tests at different frequencies. Moreover a new technique for crack closure measurements is introduced.

In references [1-4] it is found that there is more crack closure in vacuum than in air and that crack closure can depend on the crack length. Elber [5] observed crack closure under cyclic tension loading on Al 2024 T3 specimens. He introduced the effective stress intensity interval ΔK_{eff}. The crack growth rate da/dN is assumed to be a function of this $\Delta K_{eff} = U\,\Delta K$ only. Elber found empirically:

$$\Delta K_{eff} = (0.5+0.4R)\Delta K \qquad -0.1 \le R \le 0.7 \qquad 7.1$$

ΔK_{eff} is also defined as:

$$\Delta K_{eff} = K_{max} - K_{op} \qquad 7.2$$

K_{max} is the maximum value of K. K_{op} is the value of K where the crack is just fully open. K_{op} is a measure for the crack opening behavior. An equivalent parameter is K_{cl}, the value of K where the crack starts closing. Several methods to measure crack closure are discussed by Schijve [6]. In this chapter we use the potential drop method for closure measurements. Similarly to all other methods, this method has its specific difficulties. Significant aspects are oxide layers on fracture surfaces, asperities causing electrical short-circuiting and the effect of plasticity on the electrical resistance. The important question is whether an "electrically closed" crack is also "mechanically closed". Because it is difficult to answer this question, another approach is used. Instead of the situation of a

closed crack, an open crack is considered. It is assumed that when there is no electrical contact there will also be no mechanical contact, thus an "electrically open" crack is always "mechanically open" too. This is not necessarily true for an "electrically closed" crack, i.e. an "electrically closed" crack is not always "mechanically closed".
It turned out to be impossible to measure crack closure contact continuously in lab air during constant amplitude or constant ΔK tests with the potential drop technique, probably due to corrosion (oxidation) of the crack flanks. Oxide layers are a very good electrical insulator and that violates our basic assumption about the equivalence of "electrically open" and "mechanically open" cracks. However, with a special technique the closure measurements were possible in lab air, after loading transitions (at the same K_{max} and lower $R = K_{min}/K_{max}$). The closure level can then be measured during a short number of the underload cycles. The results are compared with results from tests performed in vacuum.

7.2 A New Crack Closure Measurement Technique

The closure measurements are performed on center cracked tension specimens (width 100 mm, thickness 5 or 6 mm) of 2024-T3 in lab air and in vacuum with the pulsed direct current potential drop apparatus (Howden), that is normally used for crack length measurement. In the latter case the crack length is found by triggering the apparatus to measure the crack length at the maximum value of the force signal.
The apparatus can also be used to measure the crack length at the minimum value of the force signal. The difference between the two crack lengths is an indication for the amount of closure, but it does not allow to find K_{op} or K_{cl} . To find these K-values we use an external trigger signal to get a large number of crack length measurement points in a full fatigue load cycle. The points where the crack starts closing (K_{cl}) and where the crack is just fully open (K_{op}) can then be obtained. In figure 7.1 results of about 30 cycles are shown for a test performed in air. During every single cycle 400 measurements of the crack length were made. A loading transition with the same K_{max} and an R transition from 0.7 to 0.1 is shown. As soon as the potential drop signal decreases there must be some electrical contact of the crack surfaces and thus crack closure has started.
The frequency of the fatigue machine is lowered from 10 Hz to 0.05 Hz just before and in the closure measurement period to get more data points per cycle, i.e. 400 measurements in 20 seconds. The crack length *contact* area for the first cycle just after the transition was about 3 mm, according to the calibration curve

of the potential drop signal versus crack length.

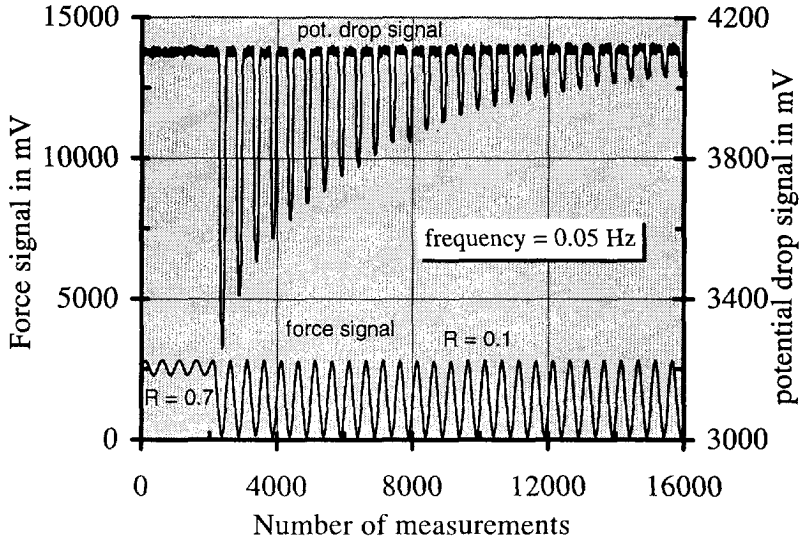

Figure 7.1. Potential drop (crack length) and Force signals. Test in air with load transition. K_{max} = 29.09 MPa√m.

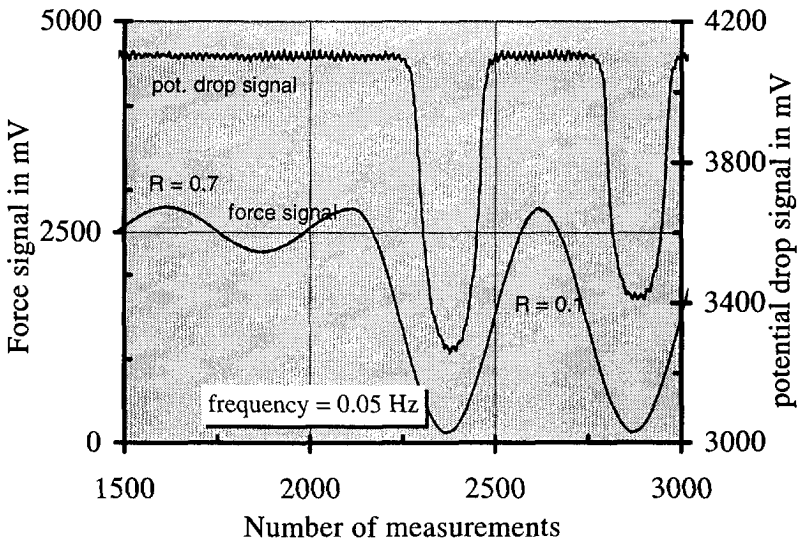

Figure 7.2. Detail of figure 7.1.

Note that the value of 3 mm crack length contact area is the same as was needed, in section 6.7, for the shear lip crack closure crack length to fit the calculation results with the experimental results.

In air the amplitude of the potential drop signal reduces quickly owing to crack closure enhanced oxidation. This is illustrated in figure 7.1 by the fast increasing minimum value of the potential drop signal with the number of cycles. In figure 7.2 a detail of Figure 7.1 is shown.

With this underload measurement technique it is possible to measure the closure level (K_{cl}) in air under some restrictions. During the underloads the value of K_{max} or S_{max} (c.a. tests) has to be the same as before the underloads in order to have the same closure build up during crack growth. Also the fracture mode can be of influence as will be shown later.

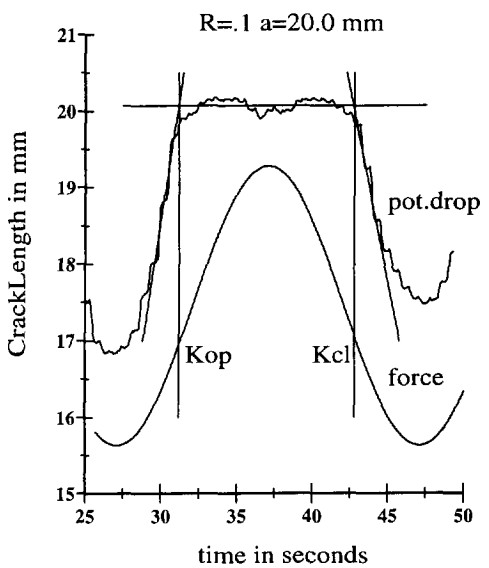

Figure 7.3. Tangency construction for measuring K_{op} and K_{cl}. R=0.1.

The underloads are obtained by lowering the R-value. For closure measurements as a function of the crack length this procedure can be applied every 5 mm for example. It implies that K_{cl} during a fatigue test is periodically obtained by inserting a small block of underload cycles with the same K_{max} . Note that we measure the closure of the underloads. The results are found by taking the mean values of the underload cycles (normally about 5 to a maximum number of 10).

The number of underloads is much too small for the development of shear lips. The measurement technique is thus only capable of finding closure values for a crack in the tensile mode. There is in practice no systematic change in closure results during the small number of underloads. It seems that crack closure adjusts itself immediately in the tensile mode. It is possible to find both K_{cl} and K_{op} by this procedure. The principle of the measurement technique is shown in figure 7.3 for one underload cycle of a test in air. In this figure the potential drop signal is converted to open (apparent) crack length in mm. There is a small phase difference between the crack length signal and the force signal, see figure 7.2. It is assumed that the minima of the load signal and the potential drop signal have to be synchronized. The correction is achieved by setting the minimum values of both signals at the same time. Figures 7.3 and 7.4 are corrected for this phase difference. K_{cl} and K_{op} are then obtained by adopting the three tangent lines presented in figure 7.3.

The tangency construction is somewhat ambiguous. The horizontal line represents the time that the crack is fully open. The horizontal line can be found by taking the mean of the points on the plateau. It will be clear from figure 7.1 that this time is not much influenced by oxidation, contrary to the minimum crack length measured. A small change of the plateau width is probably due to a change of the closure level after the load transition. This change in closure level is probably due to enhanced oxidation by fretting.

In figure 7.5 the signals are presented in a more conventional way by plotting the open crack length as a function of the load by eliminating the time. The closure level can then be found as the load where the graph becomes horizontal (i.e. no change of opened crack length). This latter method is not used in this chapter. The method described in figure 7.3 is preferred because more information is found about K_{op} and K_{cl} separately. In figure 7.5 a large number of cycles is chosen to show qualitatively that the closure level remains the same for all these cycles.

In figure 7.4 the result for a test in vacuum is shown . In vacuum the measured minimum crack length remains the same. We do not need underloads then for the closure measurement.
The measurement technique in vacuum can be the same as in air (figure 7.3), although the method of figure 7.5 (same test result as given in figure 7.4) can also be used.

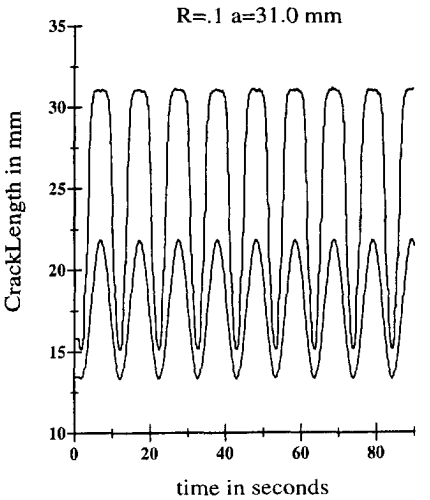

figure 7.4. Apparent Crack Length and Force Signals. Test in Vacuum.

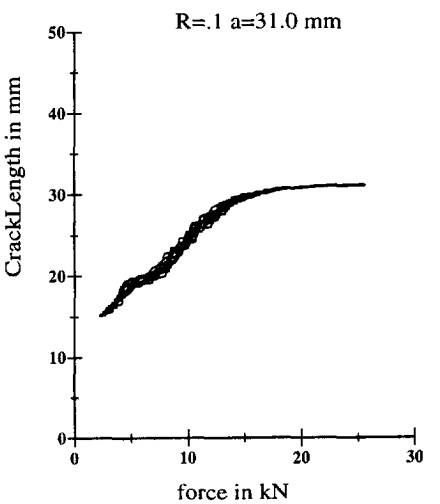

figure 7.5. Apparent Crack Length against Force. Test in Vacuum.

7.3 Crack Closure Relations

In section 4.3.5 it was shown that a closure function U = a +bR (+cR^2) had the

same correlating abilities for $t_{s,eq}$ and da/dN, as long as the ratio of the coefficients in the U relation is the same. Therefore an infinite number of U functions exist with the same correlating potential. It is necessary to have (at least) one absolute measurement of ΔK_{eff} to find a realistic U relation. With the new closure measurement technique we can achieve an absolute value of ΔK_{eff} in two ways. The first was already discussed and the principle was shown in figure 7.3. In the second method R is varied (increased) until no "electrical" crack closure can be measured. The lowest R that shows no electrical contact of crack flanks is assumed to be the R value for which $\Delta K_{eff} = \Delta K$ or $U = 1$. In this way the general U relation can be scaled up to a realistic U relation. Both closure measurement methods are used below in the evaluation of test results obtained in vacuum. Later we will discuss some results from tests in air.

In figure 7.6 da/dN results as a function of ΔK are presented for 3 constant amplitude tests at R-values of 0.7 , 0.3 and 0.1 respectively. The tests were performed in vacuum (about 10^{-6} Torr = 133 10^{-6} N/m^2). The frequency was 10 Hz. The same results are plotted in figure 7.7 against ΔK_{eff} calculated with the quadratic crack closure relation found by Schijve in air (2). This relation is:

$$U = 0.55 + 0.33R + 0.12R^2 \qquad -1 < R < 1 \qquad 7.3$$

The correlation of the da/dN data by the crack closure function $\Delta K_{eff} = U\Delta K$ is reasonable. This means, as discussed above, that at least the ratio of the three coefficients in equation 7.3 with respect to each other are correct. The absolute value of the coefficients however can be different from the values found by Schijve in air, i.e. multiplying all coefficients in equation 7.3 by a factor q gives the same correlation. Of course it will be possible to find other U relations that correlate the data somewhat better. We will not use such "exotic" relations, because relation 7.3 is good enough and has a general acceptance in the literature.

The coefficients in equation 7.3 are normalized. Their sum equals 1. It implies that it was assumed that $\Delta K_{eff} = \Delta K$ for $R = 1$.
It is amazing that relation 7.3 found for tests in air can also correlate tests in vacuum so well. However, we cannot assume a priori that equation 7.3 is also absolutely valid for crack growth tests in vacuum.

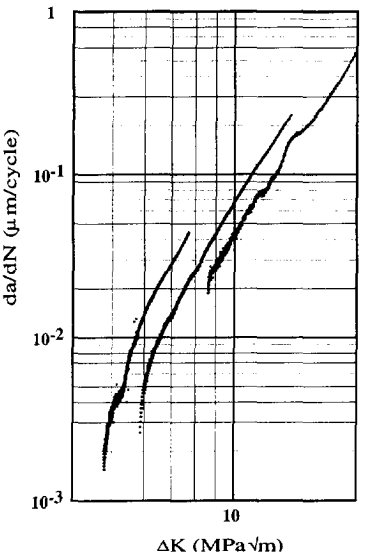

Figure 7.6. da/dN versus ΔK for R=0.7, 0.3 and 0.1 from left to right respectively. Tests in Vacuum at 10 Hz.

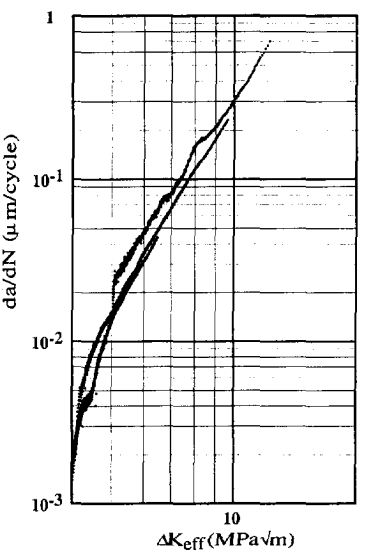

Figure 7.7. da/dN versus ΔK_{eff} for R=0.1, 0.3 and 0.7 from left to right respectively. Tests in Vacuum at 10 Hz.

In order to find the absolute values of the coefficients of the quadratic crack

closure formula we performed some constant amplitude fatigue tests in vacuum at higher R-values.

In vacuum it is not necessary to use underload cycles as in air to measure crack closure. There is no oxidation of the crack flanks and stable signals are obtained as shown in figures 7.4 and 7.5. The intention was to find the R value above which no crack closure effect could be measured.

The effect disappeared in the noise of the potential drop signal for $R \geq 0.7$. The effect for a test with $R = 0.7$ is shown in figure 7.8. The crack length measured by the potential drop apparatus remains about the same between the maximum and minimum loads. A test with $R = 0.8$ showed the same result with the same amount of noise (equivalent to about 0.4 mm crack length). A test with $R = 0.65$ showed a small effect.

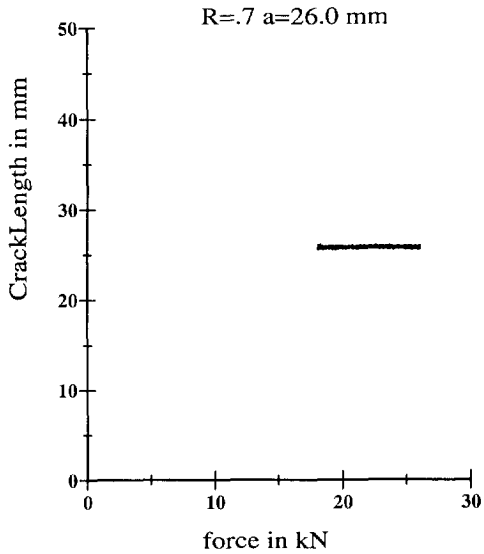

Figure 7.8. Crack Closure Test in Vacuum. Same Scale as in figure 7.5. Result from 50 cycles.

Based on these observations it is assumed that for $R \geq 0.7$ the crack closure effect does not occur any more in vacuum.

This means that $\Delta K_{eff} = \Delta K$ and $U = 1$ for $R = 0.7$. The consequence for the quadratic U relation is that all three coefficients have to be multiplied by a factor q with: $q(0.55 + 0.33R + 0.12R^2) = 1$ for R=0.7. This leads to a new crack

closure relation for fatigue crack growth tests of Al-2024 in vacuum:

$$U = 0.66 + 0.39R + 0.14R^2 \qquad 7.4$$

However, there is a problem because equation 7.4 implies less crack closure than in air (equation 7.3). It was expected that K_{cl} and K_{op} are higher in vacuum than in air, due to the rougher fracture surfaces in vacuum. More crack closure would not be contradicted by the well-known fact that da/dN is lower in vacuum. This consideration leads to the conclusion that the coefficients in relation 7.4 have to be lower with the same mutual ratio. Apparently there is a contradiction.

The absolute value of U can also be found with the other method. We performed crack closure measurements for a test in vacuum with R = 0.1 (shown in figure 7.4). The mean results for a number of cycles are $U_{open} = 0.50$ and $U_{closure} = 0.35$, which is less than found in air with equation 7.3. If this result is compared with that of equation 7.4, the conclusion is that there probably is some closure at higher R-values (above R = 0.7), which is lost in the noise. Equation 7.4 is then not correct.

If we calculate the K_{cl} and K_{op} values for the test in air shown in figure 7.3, the mean results for a number of cycles are $U_{open} = 0.67$ and $U_{closure} = 0.62$, which is more than U = 0.58 predicted by equation 7.3 for R = 0.1 for the underloads in this test. The width of the plateau where the crack is fully open is a measure for the closure. This width is not influenced by oxidation (as far as the effect is measurable in air).

If we use the test results for air and vacuum of K_{cl} and K_{op} and take the mean values of U_{open} and $U_{closure}$ we find:

$$U = 0.61 + 0.36R + 0.13R^2 \qquad 7.5$$

for the test in air. For the test in vacuum we find:

$$U = 0.40 + 0.24R + 0.09R^2 \qquad 7.6$$

In both cases the same ratios of the coefficients as in equation 7.3 are used. In order to understand the result in air (equation 7.5) it should be remembered that the result was found in a test using R = 0.7 followed by underloads at R = 0.1 to measure the crack closure (K_{cl} and K_{op}). The fracture surface geometry was flat tensile mode due to the high R-value. A similar test at R = 0.1 alone will induce a complete shear lip development after some crack growth. Thus we performed a closure measurement during the unstable tensile mode situation. This is the

reason that U in equation 7.5 is higher than U found by Schijve, equation 7.3. This means that the closure measurement technique in air is not able to measure the stable situation with complete shear lips at R = 0.1.

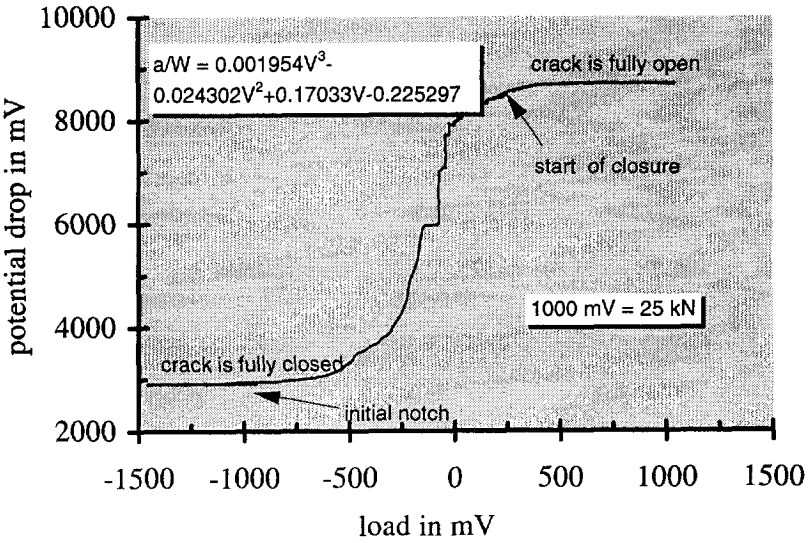

Figure 7.9. "Electrical" crack length dependence of a decreasing Force.

The conclusion is therefore that we can measure crack closure in vacuum directly, but that in air crack closure can only be measured during a few cycles in the unstable tensile mode.

In reference [11] a ratio of about 3 is reported for da/dN in air and vacuum over a large range of ΔK values. At higher ΔK values the da/dN - ΔK curves coincide. The same ratio is found by the present author, compare for example the results shown in figure 7.7 (in vacuum) with the results shown in figure 2.6 (in air). Because we also found a da/dN ratio of about 3 between fatigue crack growth in the tensile mode and complete shear mode(see chapter 5), we will investigate if the different U relations for crack growth in air and vacuum can be related by a shear lip correction.
The relation adopted in section 5.4, $\Delta K_{eff} . \ell$ = constant, is used. With this relation it is possible to correct U (equation 7.5), which was found for a tensile mode situation, to be valid for a complete shear situation. For a shear lip angle of 45° we calculate for U in air with *complete* shear lips:

$$U = 0.43 + 0.25R + 0.09R^2 \qquad 7.7$$

This result is almost equal to the vacuum U function (equation 7.6) found. Thus it seems that the effect on U by changing to fatigue in vacuum can be attributed mainly to surface roughness caused by shear lips. This can be an explanation for the fact that the same values for K_{op} and K_{cl} have sometimes been found in air and vacuum in the literature. Probably then in both cases shear lips were present. *Thus the same K_{op} and K_{cl} are expected when in both environments fracture surfaces are in the complete shear mode.*

To explain the difference between the closure relations in air, equation 7.5 for tensile mode and equation 7.7 for shear mode, with the Schijve closure function given in equation 7.3, it can be noted that the latter closure function was found from constant amplitude tests performed in air. The crack started in the tensile mode and slowly transformed into the shear mode as the crack length increased. It is not strange therefor that this U relation lies between the limits representing flat tensile mode and complete shear mode.

A matter of concern for the present closure measurement technique is formed by the fact that there might be an influence of the amount of crack flank pressure. In order to investigate the effect of premature contact or pressure on the crack flanks on the results of the potential drop method another experiment was performed. A center cracked tension specimen was prepared with an initial notch (saw cut) of about 5.2 mm length. After this the crack was allowed to grow in vacuum by constant amplitude fatigue cycling until it had a length of about 42 mm length. The growth was then stopped at the maximum value of the load (26 kN). Next the load was reduced slowly until a compression of about -35 kN. The result is shown in figure 7.9. The crack length as recorded by the potential drop apparatus, reduces from 42 mm, where the crack is fully open, to 5.2 mm at the initial saw cut, meaning that the fatigue crack is completely closed. The initial notch length is reached at about -15 kN. Without closure (and of course plasticity before the tip) we would expect to reach the initial notch length at 0 kN. It seems logical to assume that a certain amount of pressure is needed to reach the original crack length, owing to plasticity and the crack closure wedge that has grown during the crack growth period. Increasing the pressure until -35 kN does not change the outcome of the potential drop apparatus any more, meaning that the amount of pressure is not an important factor in this test method.

7.4 Crack Closure of Smooth and Rough Shear Lips

Recent constant amplitude tests in vacuum indicate a frequency dependent

behavior of the shear lips similar to the behavior in air [8-10]. In chapter 6, figure 6.10, it was shown that application of constant ΔK (under)load cycles at ΔK_{eff} = 16 Mpa$\sqrt{m}$ resulted in a considerable decrease of da/dN at 10 Hz and no decrease at 0.1 Hz for a test in air. A study of the fracture surfaces showed a very rough surface with big shear lips at 10 Hz. A continuous initiation of new shear lips within older ones occurred. This phenomenon was discussed in chapter 4, section 4.4, and it was shown in figure 4.27.
The fracture appearance at 0.1 Hz was different. Smooth shear lips without initiation of new ones occur. There is no change (no decrease) in da/dN as a function of the crack length (see figure 6.10).
Figure 7.10 shows the da/dN result of a constant ΔK test at 0.5 Hz. A decrease of da/dN, as found in this work (see chapters 4, 5 and 6) for tests at 10 Hz at ΔK_{eff} > 5.5 Mpa$\sqrt{m}$, is absent at 0.5 Hz, probably due to the regular shear lip forming.

The aim of the present section is to investigate if the closure behavior of smooth and rough shear lips is different, as should be expected from the da/dN behavior mentioned above. As we did show, the closure behavior of a crack in the tensile mode and in the shear mode is different. It is suspected that also the crack closure behavior of cracks with smooth shear lips is different from that of cracks with rough shear lips.
In order to shed more light on the crack closure phenomenon, as affected by the loading frequency and the type of shear lips (smooth or rough), the following test series of constant ΔK tests were carried out. Tests were performed in air until a crack length of 25 mm was reached. Then a sawcut (with a width of about 3 mm) was made along the fatigue crack to remove the plastic deformation in the wake of the crack. This eliminates the material responsible for the occurrence of crack closure. The saw cut was stopped at a short distance behind the existing fatigue crack (at a = 25 mm). Then the fatigue test was continued to see the effect of the crack flank material removal.
In the case of a tensile mode crack, and a crack with smooth shear lips, removal of crack flank plasticity until 1 mm behind the crack tip showed no change in da/dN (see figures 7.11 and 7.12). The crack flanks had no contact in the areas of the removed material. In the case of rough shear lips it was more difficult to remove crack flank material. Here an effect on da/dN is visible, as shown in Figures 7.13 and 7.14. In these tests material was removed until 3 mm and 1 mm behind the tip respectively.

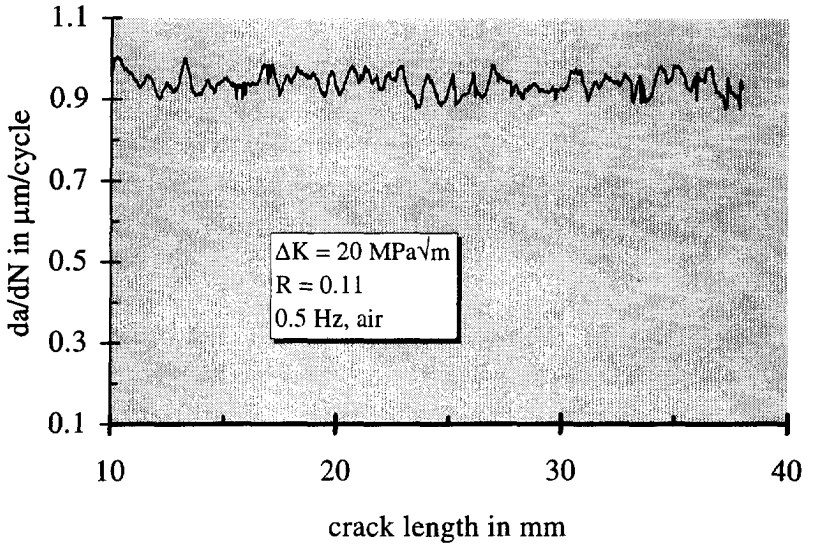

Figure 7.10. da/dN in case of smooth regular shear lips, test in air at 0.5 Hz.

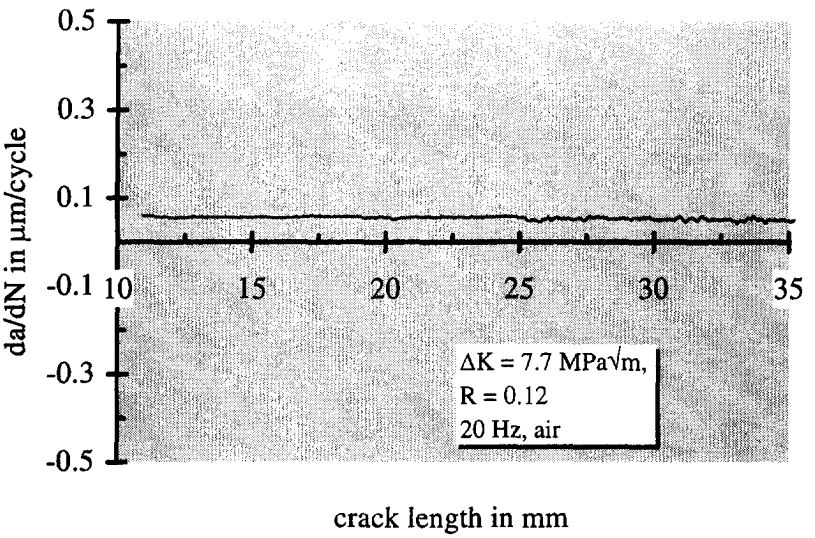

Figure 7.11, da/dN in tensile mode, test in air at 20 Hz. At a=25 mm the crack flank material is removed until a= 24 mm.

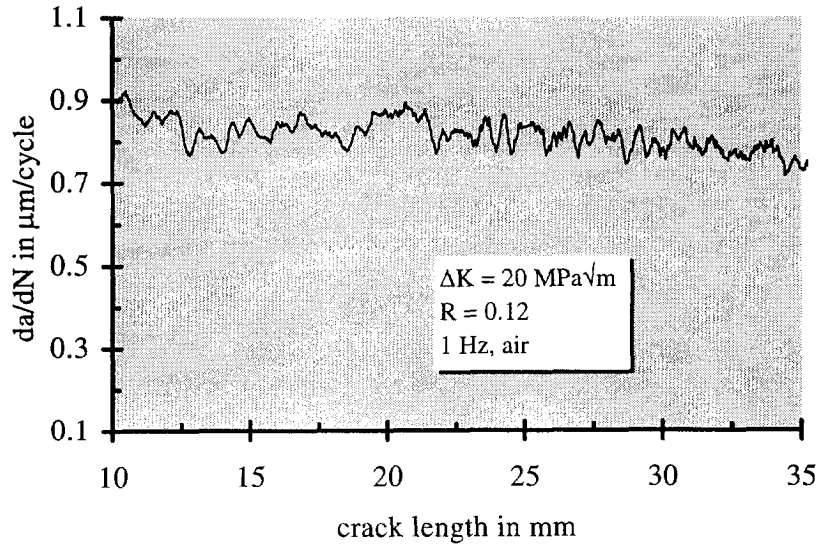

Figure 7.12, da/dN in case of smooth regular shear lips, test in air at 1 Hz. At a=25 mm the crack flank material is removed until a= 24 mm.

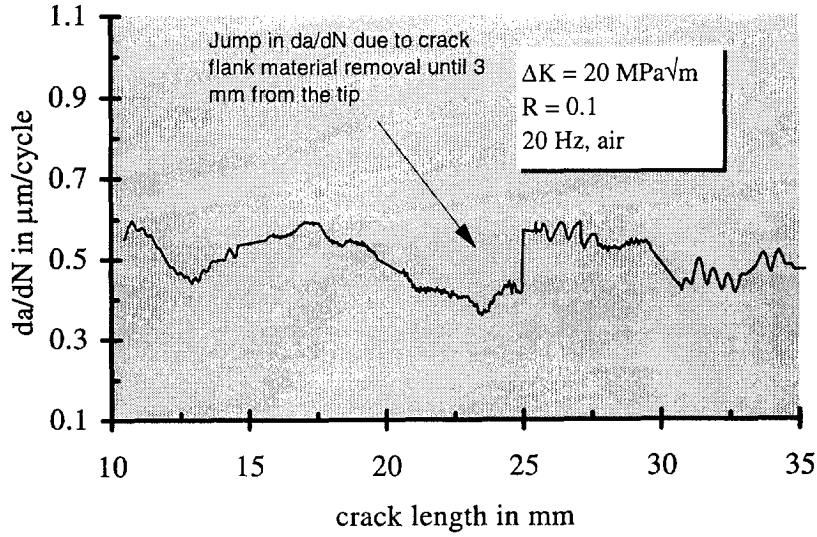

Figure 7.13, da/dN in case of rough, irregular shear lips. At a=25 mm the crack flank material is removed until a= 22 mm.

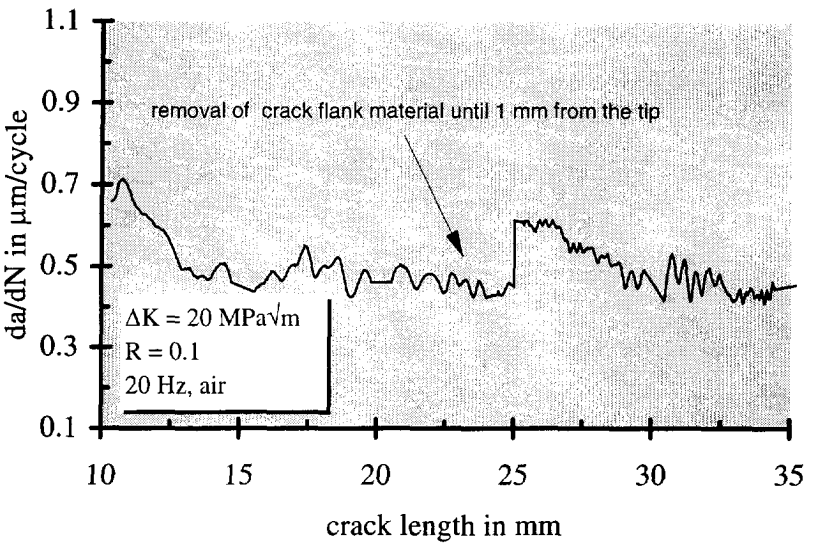

Figure 7.14, da/dN in case of rough, irregular shear lips. At a=25 mm the crack flank material is removed until a= 24 mm.

In figures 7.10 - 7.14 the same scale intervals were used for the da/dN axis in order to allow a direct comparison of the scatter in these figures. From the tests where crack flank material was removed we can conclude that fatigue cracks in the tensile mode and fatigue cracks with smooth shear lips experience a very localized closure effect (if at all), namely within 1 mm from the crack tip. Beyond 1 mm from the tip no effect is measurable, i.e. crack flanks do not touch in these areas. For rough shear lips the closure effect extends more than 3 mm from the tip. An analogous test with removal of crack flank material until 10 mm from the tip showed no jump in da/dN. This implies that the closure contributions start from a distance from the crack tip less than 10 mm and more than 3 mm. For both tests with crack flank removal until 1 and 3 mm the jump in da/dN is about the same (0.16 µm/cycle). If a slope m=4 in the Paris law for da/dN versus ΔK_{eff} is used (see figure 7.7), it follows that the jump in figures 7.13 and 7.14 leads to a change in ΔK_{eff} of about 8%. The total crack closure effect is probably much larger, since the contribution of the dominant last mm closest to the tip cannot be measured in this way. By performing other tests at different frequencies it was generally found that tests at frequencies below 1Hz show smooth shear lips in air, whereas above 2.5 Hz they become rough. In vacuum the transition frequencies for smooth to rough shear lips are somewhat lower, about 0.2 Hz to 2 Hz

7.5 Conclusions

1. It is possible to find the onset of crack opening and closure with the potential drop apparatus.

2 It is at this moment possible only to find an approximate upper bound R value above which the crack flanks make no electrical and thus no mechanical contact.

3. The quadratic closure function for fatigue tests on Al 2024 in vacuum is :

$$U = 0.40 + 0.24R + 0.09R^2$$

4. The quadratic closure function for fatigue tests on Al 2024 in air (flat tensile mode) is :

$$U = 0.61 + 0.36R + 0.13R^2$$

5. The quadratic closure function for fatigue tests on Al-2024 in air, corrected for the presence of shear lips is :

$$U = 0.43 + 0.25R + 0.09R^2$$

This is about the same as in vacuum. Thus the effect on U in vacuum can be attributed mainly to the surface roughness caused by shear lips.

6. Schijve's crack closure function was found from constant amplitude tests that started in the tensile mode and slowly transformed to the shear mode. This U relation lies between the limits of U in the flat tensile mode and in complete shear mode in air:

$U = 0.61 + 0.36R + 0.13R^2$ (tensile mode)

$U = 0.55 + 0.33R + 0.12R^2$ $-1 < R < 1$ (Schijve)

$U = 0.43 + 0.25R + 0.09R^2$ (shear mode)

7. Crack closure is a localized phenomenon for fatigue cracks in the tensile mode and in the shear mode with regular shear lips. It is not found to extent more than 1 mm from the crack tip.

8. Crack closure in the shear mode with irregular shear lips extends over more than 3 mm and less than 10 mm behind the crack tip for the loading situation discussed in this chapter.

9. The appearance of shear lips, in air as well as vacuum, depends on the frequency. Higher frequencies promote irregular shear lips with high closure, lower frequencies promote regular shear lips with little crack closure.

7.6 References

1. P.E. Irving, J.L. Robinson and C.J. Beevers, Engng. Fract. Mech. Vol. 7, 1975, pp. 619-630.
2. N. Ranganathan, J. Petit and B. Bouchet, Engng. Fract. Mech. Vol. 11, 1979, pp. 775-789.
3. M.C. Lafarie-Frenot, J. Petit and C. Gasc, Fat. Eng. Mat. Struct., Vol 1, pp. 431-438, 1979.
4. J. Petit, B. Bouchet,C. Gasc and J. De Fouquet, Fracture 1977, Vol. 2, ICF4, Waterloo, Canada, pp. 867 - 872.
5. W. Elber, A.S.T.M S.T.P 486, 230- 242 (1971).
6. J. Schijve, A.S.T.M S.T.P 982, 5- 34 (1988).
7. J. Zuidema, A calculation of the effective ΔK under various fatigue loading conditions, in Proceedings of ECF 9. conference pp 391 - 396 ,Varna, Bulgaria, 1992.
8. M. Kanaar, Master Thesis T.U. Delft, February 1992.
9. J.P. Krabbe, Master Thesis T.U. Delft, May 1994.
10. F.A. Veer, Doctor Thesis T.U. Delft, October 1993.
11. H.L. Ewalds, F.C. van Doorn and W.G. Sloof, ASTM STP 801, pp. 115-134, 1983.

8. General Discussion and Conclusions

8.1. Introduction

It is remarkable that crack closure as a phenomenon was overlooked for a long time before it was discovered by Elber.
The occurrence of shear lips on fatigue fracture surfaces was recognized long ago. However, the effect of shear lips on fatigue crack growth was largely disregarded, probably in view of so many other complicating influences, especially the predominant effect of crack closure. The present investigation was primarily carried out to fill this gap in our knowledge. The 2024 T3 Aluminium alloy was chosen for testing, because fatigue crack growth in this alloy does clearly exhibit the shear lip phenomenon. Moreover, the 2024 T3 alloy is abundantly used in aircraft structures because of its favorable fatigue damage tolerant properties.
In this last chapter the major observations of the present investigation and their significance are summarized first. The last section recapitulates specific conclusions in detail.

8.2. General observations

Shear lips have been extensively observed in large numbers of fatigue crack growth tests. Several systematic trends of the shear lip development were found. In this chapter an attempt will be made to come to a synthesis of some important facts discussed in the previous chapters. Fatigue crack growth is a complex physical process. In this process an important role is played by fatigue crack closure. Unfortunately, the results of measuring crack closure often depend on the measurement technique used.
In chapter 4 it is found that shear lips grow in width in a constant ΔK test until

an equilibrium value of the shear lip width is reached. The width is dependent on ΔK_{eff}, and in a certain sense also on the material thickness. The frequency also has an influence on the equilibrium shear lip width.
During shear lip growth the crack growth rate da/dN decreases. The wider the shear lip, the larger the decrease of da/dN.
In chapter 5 it was shown that the crack growth rate, going from tensile mode to complete shear, decreases by a factor of 3. Finite element calculations indicate that shear lips can reduce the mode I K factor by about 40%. This fact alone can lead to a decrease in da/dN by a factor of about 7 to 8 when a Paris curve with a slope m= 4 is used, or about 5 when m=3 is used. Thus the effect of shear lips on K_I alone cannot explain the observed decrease in da/dN.
Therefore a model, also involving crack closure and crack growth resistance, is presented in chapter 5. The model explains a da/dN decrease by a factor 3, when a Paris exponent of 3 is used, and also gives an explanation for the two slopes in log da/dN - log ΔK relations as are often quoted in the literature. The lower slope of the two is material thickness dependent. The crack growth mechanism is assumed to be the same in tensile and shear parts, while the reduction in da/dN is attributed to a shear lip effect on ΔK, on crack closure and on crack growth resistance.
In chapter 6 the results indicated a significant role of (extra) crack closure due to shear lips. To explain the results it was necessary to assume a long part of the crack length to be closed at K_{min}. However, it was not immediately clear why. The concept of smooth and regular versus rough and irregular shear lips was then introduced. The retardation after underloads was found to be due to a significant crack closure wedge accompanying rough shear lips.
In chapter 7 it was shown that the tensile mode and regular, smooth shear lips have no or only a small effect on da/dN in a constant ΔK test, while the development of irregular, rough shear lips has a much larger effect. It was also shown that the higher crack growth rate in air, compared to that in vacuum, could be largely explained by the presence of rough shear lips in the latter case. The difference becomes nearly zero when rough shear lips develop also in air at higher ΔK.

8.3. The Interaction of Crack Driving Force, Crack Growth Resistance and Crack Closure in the Case of Shear Lips

An inherent problem of the analysis of the various shear lip observations is the question whether certain influences are due to changes either of the crack driving force, or the crack growth resistance, or both. In this respect the following facts

were ascertained:

- there is a shear lip effect on K (chapters 4, 5)
- there is a shear lip effect on closure (chapters 4, 5, 6, 7)
- there is a shear lip effect on crack growth resistance (chapter 5).

Let us assume that when a shear lip is formed (regular or irregular) there is a decrease in K_I of 40%, as indicated by finite element calculations. Let us also assume that mode II and mode III crack growth can be neglected in comparison with mode I growth in the situation of a growing crack in a center cracked tension specimen under uniaxial tensile loading conditions. For smooth shear lips (obtained at low frequencies) no decrease in da/dN, in a constant ΔK test with growing shear lips, is found despite the reduction in K. For smooth shear lips also little or no (extra) closure is found (chapter 7). These facts point to the conclusion that the effect of shear lips on crack growth resistance must cancel the effect of shear lips on K.

This conclusion is supported by some reasonable physical arguments. The crack growth resistance is mainly due to the energy involved in plastic deformation at the crack tip. The plastic zone size depends on K. Then it seems reasonable to expect that if there is a decrease in K, thus a lower driving force, there will also be a smaller plastic zone, leading to a lower crack growth resistance. Thus the lower driving force will be partly compensated for by a lower crack growth resistance in the case of smooth shear lips. Of course this explanation is very rough.

For rough shear lips, at higher frequencies, the same argument with respect to driving force and crack growth resistance can be adopted. The only difference now is that a significant crack closure is present. This closure is responsible for the observed decrease in da/dN at growing shear lips and for retardation in da/dN after underloads.

An alternative explanation on the difference in behavior of smooth and rough shear lips can be given based on a contribution of K_{III} to crack growth. Finite element calculations predict both a decrease in K for mode I of 40 % and an increase in K for mode III of zero to 40% of the original mode I K value. If mode III crack growth is not neglected in the case of shear lips, then smooth shear lips are expected to lead to higher crack growth rates than rough shear lips do. The reason is the much higher mode III crack closure in the case of rough shear lips. It seems reasonable to expect that in the combined mode I plus mode III crack growth the mode III crack growth rate is higher than in pure mode III, because the tensile loading that opens the crack in mode I reduces the mode III crack

closure. For smooth shear lips this opening of the crack is possibly just enough to find a da/dN that is about equal to da/dN resulting from mode I loading at the same ΔK. For rough shear lips the mode III closure may be too high to be overcome by the mode I opening.

8.4. Implications for Failure Analysis and Fractography

In chapter 4 relations between the equilibrium shear lip width $t_{s,eq}$ and ΔK_{eff} (using the standard Elber formula) were found. A given ΔK_{eff} value ultimately leads to a unique $t_{s,eq}$ value. This relation can be reversed and used as a basis for extra information in the case of failure analysis and fractography. When a failed component shows a shear lip, the width of the shear lip is an indication for da/dN or for the applied ΔK_{eff}, or ΔK. This is in general not true for tests with large changes in ΔK, where da/dN and $t_{s,eq}$ are both dependent on the load history and not a measure for the momentary applied ΔK.
From the shear lip width it is possible to get a global impression of da/dN, and from striation measurements we get a local da/dN. Of course caution is needed in the interpretation of the results, as different loading conditions can lead to the same shear lip width, just as it is possible with da/dN found from striation measurements. Information from shear lip width is thus not sufficient but supplementary to other characteristics like striation width measurements, beach markings, etc. Another parameter accompanying shear lips is the roughness or smoothness of the shear lips. This factor gives information about the frequency and about the amount of crack closure. Fluctuations in shear lip width indicate loading transitions. The conclusion of this section is that large shear lips point to a high ΔK_{eff} (high loading) and that rough shear lips point to a high frequency.

8.5. Implications for Fatigue Crack Growth Prediction Models based on Closure

In fatigue crack growth prediction models based on crack closure results from laboratory constant amplitude tests are often used. During variable amplitude loading in practical situations the loading spectra seldom result in large shear lips. The cracks are mainly in the tensile mode. Under laboratory circumstances constant amplitude tests often show a transition from tensile to slant crack growth. It is shown in chapter 5 that a crack in the tensile mode propagates about three times faster than an equivalent crack in a completely slant situation. Thus when results from constant amplitude tests are used in the prediction this is only allowed when the fracture modes of constant amplitude test specimens and variable amplitude specimens are the same. When the fracture surface is not

considered there can be a breakdown of similitude. In practical situations with a very low number of high load excursions the effect will be negligible. If the number of loading "spikes" is high it is better to use the extrapolated tensile mode data (see chapter 5). Another very simple safety procedure would be to magnify the da/dN of all "spikes" by a factor of 3, to be conservative.

8.6. General Conclusions

1. A satisfactory mathematical description of the shear lip width behavior under constant stress intensity loading could be given. Relation 4.3 is the basis of the description.
2. It was possible to predict shear lip width behavior under constant stress amplitude loading by using the mathematical description found in constant ΔK tests.
3. The effect of frequency on the shear lip width could be described. Both ΔK and frequency effects could be combined in a general shear lip width description (equation 4.31). The da/dN in tensile mode was found to be independent of the frequency. The effect of the frequency on da/dN could be associated with the effect of the frequency on the shear lip width.
4. An explanation could be given of the fracture path (in fast static fractures) of fracture surfaces in single and in double shear.
5. An effect of the fracture mode on K (and/or K_c) was found. The large difference between the results found in fatigue tests and in tensile tests could not be explained satisfactorily
6. The increase of the shear lip width under constant ΔK loading decreases the crack growth rate da/dN.
7. The two slopes in the da/dN - ΔK curves on a log-log scale are due to the impeding action on da/dN by the growing shear lips in the transitional area between pure tensile mode and pure shear mode.
8. The formula found for the tensile mode crack growth, equation 5.6, is important for fatigue crack growth prediction under variable amplitude loading where the fracture surface is expected to remain flat.
9. The crack growth rate in the case of shear lips can reasonably well be described by a model based on $\Delta K_{eff} . \ell$ = constant (ℓ is the transverse crack front length) and by adopting a similarity approach.
10. The thickness effect on da/dN is dependent on the change of the transverse crack front length; for low ΔK_{eff} (pure tensile mode) and high ΔK_{eff} (pure shear mode) no thickness effect is observed.
11. The tensile growth rate can be described by Elber's crack closure

formula. A good description includes an effective threshold K value.

12. The prediction of da/dN in the shear mode is based on the transverse crack front length.

13. An explanation for the observed temporary decrease of da/dN in some constant amplitude tests could be given, based on the transition of the tensile mode to the shear mode.

14. The maximum reduction in da/dN, from a pure tensile situation to a complete shear situation, is by a factor of about 3.

15. The application of overloads always causes delayed retardation on subsequent crack growth. Larger numbers result in more retardation.

16. The application of large numbers of underloads always cause delayed retardation on subsequent crack growth when the applied ΔK of the underloads is so high that shear lips will develop on the fracture surface. Larger numbers and a high frequency enhance the retardation.

17. The application of one or a small number of underloads has no effect on subsequent crack growth.

18. The crack length affected by the underloads extends far more than the physical presence of shear lips, indicating that shear lips not only have an effect on K but also on K_{op}. The affected crack length is also much larger than the monotonic plastic zone size.

19. Tests with underloads at a lower frequency indicate that the reduction in crack growth rate during application of the underloads and the delayed retardation after the underloads are largely caused by irregularities of the shear lips. A smooth regular shear lip as is found at 0.1 Hz has only a slight effect, indicating that crack closure caused by an irregular shear lip is the most important delaying mechanism.

20. It is possible to find the onset of crack opening and closure , in air and vacuum, with the potential drop apparatus.

21 It is at this moment possible to find only an *approximate* upper bound R value above which the crack flanks make no electrical and thus no mechanical contact.

22. The quadratic crack closure function for fatigue tests on Al-2024 in vacuum is :

$$U = 0.40 + 0.24R + 0.09R^2$$

23. The quadratic closure function for fatigue tests on Al-2024 in air (flat tensile mode) is :

$$U = (0.61 + 0.36R + 0.13R^2)$$

24. The quadratic crack closure function for fatigue tests on Al-2024 in air, corrected for the presence of shear lips is :

$$U = 0.43 + 0.25R + 0.09R^2$$

This is about the same as in vacuum. Thus the effect of vacuum on U can be attributed mainly to the surface roughness caused by shear lips.

25. Schijve's crack closure function was found from constant amplitude tests that started in tensile mode and slowly transformed to shear mode. His U relation lies between the limits of U in the flat tensile mode and in the complete shear mode in air:

$$U = 0.61 + 0.36R + 0.13R^2 \qquad \text{(tensile mode)}$$

$$U = 0.55 + 0.33R + 0.12R^2 \qquad -1 < R < 1 \qquad \text{(Schijve)}$$

$$U = 0.43 + 0.25R + 0.09R^2 \qquad \text{(shear mode)}$$

26. Crack closure is a localized problem for fatigue cracks in the tensile mode and in the shear mode with regular (smooth) shear lips. It is not found to extend more than 1 mm from the crack tip.

27. Crack closure in the shear mode with irregular (rough) shear lips extends over more that 3 mm and less than 10 mm from the crack tip for the loading situation discussed in chapter 7.

28. The appearance of shear lips, in air as well as in vacuum, is dependent on the frequency. Higher frequencies promote irregular shear lips with a high closure influence, lower frequencies promote regular shear lips with little crack closure influence.